ISSN 1936-5330

kc FED Research Working Papers

Housing Market Value Impairment from Future Sea-level Rise Inundation

David Rodziewicz, Christopher J. Amante, Jacob Dice,
and Eugene Wahl

July 2020
RWP 20-05
http://doi.org/10.18651/RWP2020-05

Federal Reserve Bank of Kansas City

Housing Market Value Impairment from Future Sea-Level Rise Inundation

David Rodziewicz, Christopher J. Amante, Jacob Dice, and Eugene Wahl*

July 16, 2020

Abstract

The rate of future global sea-level rise will likely increase due to elevated ocean temperatures and increases in land-ice melt. Nearly 40 percent of the U.S. population lives in coastal communities, and coastal properties are expected to become more prone to coastal flooding in the coming decades due to relative sea-level rise caused by both global and local factors. Understanding how this projected sea-level rise translates to lost economic value is critical to the decisions of insurance companies, banks, governments, investors, and regulatory agencies. We use probability distributions of local sea-level rise projections, National Oceanic and Atmospheric (NOAA) coastal digital elevation models, and CoreLogic housing data to estimate a range of housing market value impairments from future sea-level rise in 15 major U.S. coastal cities as well as the associated timing of those impairments. Our estimates include only residential properties with four or fewer units and thus provide a lower bound estimate of economic risk from sea-level rise. We estimate that within these 15 major U.S. coastal metros, sea-level rise will inundate between 2,000 and 28,000 properties by 2100 in a relatively low greenhouse gas concentration scenario and between 7,000 to 77,000 properties under an unlikely, extreme greenhouse gas concentration scenario. These estimates equate to direct economic losses between $0.1 to $1.8 billion under the low greenhouse gas scenario and $3.8 to $50.6 billion under the high scenario.

Keywords: Climate Risk, Climate Economics, Sea-level Rise, Natural Hazards, Housing

JEL Classification Codes: Q54, R3, D89

*The views expressed here are those of the authors and are not attributable to the Federal Reserve Bank of Kansas City, the Federal Reserve System, or the National Oceanic and Atmospheric Administration. Rodziewicz: Federal Reserve Bank of Kansas City, Research Department, 1 Memorial Dr, Kansas City, MO 64198 (email: david.rodziewicz@kc.frb.org); Amante: Cooperative Institute for Research in Environmental Sciences (CIRES), University of Colorado Boulder at the National Oceanic and Atmospheric Administration (NOAA), National Centers for Environmental Information (NCEI), 325 Broadway, Boulder, CO 80305, DSRC 1B118 (email: christopher.amante@noaa.gov); Dice: Federal Reserve Bank of Kansas City, Research Department, 1 Memorial Dr, Kansas City, MO 64198 (email: jacob.dice@kc.frb.org); Wahl: National Oceanic and Atmospheric Administration (NOAA), National Centers for Environmental Information (NCEI) (retired), (email: generwahl@yahoo.com); Keywords: Climate Risk, Climate Economics, Sea-level Rise, Natural Hazards, Housing Markets.

1 Introduction

Climate change is a persistent and substantial threat to society and the functioning of our economic systems (USGCRP, 2018). Climate change impacts are already manifesting through more frequent and extreme weather events (NOAAa, 2019), higher temperatures (IPCC, 2014), and rising seas (Sweet et al., 2017). Sea-level rise (SLR) is one of the more pernicious consequences of climate change and will likely negatively impact large portions of the United States (U.S.) population and economy in the coming decades. Roughly 40 percent of the U.S. population lives in coastal communities (NOAAb, 2019), with approximately 7 million people and 1.9 million homes at elevations within 1.8m (6ft) above sea-level (Hauer et al., 2016; Rao, 2017). As sea-levels slowly rise, these locations will likely face increased nuisance flooding (Moftakhari et al., 2015; Sweet et al., 2017), enhanced storm surge inundation (Amante, 2019), and permanent change of coastlines. In extreme cases, some coastal areas may experience out-migration, and city planners may need to implement policies to facilitate population departure (Wrathall et al., 2019). Rising sea-levels over the next century will potentially disrupt housing markets and cause large economic losses.

1.1 Climate Change, Sea-level Rise, and Economics

Estimates of the economic costs of climate change date back nearly 30 years (Smith and Tirpak, 1989; Nordhaus, 1991) and estimates of the economic costs of SLR date back more than 20 years (Fankhauser, 1995). Today, theoretical economists and macroeconomists continue to refine estimates for the social cost of carbon (Stern, 2008; Gillingham and Stock, 2018; Pindyck, 2019) and the broad economic consequences of climate change (Bansal et al., 2016; Colacito et al., 2018; Auffhammer, 2018). Recent empirical research suggests that properties prone to coastal flooding from hurricanes have lower values than similar properties in unaffected areas (Ortega and Taspinar, 2018). Multiple markets prone to SLR inundation are also starting to

witness slower price appreciation growth (Mcalpine and Porter, 2018). Furthermore, properties most prone to SLR inundation may face lower valuations compared with similar properties in less prone areas (Bernstein et al., 2019).

The banking and finance world are also starting to consider the economic impacts of climate change. In 2015, Mark Carney, the governor of the Bank of England, gave one of the first speeches on the role of central banks in a changing climate. Carney described the challenges and risks of climate change as the "Tragedy of the Horizon" and stated that the cost of climate change will most likely be felt by future generations, beyond typical business and political cycles (Carney, 2015).[1] Longer-term climate impacts may pose issues for businesses, investors, and financial institutions in the coming decades. In particular, attention is being focused on increased physical impacts from climate change, such as fires, floods, and hurricanes. Markets also face transitional risks that may take the form of carbon policy changes, shifts in technology (e.g., from fossil fuel technology to renewables) and changes in investor preferences toward more environmentally sustainable business practices (FSB-TCFD, 2017). In recent years, central banks around the world started to examine their potential role in mitigating economic risks from climate change and the unique risks banks face from climate change, such as investments in areas more prone to extreme weather events (NGFS, 2017; Campiglio et al., 2018; BOE, 2019). Private financial institutions are also starting to consider climate change impacts within their own businesses and investment strategies, signaling the reallocation of financial capital away from carbon intensive industries, such as coal and other fossil fuels, towards more sustainable, renewable energy sources (Black Rock, 2019; CoBank, 2019; Goldman Sachs, 2019). Through these multiple outlets, the banking and finance sector is beginning to consider the economic effects that climate change may pose in the coming decades.

However, as the awareness of climate change grows, risk practitioners face a series of chal-

[1]Robert Solow coined the term "intergenerational equity" in 1974 to describe a similar phenomena relating to exhaustible nature resources (Solow, 1974).

lenges. A primary challenge for economists and financial analysts is understanding climate science and accurately linking climate change to some measure of economic or financial risk. Recent plain-language articles on climate help bridge the knowledge gap between economists and climate science and outline the economic implications of climate change (Hsiang and Kopp, 2018; Auffhammer, 2018; Gillingham and Stock, 2018). Two additional challenges risk practitioners face are understanding the uncertainties associated with climate projections and accounting for the economic or financial value linked to those climate projections. Uncertainty in climate projections needs to be accounted for when estimating the economic implications of climate change, especially when assessing the potential impacts of future SLR on the U.S. housing market. For example, depending on carbon emissions, land-use changes, and other global, regional, and local factors that affect sea-levels, SLR could displace between 4 - 13 million people in the U.S. over the next century (Hauer et al., 2016). Coastal communities are facing a wide-range of risks, with differing social, economic, and financial costs. Properly accounting for the range of economic and financial risks that results from climate change and SLR uncertainty is crucial to accurately balance the financial costs and benefits of potential policy choices.

1.2 Climate Change Uncertainty and Sea-level Rise

1.2.1 Climate Models, Scenarios, and Uncertainty

Accounting for climate change uncertainty is critical for estimating the range of economic costs associated with future SLR. Hawkins and Sutton (2009) separate total climate change uncertainty into three broad categories: climate scenario uncertainty, internal climate variability (i.e., natural climate variability separable from human influences), and model uncertainty. In concert, these sources of climate uncertainty can affect economic decision-making and the costs attributed to climate change impacts such as SLR inundation (Heal and Millner, 2014).

Future atmospheric greenhouse gas (GHG) concentrations are one major source of climate

uncertainty. The scientific literature and climate policy publications outline a series of commonly used, independent scenarios known as Representative Concentration Pathways (RCP), e.g., RCP 2.6, 4.5, 6.0, and 8.5 (Moss et al., 2010; IPCC, 2014). Each RCP scenario is associated with a given level of future atmospheric greenhouse gas (GHG) concentrations that results from differing socioeconomic, technology, and biophysical assumptions in specific integrated assessment models (IAMs). As a result of these independent assumptions, the RCP scenarios depict progressively higher levels of GHG concentrations, elevated global temperatures, and, by extension, accelerated increases in global sea-levels. For example, under RCP 2.6, global GHG concentrations are projected to rise modestly to 490 ppm by 2100, global mean temperatures are projected to rise by 1.5°C, and global mean sea-level is projected to rise by 49 cm. Under RCP 8.5, GHG concentrations are projected to rise to 1370 ppm by 2100, mean temperatures are projected to rise by 4.9°C, and global mean sea-level is projected to rise 79 cm (Moss et al., 2010; Rogelj et al., 2012; Wayne, 2013; Kopp et al., 2017).[2] As these data demonstrate, climate scenario uncertainty contributes to a wide range of potential outcomes, and is especially important on longer-term horizons (>60 years; Hawkins and Sutton (2009)). By extension, the economic consequences of climate change can be very different solely based on the climate scenario.

Analysts and social science researchers (who may have limited knowledge of climate science) are often charged with making a judgement on which RCP scenario(s) to analyze. The RCP scenarios are independent and result from different combinations of economic, technological, demographic, policy, and energy source futures. Practitioners are often required to make a value judgment on climate scenarios or analyze the economic effects of each climate scenario, arriving at a range of outcomes. This approach, while useful, is limited as it doesn't account for uncertainty within each of the RCP scenarios.[3]

[2]Under current carbon emission policies and energy transitions, empirical evidence would suggest that RCP 8.5 is less likely, and in reality, we are currently closer to a medium GHG concentration scenario (RCP 4.5)(Hausfather and Peters, 2020). Recent research accounted for economic risks associated solely with GHG scenarios (e.g., RCP 2.6, 4.5, and 8.5)(Zillow, 2018). Our work is in line with those results, but includes uncertainty around those commonly analyzed scenarios.

[3]Government agencies such as the National Oceanic and Atmospheric Administration (NOAA) have also

The second and third major sources of climate uncertainty are internal climate variability (natural variability) and modeling uncertainty. In the near term (<20 years), a majority of climate uncertainty is driven by internal variability, i.e., natural climate variability (climate variation separable from human influences); this is especially true for regional scenarios (Hawkins and Sutton, 2009). The global climate system is chaotic, which makes it sensitive to the initial model parameters. In the medium-term (20-50 years), model uncertainty, or the spread of estimates across various climate models, is the main contributor to climate uncertainty (Hawkins and Sutton, 2009). As previously mentioned, global climate scenarios (i.e., GHG concentration scenarios) contribute most to total uncertainty when time horizons exceed 60 years into the future (Hawkins and Sutton, 2009; Heal and Millner, 2014).[4] It is important to account for these various sources of climate change uncertainty to estimate the range of economic costs associated with future SLR over the next 80 years.

1.2.2 Sea-level Rise Uncertainty

Large climate change uncertainty contributes directly to a range of future SLR projections through the end of the century and can make it challenging to assess potential economic costs from SLR. Under the low GHG concentration scenario (RCP 2.6), projections for global mean SLR range from 0.3 to 0.8 meters (5^{th} to 95^{th} percentiles) by the end of the century (Kopp et al., 2017). Under the high GHG concentration scenario (RCP 8.5), mean SLR is expected to range from 0.5 to 1.2 meters (5^{th} to 95^{th} percentiles; Kopp et al. (2017)). Uncertainty in local SLR projections can be even more extreme. Kopp et al. (2014, 2017) provide local sea-level projections that are informed by a combination of expert community assessment, expert

created their own SLR projections with the intent of making climate risk information more accessible to the non-scientific public. However, easy-to-use scenarios can mask uncertainty around the underlying climate scenarios. For example, NOAA created their own SLR projections that are based on the underlying GHG concentration scenarios which obfuscate from the uncertainty within each of those climate scenarios (Sweet et al., 2017; NOAAc, 2019; Kopp et al., 2014). NOAA outlines 5 SLR pathways (e.g., low. . . extreme) for each of its local tidal stations. These pathways are based on exceedance thresholds, which utilize parametric uncertainty, but does not map easily to parametric distributions of uncertainty within each GHG scenario (RCP 2.6, 4.5, 8.5).

[4]Figure 3 in Hawkins and Sutton (2009) illustrates the change in contribution to climate uncertainty over time from the three sources: scenario uncertainty, internal variability, and model uncertainty.

elicitation, and process modeling, and incorporate the various sources of climate uncertainty within GHG concentration scenarios (e.g., RCP 2.6, 4.5, and 8.5).[5] For example, future SLR estimates for Miami, Florida range from 0.2 and 1.0 meters under RCP 2.6 and between 0.4 to 1.4 meters under RCP 8.5, by the end of the century (Kopp et al., 2017). SLR estimates for New York City (NYC) are even more uncertain, ranging from 0.2 to 1.2 meters for RCP 2.6 and from 0.4 to 1.7 meters for RCP 8.5, through 2100 (Kopp et al., 2017). Other additional factors, such as accelerated Antarctic ice sheet melt can further exacerbate uncertainty in mean sea-level and local SLR projections through the end of the century, amplifying the range of economic impacts from SLR (Deconto and Pollard, 2016).[6]

This research incorporates uncertainty in future SLR projections caused by global climate change and regional and local processes to estimate a range of future U.S. housing market value impairments. Specifically, we use probability distributions of local SLR projections, National Oceanic and Atmospheric (NOAA) coastal digital elevation models (DEMs), and CoreLogic housing data to estimate housing market value impairment from future SLR inundation in 15 major U.S. coastal metros.

2 Methods and Data

2.1 Discount Rates, Time Value, and Value Impairment Estimates

An important factor in estimating the impaired value of the U.S. coastal housing market is the timing of impairment from SLR. Intuitively, a property that is impacted by SLR sooner should see a higher value impairment than a property that is affected by SLR at a later date. Determining the timing of impairment is an important component of this research in estimating total value at risk. Another important consideration is the discount rate used to estimate the

[5]These are the estimates utilized by NOAA for their local SLR projections Sweet et al. (2017).

[6]See supplemental material Section 6.3 for a detail description of the effect of Antarctic ice sheet melt on housing market impairments.

impaired value. A common method to account for value over time (i.e., time value of money) is by using a discounted cash flow methodology. Discounted cash flow methods value an asset based on future cash flows by discounting future cash flows by some interest rate (i.e., discount rate) over a period of time. The value of an asset is calculated as the sum (or integral) of the discounted values of all future cash flows. This method can be applied to value any asset with relatively consistent cash flow streams, such as stocks, bonds, or real estate, and is also widely used in the public policy sphere to value long-dated projects or estimate the cost of policies with long-term social consequences (Arrow et al., 2013a). We use a discounted cash flow method to account for the value at risk for a property with respect to when a property is potentially inundated by SLR.[7]

A noteworthy assumption for a discounted value methodology is the choice of a discount rate, as the discount rate has a significant effect on estimates of impaired value over time (Arrow et al., 2013a,b).[8] Despite the importance of the discount rate to long-term valuation, estimating or agreeing upon discount rates that are "socially responsible" over generational time is challenging and open for debate (Arrow et al., 2013b). Estimating the correct long-term interest rate is beyond the scope of this paper. For our baseline value impairment estimates, we use a discount rate of 0 percent, which allows us to easily communicate results in an intuitive way. Our impairment estimates are simply the current estimated property values and values are held constant over time. Additionally, a 0 percent discount rate is within the range (albeit at the lower end) of rates used by other researchers and is consistent with current conditions where risk free interest rates remain near zero throughout most of the developed world (Drupp et al., 2018). Policymakers and local governments, who might be interested in provisioning for SLR

[7]Conceptually, this type of valuation methodology accounts for the "time value of money" by acknowledging that individuals place a lower value on the future than on the present period (Samuelson, 1937). The discounted cash flow technique for valuing companies dates back to the early 1700's (Brackenborough et al., 2001) and gained popularity as a common valuation approach in the 1900's. Refer to the supplemental material section 6.2 for a detailed description of our discounted cash flow methodology based on the Gordon (1963) model, a discussion of cash flow impairment, and analysis of interest rate sensitivity.

[8]The higher the discount, the less value you place on future cash flow streams, and vis-a-versa. When thinking about impairment from SLR over time, the higher the discount rate, the lower the impairment value.

risks over time, may want to use a different (positive discount rate) for their long-term planning purposes.[9]

In addition to the discount rate assumption, our housing market impairment analysis makes a series of simplifying assumptions: First, we assume that once a property is inundated by SLR, the value of the property falls to zero, which is an assumption in line with previous research (Bernstein et al., 2019). In reality, additional flood risks from nuisance flooding or enhanced storm surge would also erode economic value well before terminal impairment from SLR inundation (Amante, 2019; Ghanbari et al., 2019; Beltrán et al., 2019). Second, our approach assumes no foresight on the part of homeowners, who would likely begin to discount property values well before terminal impairment or might take steps to protect their properties (e.g., by erecting protective flood walls). This either carries forward the value impairment or burdens the homeowner with onerous mitigation costs, both of which would reduce the home's value earlier than our estimates. From this perspective our estimates for value at risk fall on the conservative side, as we are not accounting for these additional risk factors or costs. Third, we assume that coastal markets have yet to incorporate all the risks associated with SLR into the valuation of coastal housing properties.[10] Lastly, our analysis treats the housing market as static, as we implicitly assume no population growth (or migration), no housing market growth, and no housing price appreciation. We contribute to the literature by providing a range of impairment estimates for coastal housing markets and importantly the timing of when that impairment may occur. Ultimately this simple approach allows us to estimate when properties will become

[9]Our 0 percent discount rate is the real rate of interest, which means that we assume that cash flows grow at the same rate as inflation – the growth in nominal cash flows cancels out with the inflation rate, leaving the real rate of interest or "discount rate" in our case. There is a wide array of discount rates used in the social science and public policy spheres ranging from slightly negative to 20 percent (Drupp et al., 2018). Other commonly used discount rates used for long-term housing cash flows fall in the low single digits (Giglio et al., 2014, 2015; Bernstein et al., 2019). For example, 4 percent is commonly used for carbon accounting (Nordhaus, 2013) and the Office of Management and Budget's upper range for the "social rate of time preference" extends up to 7 percent (OMB, 2003). Although we simply use a 0 percent discount rate in our baseline analysis, we provide an interest rate sensitivity analysis in the supplemental material section 6.2.

[10]Though some recent evidence suggests that property owners and investors are starting to account for these risks (Beltrán et al., 2019; Mcalpine and Porter, 2018), other evidence indicates that homeowners are not currently accounting for all risks of SLR and coastal inundation (Palm and Bolsen, 2020).

inundated, providing an estimate of direct economic loss from SLR over time.

2.2 Housing Market Data

We use CoreLogic housing information from their Deeds, Tax, and Tax History data sets to generate our housing market sample. Our housing market for the U.S. spans roughly 5.4 million unique residences across 15 major coastal metros. We use precise geo-location information (latitude and longitude) available in the housing data set to determine the respective elevation above sea-level for each property and to estimate the timing at which the property may be affected by local SLR. For each metro, we use the U.S. Postal Services' city and ZIP code data to filter the CoreLogic housing data to include only ZIP codes within the metropolitan areas (USPS, 2020). Our housing market sample is restricted to single-family houses, townhomes, and 2-4 unit residential buildings.[11] Finally, our housing data set includes historical pricing information – sales price, market value, and assessed value. We index the most recent property value available in our data set to the current time period (2020) using CoreLogic ZIP code and county-level combined single-family housing price indexes. Adjusting values to the current year gives us an estimate of the current value of each property and the total estimated value of the housing stock within each of the 15 metros.

2.3 Local Topography, Geospatial Data, and Matching Methodology

2.3.1 Local Topography

The local topography has a large effect on the modeling of future coastal inundation from SLR and the impairment of individual housing markets. Much of the Atlantic and Gulf Coasts of the U.S. consist of low-lying areas with small terrain slope, which results in wide swaths of potentially flooded areas and impaired housing markets. Conversely, the Pacific Coast of the

[11] We exclude properties with a value estimate of less than $10K and trimmed the housing sample within each metro, removing any properties in the upper 0.00001 percentile of the value distribution.

U.S. has many elevated areas with large terrain slope adjacent to the coastline, resulting in narrower swaths of land prone to SLR inundation and future impaired housing markets. DEMs depict the local topographies and are essential to modeling coastal flood risk and the future impairment of housing markets.

Accurate, high-resolution DEMs are needed to both delineate areas with low elevations below a projected sea-level and to determine hydrologic connectivity. Natural terrain features (e.g., gullies, hills) and man-made terrain features (e.g., culverts, levees) can enhance or impede the flow of water and affect flooding at inland elevations (Li et al., 2009; Poulter and Halpin, 2008; Gesch, 2009; Zhang et al., 2013; Amante, 2019). The spatial resolution of the DEM is an important factor in coastal flood modeling, as it determines the ability to resolve these terrain features (e.g., gullies, hills, culverts, and levees) that can affect hydrologic connectivity. This ability is especially important for modeling the future housing impairment for coastal regions with low-lying areas protected by terrain features at present-day sea-levels. For example, the DEMs for NYC and Miami have spatial resolutions of 3m and 5m, respectively. These spatial resolutions are assumed to be able to resolve the most important terrain features that could enhance or impede water flow, but the effect of the DEM spatial resolution is not rigorously quantified in our analysis.

Furthermore, potential differences between DEM values and the "true" elevation represents the DEM uncertainty, and such uncertainty can cause differences in the modeled coastal flood risk (Amante, 2018, 2019) and, subsequently, in housing impairment estimates. There are many sources of DEM uncertainty, including the spatial resolution, interpolation method, and elevation measurement uncertainty (Amante and Eakins, 2016; Amante, 2018). The vertical uncertainty of topographic elevation measurements using modern light detection and ranging (lidar) technology is generally on the order of 10-20 cm at one standard deviation (Amante, 2018, 2019). This study does not incorporate DEM uncertainty into the analysis. Modeling a single SLR projection at

yearly time steps generally results in the SLR increment to be smaller than the DEM uncertainty, and can lead to questionable results (Gesch, 2018). However, the uncertainty in topographic DEMs derived from lidar measurements is much smaller than the uncertainty in SLR projections due to different RCP scenarios, and the full SLR probability distributions within a given RCP scenario provided by Kopp et al. (2014, 2017). Previous research indicates that the DEM uncertainty has a much smaller effect on the modeled area prone to coastal flooding than the uncertainty in SLR projections, especially in more distant decades (Amante, 2019).

2.3.2 Geospatial Data and Matching Methodology

We use geospatial data from NOAA's Sea Level Rise Viewer (NOAAd, 2019), which captures local topographic features, in order to estimate the timing of inundation and associated housing market impairment for the 15 metros. We use NOAA's Sea Level Rise Viewer DEMs to determine each property's respective elevation above sea-level at approximately high tide. Specifically, the DEMs indicate the relative elevations above the tidal datum of Mean Higher High Water (MHHW), which is the average of the higher high water height of each tidal day observed over the National Tidal Datum Epoch. We also use NOAA's Sea Level Rise Viewer inundation shapefiles, which delineate areas that will be inundated at one-foot increments of SLR above MHHW (0-10ft). These shapefiles were generated from NOAA's Sea Level Rise Viewer DEMs (NOAAd, 2019), and provide validation that a property is inundated at its respective elevation above sea-level by accounting for hydrologic connectivity. Depending on the local topography and built-environment, some low-lying areas along the coast may be protected by natural levies or structures and might not be inundated (i.e., not hydrologically connected) until sea-level rises well above their actual measured elevation (Poppenga and Worstell, 2015). For this reason, it is important to account for hydrologic connectivity when estimating the inundation height and associated timing of impairment for a property.

We use both the property elevations from the DEMs and the one-foot increment shapefiles to

refine our estimates of the timing of inundation for each property.[12] The NOAA Sea Level Rise Viewer shapefiles consider both the elevation and hydrologic connectivity when delineating areas prone to SLR inundation at 1ft intervals. However, additional temporal granularity is needed to refine estimates of the year of inundation for each property. This is especially true with the 10^{th} percentile of SLR projections associated with RCP 2.6. For example, in the city of Miami, it takes approximately 100 years for local sea-level to rise 1ft at the 10^{th} percentile projection associated with RCP 2.6. The many years between one-foot intervals of SLR provides coarse estimates of the timing of housing market impairment. Accordingly, we use both the property elevation from the DEM and the location of the property within the NOAA Sea Level Rise Viewer shapefiles that considers hydrologic connectivity to estimate the timing of inundation. See section 6.1 in the supplemental material for more details on our method of using both the NOAA Sea Level Rise Viewer DEMs and shapefiles to refine the estimates of housing market impairment.[13]

2.4 Local Sea-Level Projections and Data

2.4.1 Local Sea-Level Projections

Coastal flooding occurs at the land-water interface, and, therefore, local information on the relative vertical movement between the land and water surface is required to model future flood risk and associated housing market impairment. Local sea-level projections account for both potential vertical movement in the land topography and changes in water levels. Local land topography can uplift or subside due to both long and short-term local or regional processes that include loss of glacial ice (glacial isostatic adjustment), human extraction of ground water,

[12] We convert all DEMs from the original vertical datum of the North American Vertical Datum of 1988 (NAVD88) and vertical units of meters to the same vertical datum (MHHW) and vertical units (feet) as the Sea Level Rise Viewer inundation shapefiles using NOAA's VDatum conversion tool (NOAAe, 2019).

[13] Any property that has a negative DEM elevation is excluded from the sample, as this implies the property may already be inundated at high tide. This rare occurrence of a negative DEM elevation could be due to conversion of the DEM vertical datum from NAVD88 to MHHW or an inaccurate spatial reference on the property. We exclude roughly 3300 properties (0.06% of the property sample) in this fashion.

and tectonic processes (Horton et al., 2015; Church, 2013). Changes in local water levels can also deviate from the global mean due to differences in ocean temperature, salinity, and currents (Nerem and Mitchum, 2001; Cazenave and Nerem, 2004; Lombard et al., 2005; Milne et al., 2009). Additional regular fluctuations of the climate system known as oscillations or "modes", can also affect local sea-levels. For example, the local sea-level in NYC is affected by climate modes such as the North Atlantic Oscillation (Barnston and Livezey, 1987; Hurrell, 1995; Han et al., 2017) and the Atlantic Multidecadal Oscillation (Trenberth and Shea, 2006; Wang and Zhang, 2013; Han et al., 2017). Additional research is needed to understand how these climate modes can affect regional and local sea-level projections (Han et al., 2017). These regional and local factors that affect the relative vertical movement between the land and water surfaces necessitate using local SLR projections to accurately model future coastal flooding from SLR and associated individual housing market impairments.

2.4.2 Local Sea-Level Rise Data

We use local sea-level projections for Permanent Service for Mean Sea-Level (PSMSL) tidal stations from Kopp et al. (2014, 2017) to estimate a range of future housing value impairments. Our analysis uses SLR projections from 2020-2100 for three different climate scenarios (i.e., RCP 2.6, 4.5. and 8.5) and includes the SLR uncertainty around each of the RCP scenarios (0.10, 0.25, 0.50, 0.75, and 0.90 percentiles). These SLR projections account for the wide-range of climate and sea-level uncertainty, allowing for an analysis of SLR housing impairment at the local level, while remaining climate scenario agnostic.[14] We determine the local SLR projections based on the nearest PSMSL tidal station to the centroid of the ZIP code shapefile. These local SLR projections then determine the potential year of inundation and impairment value for properties in a given ZIP code. Finally, we aggregate the housing market impairment estimates

[14]The local SLR projections in Kopp et al. (2014) may underestimate SLR as they do not include feedback loops in Antarctic ice sheet melt included in Deconto and Pollard (2016). We provide an aggregated impairment analysis for the 15 metros under Deconto and Pollard (2016) in the supplemental material section 6.3 of this paper.

to both the individual metro level and across all 15 U.S. metros for each RCP scenario.

3 Results

Our results provide a range of housing market value impairment estimates for 15 major U.S. coastal metros and the associated timing of those impairments. We provide an aggregated estimate of the range of housing market value impairment for the U.S. coastal region based on our sample of 15 major coastal cities. We also highlight the results of two select cities with different terrain and housing characteristics (NYC and Miami). Specific impairment analyses for the remaining metros are provided in the supplemental material.

3.1 15 U.S. Metro Total

Our aggregated results for the U.S. coastal region comprise 15 major coastal metros (including NYC and Miami).[15] These results incorporate local geographic and housing market factors, which contribute to unique impairment profiles within the individual cities. Our aggregated sample (i.e., all 15 metros) for the U.S. has roughly 5.4 million housing units and our compiled national results have a smoother impairment profile than the individual cities. Additionally, our analysis focuses on larger at risk metros, which provide a crude estimate for U.S. housing market value at risk from SLR through 2100 (see figure 1, tile a-d).

We estimate that within these 15 major U.S. coastal cities, 8,900 (range 2,000 to 27,700), 12,200 (range 3,200 to 38,700), 22,000 (range 6,700 to 77,200) properties will be inundated by 2100 at the 50^{th} percentile under RCP 2.6, 4.5, and 8.5, respectively, which equates to 0.2% (range 0.04-0.5%), 0.2% (range 0.06-0.7%), and 0.4% (range 0.1-1.4%) of our 5.4 million property

[15]The 15 metros in this analysis are: NYC, Washington D.C. area (i.e., Washington D.C., Alexandria, Arlington, Bethesda, Chevy Chase, Hyattsville, Silver Spring, etc...), Norfolk (i.e., Norfolk, Portsmouth, and Virginia Beach), Wilmington, Charleston, Jacksonville, Fort Lauderdale, Miami (i.e., Miami and Miami Beach), Mobile, Galveston, Houston (i.e., Houston, Pasadena, La Porte, and Galena Park) San Diego, Los Angeles (i.e., Los Angeles and Long Beach), San Francisco Bay Area (i.e., San Francisco, San Jose, Oakland, Fremont, Hayward, Sunnyvale, Santa Clara, Berkeley, Daly City, Alameda etc...), and Seattle. See supplemental material for summary statistics and detailed impairment results on each individual metro.

sample (figure 1, tile c). For those properties that are identified as impaired (inundated) by 2100, the average year of impairment is 2072 (standard deviation 18 years), 2074 (standard deviation 18 years), and 2077 (standard deviation 17 years) under RCP 2.6, 4.5, and 8.5, respectively.

Measuring housing market value at risk for our 15 city sample through 2100, we estimate that $5.0 billion (range $0.9 to $17.3 bil), $7.0 billion (range $1.5 to $25.0 bil), and $13.7 billion (range $3.8 to $50.6 bil) of total housing value is at risk under the low (RCP 2.6), medium (RCP 4.5), and high (RCP 8.5) GHG concentration scenarios, respectively. Under these scenarios, this equates to 0.2% (range 0.03-0.6%), 0.2% (range 0.05-0.8%), and 0.4% (0.1-1.61%) of our estimated $3.1 trillion housing market (see tile b and d).

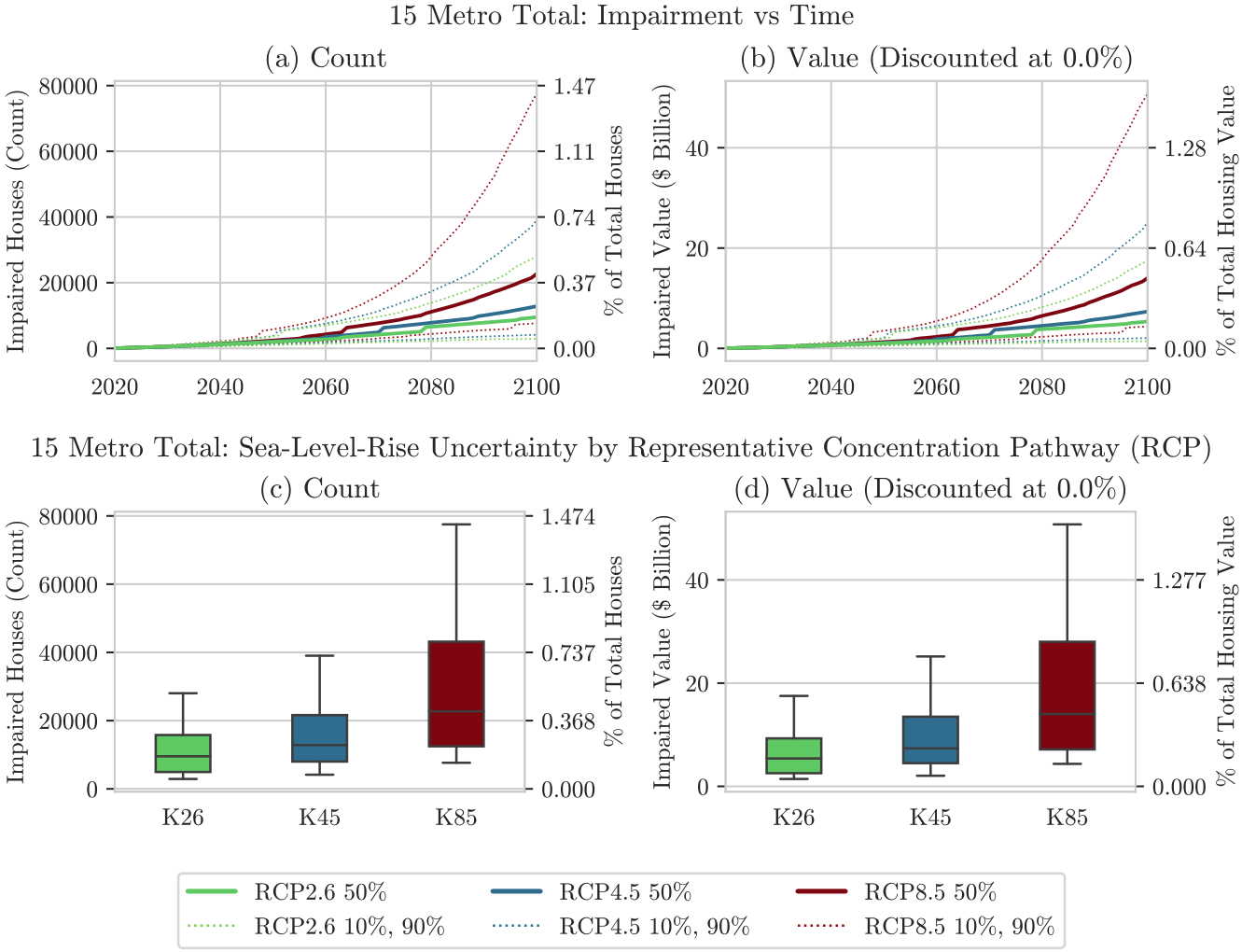

Figure 1: 15 Metro Summary

Across our 15 metro sample, we determine that the Galveston, TX, Charleston, SC, and Norfolk, VA have the largest percent impairment values for RCP scenarios 2.6, 4.5, and 8.5, respec-

tively. Washington D.C., Seattle, WA, and Houston, TX have the smallest percent impairment values for RCP scenarios 2.6, 4.5, and 8.5, respectively. The "Metro Summary Statistics and Results" table (see supplemental material) provides a detailed summary of impairment counts and values through 2100 across the 15 metros for local SLR projections associated with the 50^{th} percentiles of RCP scenarios 2.6, 4.5, and 8.5.

3.2 New York City

NYC is the most populous city in the U.S. and is expected to experience local SLR that exceeds the global average due to global, regional, and local processes (Amante, 2019; Kopp et al., 2017). Figure 2 (tile a) shows a map of greater NYC and the land area that falls within 1.8m (6ft) of local SLR. SLR projections for each climate scenario (RCP 2.6, 4.5, and 8.6) and their respective uncertainty bands between 10^{th} and 90^{th} percentiles are outlined in figure 2 (tile b). Local sea-level is expected to increase by 0.60m, 0.73m, and 0.94m through 2100 under the low (RCP 2.6), medium (RCP 4.5), and high (RCP 8.6) GHG concentration scenarios (50^{th} percentile), respectively (Kopp et al., 2017). Our housing sample for NYC has roughly 659,000 unique single-family houses compared with an estimated population of approximately 8.4 million people (Census, 2020). Due to a relatively low concentration of single-family houses in the metro, a positively sloping topographic gradient, and few homes in areas at risk of SLR (directly on the coast with low elevation), we find limited risk to NYC 's single family housing market through 2100 (see discussion section for a more detailed description of local factors contributing to these impairments).

We estimate that 256 (range 16 to 1,645), 496 (range 47 to 2,833), and 1,223 (range 132 to 7,405) properties will be inundated by 2100 in NYC at the 50^{th} percentile of RCP 2.6, 4.5, and 8.5, respectively. This equates to 0.04% (range 0.0-0.3%), 0.08% (range 0.01-0.4%), and 0.2% (0.02-1.1%) of our 659,000 property sample under those scenarios (tile e). For the properties

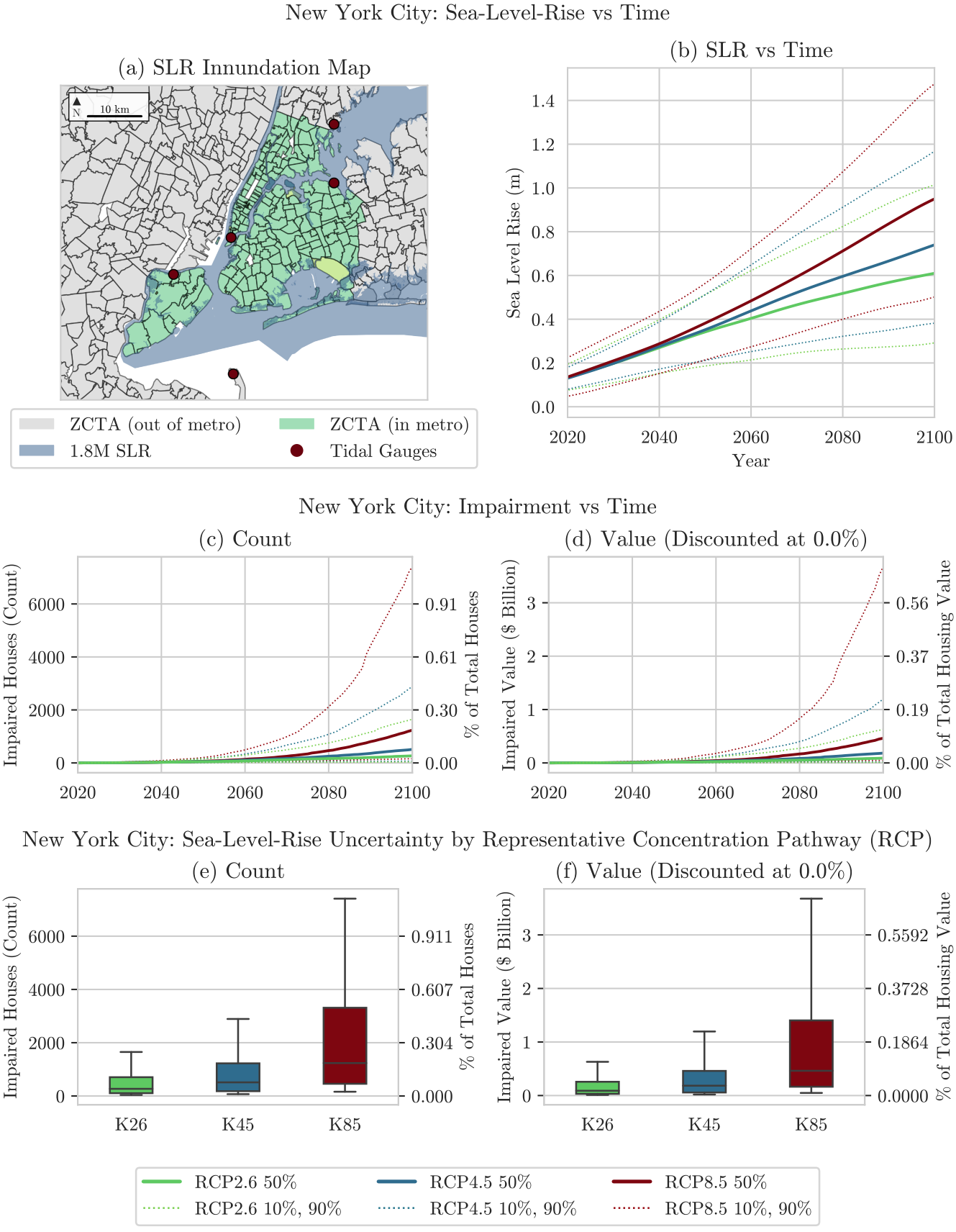

Figure 2: New York

a) Map of NYC and 1.8m (6ft) inundation area; b) SLR Path and 10-90th uncertainty band for representative concentration pathways RCP 2.6 (green), 4.5 (blue), and 8.5 (red); c) Inundation path and uncertainty bands for impaired property counts (left vertical axis) and percent of housing market (right vertical axis) for RCP 2.6, 4.5, and 8.5; d) Inundation path and uncertainty bands for total value at risk using discount rate 2.6% (left vertical axis) and percent of housing market value (right vertical axis) for RCP 2.6, 4.5, and 8.5; e)Box and whisker plot for impaired property counts through 2100 (left vertical axis) and share of housing market (right vertical axis) for RCP 2.6, 4.5, and 8.5 - lower whisker 10^{th} percentile, lower box 25th percentile, center line median, upper box 75th percentile, and upper whisker 90th percentile; f)Box and whisker plot for total value at risk through 2100 using discount rate 2.6% (left vertical axis) and percent of housing market value (right vertical axis) for RCP 2.6, 4.5, and 8.5 – lower whisker 10th percentile, lower box 25th percentile, center line median, upper box 75th percentile, and upper whisker 90th percentile. K26, K45, and K85 refer to results associated with RCP2.6, RCP4.5, and RCP 8.5 from (Kopp et al., 2014, 2017).

that are identified as impaired (inundated) by 2100, the average year of impairment is 2073 (standard deviation 18 years), 2077 (standard deviation 16 years), and 2082 (standard deviation 14 years) under RCP 2.6, 4.5, and 8.5, respectively.

Measuring housing market value at risk for NYC through 2100, we estimate that $0.09 billion (range $0.01 to $0.6 bil), $0.2 billion (range $0.01 to $1.2 bil), and $0.5 billion (range $0.04 to $3.7 bil)) of total housing value is at risk under the low (RCP 2.6), medium (RCP 4.5), and high (RCP 8.5) GHG concentration scenarios, respectively. Under these scenarios, this equates to 0.02% (range 0-0.12%), 0.03% (range 0-0.2%), and 0.09% (range 0.01-0.7%) of our estimated $537 billion NYC housing market (see tile d and f).

3.3 Miami and Miami Beach

Miami and Miami Beach (combined as "Miami") is also expected to experience local SLR rates that exceed the global average (Kopp et al., 2017). The image in figure 3 (tile a) shows a map of greater Miami area and the land area that falls within 1.8m (6ft) of local SLR. The results indicate that Miami's land area is more at risk of SLR inundation than NYC. In the same manner as the results presented in section 3.2 (NYC), SLR projections for each climate scenario (RCP 2.6, 4.5, and 8.6) and their respective uncertainty bands are outlined in figure 3 (tile b). Local SLR is expected to increase by 0.55m, 0.68m, and 0.84m through 2100 in Miami at the 50^{th} percentile under the low (RCP 2.6), medium (RCP 4.5), and high (RCP

8.6) GHG concentration scenarios, respectively (Kopp et al., 2017). Our housing sample for Miami has roughly 331,000 unique single-family homes compared with an estimated population of approximately 563,000 (Census, 2020). Miami has a relatively high concentration of single-family houses, flat topography with numerous low-lying areas, and a concentration of homes in areas prone to SLR inundation (on the coast at lower elevations). We find substantial risk to Miami's housing market through 2100 (see discussion section for a more detailed description of local factors contributing to these impairments).

We estimate that 199 (range 11 to 3,377), 588 (range 20 to 5,857), and 2,584 (range 107 to 12,984) properties will be inundated by 2100 in Miami at the 50^{th} percentile under RCP 2.6, 4.5, and 8.5, respectively. This equates to 0.06% (range 0-1.0%), 0.2% (range 0.1-1.8%), and 0.8% (range 0.03-3.9%) of our 331,000 property sample under those scenarios (tile e). For the properties that are identified as impaired (inundated) by 2100, the average year of impairment is 2082 (standard deviation 15 years), 2087 (standard deviation 13 years), and 2088 (standard deviation 10 years) under RCP 2.6, 4.5, and 8.5, respectively.

Measuring housing market value at risk for Miami through 2100, we estimate that $0.3 billion (range $0.02 to $3.5 bil), $0.7 billion (range $0.04 to $5.9 bil), and $2.7 billion (range $0.2 to $13.2 bil) of total housing value is at risk under the low (RCP 2.6), medium (RCP 4.5), and high (RCP 8.5) GHG concentration scenarios, respectively. Under these scenarios, this equates to 0.2% (range 0.02-2.7%), 0.5% (range 0.03-4.5%), and 2.1% (range 0.1-10%) of our estimated $131 billion Miami housing market (see tile d and f).

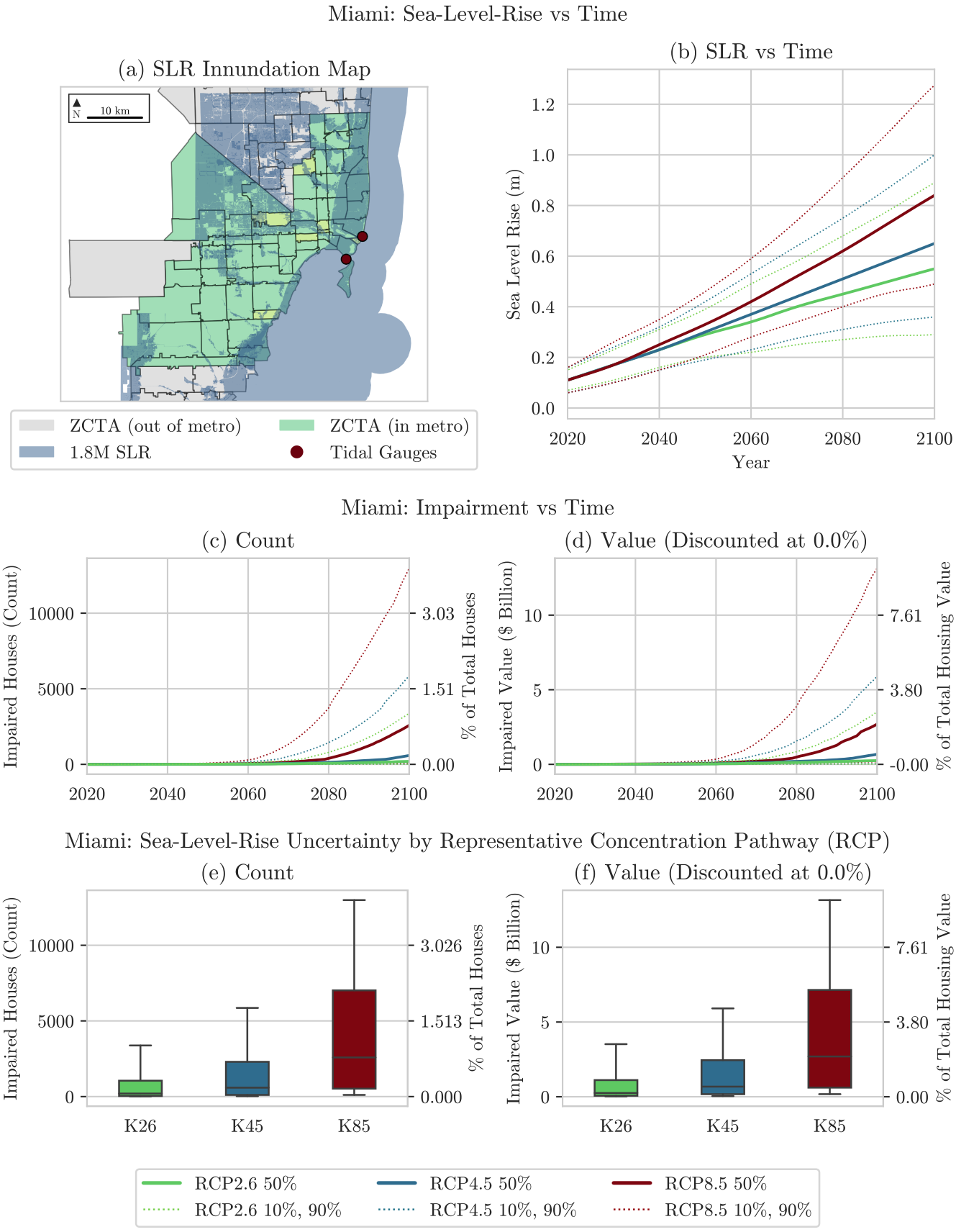

Figure 3: Miami

4 Discussion

Overall, our estimates for the direct economic costs from SLR across the 15 metro U.S. sample represent a relatively small direct economic effect to coastal single family home markets through the end of the century. Median total impairments through 2100 range between a 9,000 to 22,000 properties, $5.0 billion to $13.7 billion (RCP 2.6 to 8.5), or between 0.2% and 0.4% of our sample for both counts and value. Numerous factors contribute to our conservative lower-bound estimates for SLR impairments. We restrict our housing sample to single family, townhouses, and buildings with 4 or less units. Roughly 25% of residences in the U.S. are condominiums or multifamily with greater than 4 units. In some states, such as New York and Florida, the proportion of residences that are condominiums or multifamily is approximately 35% (Census, 2011).[16] Additionally, our analysis focuses on local SLR projections based on Kopp et al. (2014, 2017), which may underestimate other global risk factors such as accelerated Antarctic ice sheet melt (Deconto and Pollard, 2016; Kopp et al., 2017). See supplemental material section 6.3 for a sensitivity analysis of our 15 metro totals for Deconto and Pollard (2016) SLR risk compared to Kopp et al. (2014). Lastly, our analysis focuses solely on the direct economic cost from terminal impairment from local SLR, which is just one component of total costs from rising seas. Increases in nuisance flooding and storm surge inundation enhanced from SLR, as well as changing risk perceptions, would add additional costs associated with rising seas (Amante, 2019; Bernstein et al., 2019).

Despite the conservative nature of our SLR impairment estimates, our analysis provides useful insights on SLR impairment risk across the U.S. These insights include understanding differences across metros and how housing density may affect impairment at the local level. Furthermore, we generate an understanding of risk asymmetry across climate change scenarios.

[16] We exclude apartments, multifamily, and condominiums from our sample as these types of residential properties are more similar to commercial properties and are different markets than single family and townhouses. Additionally, due to size (multi-story or larger complexes) and construction in these of these types of residential building, SLR inundation may affect these properties differently. Investment for mitigation may also be applied to these types of properties in a different way than for single family homes.

Lastly, we provide estimates for the timing of SLR impairment, which may prove useful for city planners and governments.

4.1 Housing Markets and Population

Our analysis indicates that proximity of low-lying areas to the coast, the structure of coastal housing markets, and the locations of single-family houses all contribute to housing market impairment within a city. Proximity to the coast has generally been considered a positive amenity that typically drives up home prices (Benson et al., 1998). However, as expected, the proximity of single-family houses to the coast, especially in low-lying areas along the Atlantic and Gulf Coasts, makes houses more prone to SLR inundation. For example, in our Miami housing sample, 6,100 houses (1.9% of our Miami housing sample) reside within 1m of the current sea-level. In contrast, only 1,800 houses in NYC (0.3% of our NYC housing sample) reside within 1m of current sea-level. The Miami metro has a much greater concentration of properties in close proximity to low-lying areas near the coast compared to NYC, which would make those properties in Miami more subject to SLR inundation. This is precisely what we observe in our results for NYC and Miami (i.e., greater relative housing market impairment from SLR in Miami compared to NYC). Unsurprisingly, the closer a city's real estate is to sea-level, the more subject that housing market is to potential impairment from SLR inundation.

Another feature of a coastal metro that affects housing market impairments from SLR inundation is the concentration of single-family houses. Some larger, more densely populated cities, such as NYC, have a much smaller share of their population living in single-family houses than in less dense cities, such as Miami or Houston. NYC has an estimated population of 8.4 million with 3.2 million households (Census, 2020). Our housing sample for NYC contains roughly 659,000 single family homes. In contrast, Miami's estimated population is 563,000 people, with 215,000 households (Census, 2020). Our housing sample for the Miami area contains roughly

331,000 single family homes. Miami has a much higher concentration of single-family houses per capita (1.5 houses/household) than NYC (0.2 houses/household), as more people in NYC are living in commercial apartment buildings or condos (which are excluded from our housing sample). Thus, coastal metros with a greater concentration of single-family houses are more prone to housing market impairment in our analysis.

4.2 Uncertainty and Risk Asymmetry

Two consistent features within our results, both at the metro and national level, are large uncertainties in housing market impairment and asymmetry of impairment risk. First, our results consistently suggest a large impairment uncertainty within each GHG concentration scenario, such that uncertainty within each GHG scenario is larger on average than the uncertainty we find between each of the GHG scenarios (see figures 2 and 3, tile f). Using Miami's high GHG scenario (RCP 8.5) as an example, the range of impairment risk (90^{th} - 10^{th}) is $13 billion (9.9% of total market value). The range of impairment risk is $2.4 billion (1.8% of total market value) between GHG concentration scenarios (RCP 2.6 to RCP 8.5 at the 50^{th} percentile), which is a much smaller range of impairment uncertainty than within the individual GHG scenario RCP 8.5 itself. This speaks to the critical importance of including SLR uncertainty distributions when estimating value impairments within a given RCP scenario. By excluding the complete probability distributions of local SLR projections associated with each RCP scenario, any value impairment analysis would overlook a highly important source of uncertainty.

Second, our results indicate consistent asymmetric risk to the upside (positive skewness) across the three GHG concentration scenarios (RCP 2.6, 4.5, and 8.5). The upper portion of the box (50^{th} to 75^{th} percentile) is larger than the lower portion of the box (25^{th} to 50^{th} percentile). Additionally, the upper tails (to the 90^{th} percentile) are longer than the lower-tails (to the 10^{th} percentile) (see figures 1, tiles c and d), indicating strong positive risk asymmetry, which

suggests more potential impairment under a given GHG scenario than the median percentiles would indicate. Positive risk asymmetry provides some motivation for future cuts in GHG emissions, which may temper climate risk and nudge the global climate towards lower risk GHG concentration scenarios (Hausfather and Peters, 2020; IPCC, 2014). Future energy and carbon policies aside, taking into consideration the positive risk asymmetry is an important factor when assessing the overall risks coastal communities face from SLR through the end of the century.

4.3 Policy Implications, Inundation Timing, and Economic Risk

The results from our metro level analysis of SLR uncertainty and housing market impairment risk provide a series of useful insights for governments, policymakers, financial institutions, and those living in coastal communities. We estimate SLR impairments at the property and metro level, producing impairments for both property counts and value at risk, which can help expose distributional effects of SLR risk across metros. Our impairment estimate over time shed light on when SLR inundation is likely to manifest for different cities and can serve as an approximation of risk across the coastal U.S. (i.e., total of 15 coastal metros). Finally, our results may have implications for public finances and mortgage markets.

Firstly, our measures of inundated property counts (figure 1, tile a and c) and value impairments (figure 1, tile b and d) provide two different perspectives on risk exposures and can serve as an indicator of the distributional effects of SLR inundation risk. Property count inundation gives an estimate for individuals at risk (households), whereas the dollar values indicates whether higher or lower value real estate is exposed. For example, property counts and value exposures (as a share of metro totals) are roughly the same for NYC through 2100 (figure 2). Whereas Miami has lower counts and higher values (as a percent of the total metro) (figure 3). This suggests that on average Miami has relatively higher value single family homes exposed to SLR than NYC. Exposing the distributional effects of SLR risk across housing markets (e.g., high

value homes versus low value homes) can be useful when trying to understand who is most at risk from SLR inundation.

Secondly, estimating the timing of housing impairment exposures from SLR at the metro level may prove useful for city planners and local governments charged with implementing longer-term risk mitigation strategies through physical infrastructure investment (e.g., levees, seawalls, etc.) or some policy action (e.g., urban planning decisions or carbon policies). Both of these actions require a comprehensive understanding and accounting of risks over time. By analyzing 15 distinct metros in the U.S., our research identifies the unique timing of risks a city may be facing from local sea-level rise. As an illustrative example, figure 4 shows the cumulative median housing impairment (counts and values) under the medium GHG concentration scenario (RCP 4.5) through 2100 for NYC, Miami, Galveston, and Norfolk. These cumulative distribution functions provide an insight into when SLR risk might take place in a given metro relative to other metros. In Norfolk, 20% of properties are inundated by 2043, compared to 20% of properties being inundated by 2059, 2060, and 2078 in Galveston, NYC, and Miami, respectively. Comparing Norfolk and Miami, it is evident that SLR impairment takes place much sooner in Norfolk than Miami. The Galveston and NYC CDF curves require a more nuanced comparison. While both metros face a similar trajectory for impairment timing (i.e., 20% of their exposed properties become inundated by around 2060), their relative overall risk exposure is strikingly different, with 15.6% of properties inundated in Galveston through 2100 compared to a mere 0.1% in NYC. From this perspective, our results not only provide total measures of housing at risk from SLR at the local level, but also gives a sense of when impairments take place over the next 80 years, across these metros. [17]

The timing of SLR risk is important for city planners, as this information can help improve decision-making regarding where and when infrastructure could be built to reduce risks from

[17]Galveston and Norfolk are two of the more at risk metros in our sample, facing roughly 15.6% and 0.6%, respectively, of properties by count at risk from SLR through 2100 under the medium GHG scenario (RCP 4.5). This is compared to 0.1% and 0.2% for NYC and Miami, respectively. See supplemental material for a detailed description of Galveston and Norfolk results.

SLR. By producing impairment estimates over time, we provide a conservative measure of cost from SLR inundation that urban planners can compare to the benefits of mitigation (balancing costs and benefits), helping them determine optimal mitigation policies for their specific metro areas (Guthrie, 2020).[18]

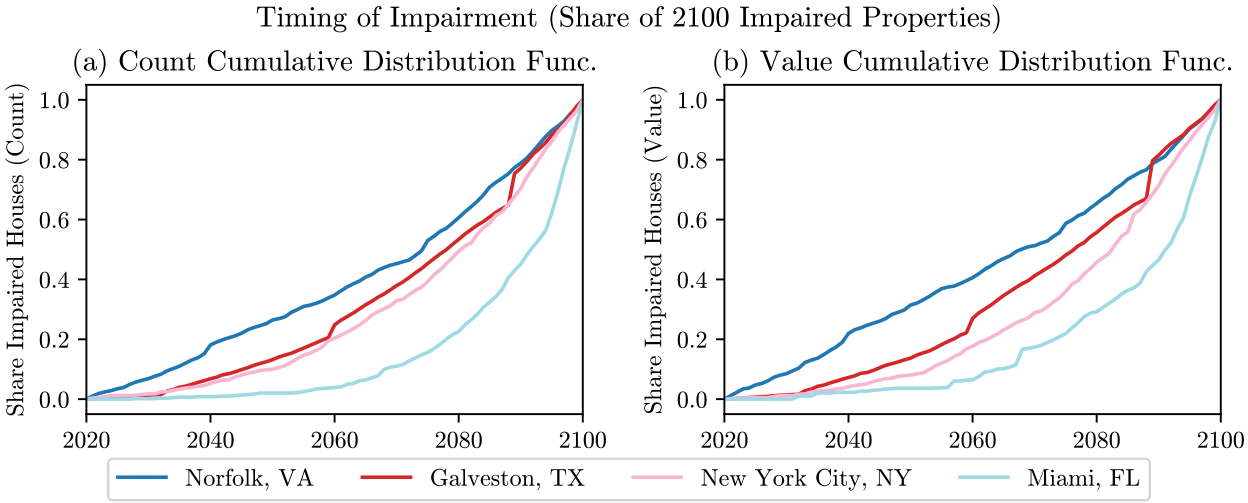

Figure 4: Cumulative Distribution Function (CDF) of Housing Impairment under RCP 4.5 (Kopp et al., 2014, 2017); Left side: CDF for property impairment counts; Right side: CDF for property value impairment.

Perhaps a less obvious implication for our research is the risk to city finances or national disaster programs from future SLR inundation. Our time series of local impairment estimates provides a rough proxy for erosion of the tax base over time within a city. As neighborhoods within a city face SLR inundation, out-migration may increase in the most at-risk areas. This out-migration, may in turn, erode the tax base for a city at a time when it needs to increase spending on infrastructure and risk mitigation. On a national scale, these same dynamics pose potential problems for the viability of disaster relief programs. As the sea-level rises and large areas of coastal cities are at greater risk from nuisance flooding and storm surge inundation, the cost to national flood insurance programs, as well as disaster relief programs, may also rise. Similar to local municipalities, higher costs may put significant strain on national flood insurance and disaster relief programs.

[18]See section 2.2 and supplemental material for a more detailed description on why accurately measuring the timing of risk is important, as well as the implications of time value of money for long-term decision making.

Lastly, our results on housing market value at risk have links to the financial sector, bond markets, and potentially financial regulatory agencies. In the same way that our housing impairment estimates provide a proxy for the erosion of a tax base at the local level, these results also provide insight into the risks local mortgage markets may face in the wake of SLR inundation. Coincident with the housing value at risk from SLR is the potential strain that may emerge in home mortgage markets. Roughly 70 percent of homeowners have a mortgage on their property (Zillow, 2013), and a negative effect on housing values may cause disruptions to home mortgage markets. Our results indicate that a majority of risk from SLR takes place toward the end of the century, which is outside the window of a standard 30-year mortgage. However, if these risks were embodied in housing values, this may reduce the creditworthiness of some outstanding mortgages as the loan to value ratios might decline.[19] Even if a house is not currently prone to coastal inundation, future SLR or changes in risk perceptions may pose challenges for selling homes or refinancing a mortgage due to concerns about the viability of that property. These secondary and more investment focused risks may be of concern to homeowners, lenders, and financial regulators. Quantifying these risks to the home mortgage markets and potential spillovers into financial institutions (including insurers and re-insurers) is beyond the scope of this project, but this is fruitful ground for additional research.

5 Conclusion

We estimate a range of housing market value impairments at the property and city level for 15 U.S. coastal metros through 2100, accounting for local topography and local SLR estimates that incorporate several sources of uncertainty. We utilize a novel spatial matching methodology, which allows us to estimate the timing of SLR inundation at the property level with refined temporal granularity. These property impairment estimates are then summed to create metro

[19]Recent survey evidence would suggest that coastal homeowners that are most at risk are reluctant to acknowledge the risks they face from SLR and coastal inundation (Palm and Bolsen, 2020).

level SLR impairment estimates over time. Our median aggregate (i.e., all 15 metros) results indicate that 9,000, 12,000, and 22,000 properties will be inundated by 2100 under the three GHG scenarios analyzed (i.e, low RCP 2.6, medium RCP 4.5, and high RCP 8.5) which equates to 0.2%, 0.2% and 0.4% of our 5.4 million property sample, respectively. These results indicate that $5.0 billion, $7.0 billion and $13.7 billion or 0.2%, 0.2% and 0.4% of value under those scenarios (RCP 2.6, 4.5, and 8.5) is at risk from SLR inundation through 2100.

With nearly 40 percent of the U.S. population living along the coast, SLR is a substantial threat to coastal communities. Our analysis provides insight into housing market value at risk for major coastal cities. These results provide a useful model for the timing of losses and asymmetry of risk from SLR inundation, which can help inform policy makers, city officials, investors, and bankers in cost-benefit decision-making related to mitigation, adaptation, and remediation policies at the local and national level. Ultimately, our research provides a useful measure for the direct economic costs from SLR inundation within coastal housing markets. Quantifying the range of future housing market value impairment is a first step in mitigating economic risks from SLR inundation. Our estimates, although only a minor portion of the total costs associated with climate change, contribute to the proper accounting of climate-related risks.

References

Amante, C. (2019). Uncertain seas: probabilistic modeling of future coastal flood zones. *International Journal of Geographical Information Science*, 33:1–30.

Amante, C. J. (2018). Estimating coastal digital elevation model uncertainty. *Journal of Coastal Research*, pages 1382–1397.

Amante, C. J. and Eakins, B. W. (2016). Accuracy of interpolated bathymetry in digital elevation models. *Journal of Coastal Research*, 76(SI):123–133.

Arrow, K. J., Cropper, M. L., Gollier, C., Groom, B., Heal, G. M., Newell, R. G., Nordhaus, W. D., Pindyck, R. S., Pizer, W. A., Portney, P. R., Sterner, T., Tol, R. S. J., and Weitzman, M. L. (2013a). Determining benefits and costs for future generations. *Science*, 341:349–350.

Arrow, K. J., Cropper, M. L., Gollier, C., Groom, B., Heal, G. M., Newell, R. G., Nordhaus, W. D., Pindyck, R. S., Pizer, W. A., Portney, P. R., Sterner, T., Tol, R. S. J., and Weitzman, M. L. (2013b). How should benefits and costs be discounted in an intergenerational context? Discussion Paper 12-53, Resources for the Future.

Auffhammer, M. (2018). Quantifying economic damages from climate change. *Journal of Economic Perspectives*, 32(4):33–52.

Bansal, R., Ochoa, M., and Kiku, D. (2016). Climate change and growth risks. Working Paper 23009, National Bureau of Economic Research.

Barnston, A. G. and Livezey, R. E. (1987). Classification, seasonality and persistence of low-frequency atmospheric circulation patterns. *Monthly Weather Review*, 115(6):1083–1126.

Beltrán, A., Maddison, D., and Elliott, R. (2019). The impact of flooding on property prices: A repeat-sales approach. *Journal of Environmental Economics and Management*, 95:62 – 86.

Benson, E., Hansen, J., Schwartz, Jr, A., and Smersh, G. (1998). Pricing residential amenities: The value of a view. *The Journal of Real Estate Finance and Economics*, 16:55–73.

Bernstein, A., Gustafson, M., and Lewis, R. (2019). Disaster on the horizon: The price effect of sea level rise. *Journal of Financial Economics*, 134(2):253–272.

Black Rock (2019). Getting physical: Assessing climate risks. Black Rock. April. https://www.blackrock.com/us/individual/insights/blackrock-investment-institute/physical-climate-risks.

BOE (2019). Bank of england consults on its proposals for stress testing the financial stability implications of climate change. Bank of England. December. https://www.bankofengland.co.uk/news/2019/december/boe-consults-on-proposals-for-stress-testing-the-financial-stability-implications-of-climate-change.

Brackenborough, S., Mclean, T., and Oldroyd, D. (2001). The emergence of discounted cash flow analysis in the tyneside coal industry c. 1700-1820* 1. *British Accounting Review*, 33:137–155.

Campiglio, E., Dafermos, Y., Monnin, P., ryan collins, J., Schotten, G., and Tanaka, M. (2018). Climate change challenges for central banks and financial regulators. *Nature Climate Change*, 8.

Carney, M. (2015). Breaking the tragedy of the horizon - climate change and financial stability. Remarks by Mark Carney, Governor of the Bank of England and Chairman of the Financial Stability Board, at Lloyd's of London. September.

Cazenave, A. and Nerem, R. S. (2004). Present-day sea level change: Observations and causes. *Reviews of Geophysics*, 42(3).

Census (2011). Historical census of housing tables. United States Census Bureau. October. www.census.gov/hhes/www/housing/census/historic/units.html.

Census (2020). Quick facts united states. United States Census Bureau. January. https://www.census.gov/quickfacts/.

Church, J. (2013). Sea level change. *In: T.F. Stocker, et al., eds. Climate Change 2013 – The Physical Science Basis: Working Group I Contribution to the Fifth Assessment Report of the Intergovernmental Panel on Climate Change*, page 1137–1216.

CoBank (2019). Rural industries and climate change. CoBank. November. https://www.cobank.com/knowledge-exchange/general/rural-industries-and-climate-change.

Colacito, R., Hoffman, B., Phan, T., and Sablik, T. (2018). The Impact of Higher Temperatures on Economic Growth. *Richmond Fed Economic Brief*.

Deconto, R. M. and Pollard, D. (2016). Contribution of antarctica to past and future sea-level rise. *Nature*, 531:591–597.

Drupp, M. A., Freeman, M. C., Groom, B., and Nesje, F. (2018). Discounting Disentangled. *American Economic Journal: Economic Policy*, 10(4):109–134.

Fankhauser, S. (1995). Protection versus retreat: The economic costs of sea-level rise. *Environment and Planning A: Economy and Space*, 27(2):299–319.

FSB-TCFD (2017). Recommendations of the task force on climate related financial disclosures. Financial Stability Board. June. https://www.fsb-tcfd.org/publications/final-recommendations-report/.

Gesch, D. B. (2009). Analysis of lidar elevation data for improved identification and delineation of lands vulnerable to sea-level rise. *Journal of Coastal Research*, pages 49–58.

Gesch, D. B. (2018). Best practices for elevation-based assessments of sea-level rise and coastal flooding exposure. *Frontiers in Earth Science*, 6:230.

Ghanbari, M., Arabi, M., Obeysekera, J., and Sweet, W. (2019). A coherent statistical model for coastal flood frequency analysis under nonstationary sea level conditions. *Earth's Future*, 7(2):162–177.

Giglio, S., Maggiori, M., and Stroebel, J. (2014). Very Long-Run Discount Rates . *The Quarterly Journal of Economics*, 130(1):1–53.

Giglio, S., Maggiori, M., Stroebel, J., and Weber, A. (2015). Climate change and long-run discount rates: Evidence from real estate. Working Paper 21767, National Bureau of Economic Research.

Gillies, S. et al. (2013–). Rasterio: geospatial raster i/o for Python programmers.

Gillingham, K. and Stock, J. H. (2018). The cost of reducing greenhouse gas emissions. *Journal of Economic Perspectives*, 32(4):53–72.

Goldman Sachs (2019). Taking the heat: Making cities resilient to climate change. Goldman Sachs. September. https://www.goldmansachs.com/insights/pages/taking-the-heat.html.

Gordon, M. J. (1963). Optimal investment and financing policy. *The Journal of Finance*, 18(2):264–272.

Guthrie, G. (2020). Adapting to rising sea levels: How short-term responses complement long-term investment. *Available at SSRN: https://ssrn.com/abstract=3571033*.

Han, W., Meehl, G. A., Stammer, D., Hu, A., Hamlington, B., Kenigson, J., Palanisamy, H., and Thompson, P. (2017). Spatial patterns of sea level variability associated with natural internal climate modes. *Surveys in Geophysics*, 38:217–250.

Hauer, M., Evans, J., and Mishra, D. (2016). Millions projected to be at risk from sea-level rise in the continental united states. *Nature Climate Change*, 6.

Hausfather, Z. and Peters, G. P. (2020). Emissions – the 'business as usual' story is misleading. *Nature*, 577:618–620.

Hawkins, E. and Sutton, R. (2009). The potential to narrow uncertainty in regional climate predictions. *Bulletin of the American Meteorological Society*, 90.

Heal, G. and Millner, A. (2014). Reflections: Uncertainty and decision making in climate change economics. *Review of Environmental Economics and Policy*, 8:120–137.

Horton, R., Little, C., Gornitz, V., Bader, D., and Oppenheimer, M. (2015). New york city panel on climate change 2015 report chapter 2: Sea level rise and coastal storms. *Annals of the New York Academy of Sciences*, 1336(1):36–44.

Hsiang, S. and Kopp, R. E. (2018). An economist's guide to climate change science. *Journal of Economic Perspectives*, 32(4):3–32.

Hunter, J. D. (2007). Matplotlib: A 2d graphics environment. *Computing in Science & Engineering*, 9(3):90–95.

Hurrell, J. W. (1995). Decadal trends in the north atlantic oscillation: Regional temperatures and precipitation. *Science*, 269(5224):676–679.

IPCC (2014). Ar5 synthesis report: Climate change 2014. Intergovernmental Panel on Climate Change.

Jordahl, K., den Bossche, J. V., Wasserman, J., McBride, J., Fleischmann, M., Gerard, J., Tratner, J., Perry, M., Farmer, C., Hjelle, G. A., Gillies, S., Cochran, M., Bartos, M., Culbertson, L., Eubank, N., Bilogur, A., and maxalbert (2020). geopandas/geopandas: v0.7.0.

Kopp, R. E., DeConto, R. M., Bader, D. A., Hay, C. C., Horton, R. M., Kulp, S., Oppenheimer, M., Pollard, D., and Strauss, B. H. (2017). Evolving understanding of antarctic ice-sheet physics and ambiguity in probabilistic sea-level projections. *Earth's Future*, 5(12):1217–1233.

Kopp, R. E., Horton, R. M., Little, C. M., Mitrovica, J. X., Oppenheimer, M., Rasmussen, D. J., Strauss, B. H., and Tebaldi, C. (2014). Probabilistic 21st and 22nd century sea-level projections at a global network of tide-gauge sites. *Earth's Future*, 2(8):383–406.

Li, X., Rowley, R. J., Kostelnick, J. C., Braaten, D., Meisel, J., and Hulbutta, K. (2009). Gis analysis of global impacts from sea level rise. *Photogrammetric Engineering & Remote Sensing*, 75(7):807–818.

Lombard, A., Cazenave, A., Traon, P.-Y., and Ishii, M. (2005). Contribution of thermal expansion to present-day sea-level change revisited. *Global and Planetary Change*, 47:1–16.

Mcalpine, S. and Porter, J. (2018). Estimating recent local impacts of sea-level rise on current real-estate losses: A housing market case study in Miami-Dade, Florida. *Population Research and Policy Review*, 37.

Milne, G., Gehrels, W., Hughes, C., and Tamisiea, M. (2009). Identifying the causes of sea-level change. *Nature Geoscience*, 2:471–478.

Moftakhari, H., AghaKouchak, A., Sanders, B., Feldman, D., Sweet, W., Matthew, R., and Luke, A. (2015). Increased nuisance flooding along the coasts of the united states due to sea level rise: Past and future. *Geophysical Research Letters*, 42(22):9846–9852.

Moss, R., Edmonds, J., Hibbard, K., Manning, M., Rose, S., Vuuren, D., Carter, T., Emori, S., Kainuma, M., Kram, T., Meehl, G., Mitchell, J., Nakicenovic, N., Riahi, K., Smith, S., Ronald, S., Thomson, A., Weyant, J., and Wilbanks, T. (2010). The next generation of scenarios for climate change research and assessment. *Nature*, 463:747–56.

Nerem, R. and Mitchum, G. (2001). *Satellite Altimetry and Earth Sciences: a handbook of techniques and applications*. Academic Press.

NGFS (2017). Network of central banks and supervisors for greening the financial system (ngfs). https://www.ngfs.net/en.

NOAAa (2019). United states billion-dollar weather and climate disasters. NOAA National Centers for Environmental Information (NCEI). https://www.ncdc.noaa.gov/billions/.

NOAAb (2019). Office of coast management: Economics and demographics. NOAA Office of Coast Management. https://coast.noaa.gov/states/fast-facts/economics-and-demographics.html.

NOAAc (2019). Tides and currents: Sea level rise trends. NOAA National Ocean Service. https://tidesandcurrents.noaa.gov/sltrends/sltrends_us.html.

NOAAd (2019). Noaa sea level rise viewer. NOAA Office of Coast Management. https://coast.noaa.gov/digitalcoast/tools/slr.html.

NOAAe (2019). Noaa vertical datum tranformation (vdatum). .version v4.0.1. National Ocean Service. https://vdatum.noaa.gov/.

Nordhaus, W. (2013). *The Climate Casino: Risk, Uncertainty, and Economics for a Warming World*. Yale University Press.

Nordhaus, W. D. (1991). To slow or not to slow: The economics of the greenhouse effect. *The Economic Journal*, 101(407):920–937.

OMB (2003). Circular a-4 regulating analysis. Office of Management and Budget. November. http:// georgewbush-whitehouse.archives.gov/omb/circulars/a004/a-4.html.

Ortega, F. and Taspinar, S. (2018). Rising sea levels and sinking property values: Hurricane Sandy and New York's housing market. *Journal of Urban Economics*, 106(C):81–100.

Palm, R. and Bolsen, T. W. (2020). Even looking at flood maps can't convince coastal residents their homes will be underwater. Fast Company.February. https://www.fastcompany.com/90461819/even-looking-at-flood-maps-cant-convince-coastal-residents-their-homes-will-be-underwater.

pandas development team, T. (2020). pandas-dev/pandas: Pandas.

Pindyck, R. S. (2019). The social cost of carbon revisited. *Journal of Environmental Economics and Management*, 94(C):140–160.

Poppenga, S. and Worstell, B. (2015). Evaluation of airborne lidar elevation surfaces for propagation of coastal inundation: The importance of hydrologic connectivity. *Remote Sensing*, 7(9):11695–11711.

Poulter, B. and Halpin, P. (2008). Raster modelling of coastal flooding from sea-level rise. *International Journal of Geographical Information Science*, 22(2):167–182.

Rao, K. (2017). Climate change and housing: Will a rising tide sink all homes? Zillow. https://www.zillow.com/research/climate-change-underwater-homes-12890/.

Rogelj, J., Meinshausen, M., and Knutti, R. (2012). Global warming under old and new scenarios using ipcc climate sensitivity range estimates. *Nature Climate Change*, 2:248–253.

Samuelson, P. (1937). A note on measurement of utility. *Review of Economic Studies*, 4(2):155–161.

Smith, J. B. and Tirpak, D. (1989). The potential effects of global climate change on the united states. Technical report, Environmental Protection Agency.

Solow, R. (1974). Intergenerational equity and exhaustible resources. *Review of Economic Studies*, 41(5):29–45.

Stern, N. (2008). The economics of climate change. *American Economic Review*, 98(2):1–37.

Sweet, W. V., Kopp, R. E., Weaver, C. P., Obeysekera, J., Horton, R. M., Thieler, E. R., and Zervas, C. (2017). Global and regional sea level rise scenarios for the united states. Technical Report NOS CO-OPS 083. National Oceanic and Atmospheric Administration.

Trenberth, K. E. and Shea, D. J. (2006). Atlantic hurricanes and natural variability in 2005. *Geophysical Research Letters*, 33(12).

USGCRP (2018). Impacts, risks, and adaptation in the united states: Fourth national climate assessment. U.S. Global Change Research Program.

USPS (2020). City state product. United States Postal Service. November. https://postalpro.usps.com/address-quality/city-state-product.

Wang, C. and Zhang, L. (2013). Multidecadal ocean temperature and salinity variability in the tropical north atlantic: Linking with the amo, amoc, and subtropical cell. *Journal of Climate*, 26:6137–6162.

Wayne, G. (2013). The beginner's guide to representative concentration pathways. *Skeptical Science*.

Wrathall, D., Mueller, V., Clark, P., Bell, A., Oppenheimer, M., Hauer, M., Kulp, S., Gilmore, E., Adams, H., Kopp, R., Abel, K., Call, M., Chen, J., deSherbinin, A., Fussell, E., Hay, C., Jones, B., Magliocca, N., Marino, E., Slangen, A., and Warner, K. (2019). Meeting the looming policy challenge of sea-level change and human migration. *Nature Climate Change*, 9(12):898–901.

Zhang, K., Li, Y., Liu, H., Xu, H., and Shen, J. (2013). Comparison of three methods for estimating the sea level rise effect on storm surge flooding. *Climatic Change*, 118(2):487–500.

Zillow (2013). 20.6 million u.s. homeowners own homes free and clear of mortgage debt. Zillow Research. January. http://zillow.mediaroom.com/2013-01-10-20-6-Million-U-S-Homeowners-Own-Homes-Free-And-Clear-Of-Mortgage-Debt.

Zillow (2018). More than 386,000 homes at risk of coastal flooding by 2050. Zillow Research and Climate Central. November. https://www.zillow.com/research/ocean-at-the-door-21931/.

6 Supplemental Material: Appendix

6.1 Combined Use of Sea Level Rise Viewer DEMs and Shapefiles

We use both the property elevation from the DEM and the location of the property within the NOAA Sea Level Rise Viewer shapefiles that considers hydrologic connectivity to refine our estimate of the timing of inundation and impairment. We first determine the most restrictive coastal inundation shapefile (i.e., lowest sea-level rise increment inundation area that the property is located within). For example, a property with an elevation from the DEM of 1.7ft may be located within the 2ft, 3ft, 4ft, ... , 10ft Sea Level Rise Viewer shapefile. We identify the most restrictive shapefile for this property to be the 2ft shapefile. In this case, we assume that the there are no large terrain or man-made barriers to inundation and estimate the year of inundation to be associated with the year at which the sea-level rise projection reaches the elevation of the property from the DEM (i.e., 1.7ft).

In other cases, a property with an elevation of 1.7ft may be located in the 4ft, 5ft, 6ft, ... , 10ft Sea Level Rise Viewer shapefile. This would occur if the property is located in an inland depression and surrounded by higher elevations from natural terrain barriers or man-made barriers such as levees that would protect the property until sea-level rises above those protective elevations. In such cases, we estimate the year of inundation to be associated with the year at which the sea-level rise projection reaches the most restrictive Sea Level Rise Viewer shapefile increment (i.e., 4ft), which gives a conservative estimate for the timing of inundation. Considering both the DEM value and Sea Level Rise Viewer shapefiles increases the granularity of our estimate of the inundation year associated with each sea-level rise projection where terrain or man-made barriers that would prevent inundation are unlikely. Figure 5 illustrates the improved precision of using both the DEM and shapefiles to determine the timing of inundation compared to only using the shapefiles.

One potential limitation of this approach is that this improved temporal granularity can lead

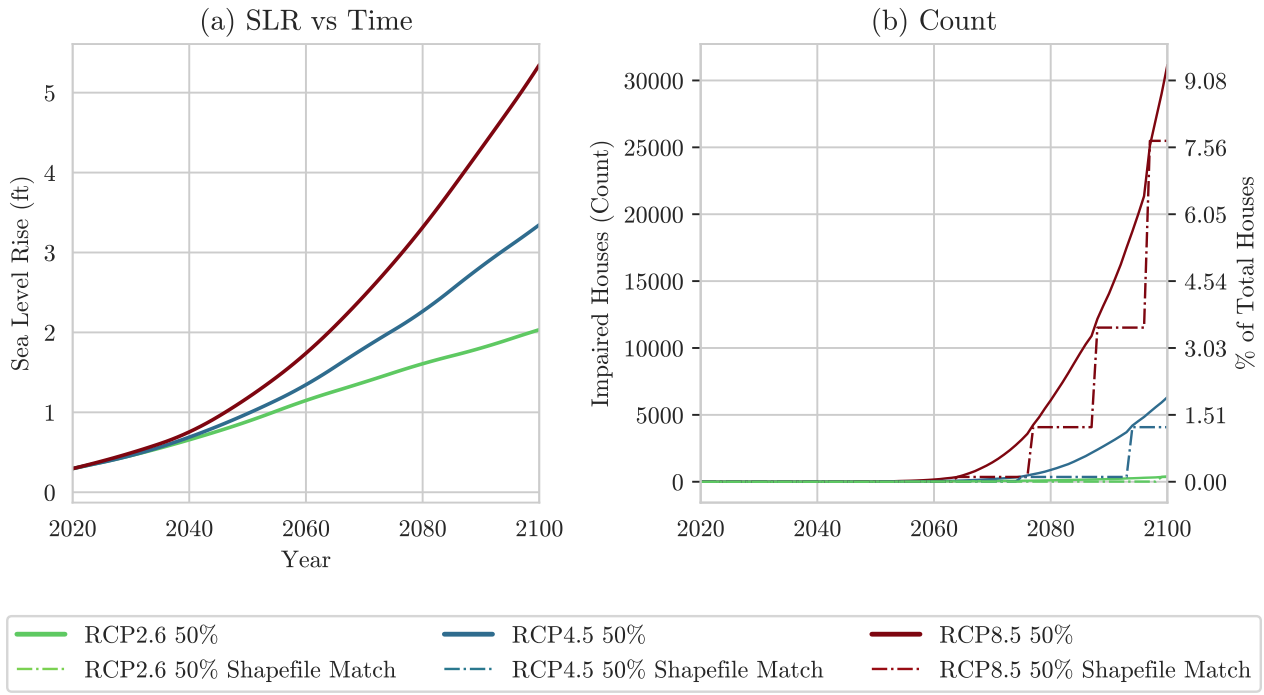

Figure 5: Combined use of Sea Level Rise Viewer DEMs and shapefiles refines impairment estimates. Left side: Sea-level rise projection for Miami. (Deconto and Pollard, 2016) Right side: Combined DEM and shapefile Match (Solid Lines) vs. Only shapefile Match (Dashed Lines)

to questionable results due to the uncertainty of the DEM. For example, the SLR increment within a year is typically on the order of millimeters, but the vertical uncertainty of the DEM is typically on the order of centimeters. As such, the annual sea-level rise increment is within the uncertainty of the DEM and can lead to questionable results for an individual SLR projection (Gesch, 2018). However, previous research indicates the DEM uncertainty (on the order of centimeters) is a much smaller contribution to the uncertainty of coastal inundation compared to the uncertainty of SLR projections (on the order of meters), especially in distant decades (Amante, 2019). Therefore, using this dual-approach to estimate the year of inundation is deemed acceptable when determining a range of future coastal housing market impairment that incorporates SLR uncertainty into the distant future (i.e., through 2100). This is because the SLR uncertainty will be a much larger contributor to the uncertainty in the housing market impairment than the DEM uncertainty that is not considered in this analysis.

6.2 Discount Cash Flow Methods and Interest Rate Sensitivity

6.2.1 Discounted Cash Flow and Cash Flow Impairment

Our analytic approach uses a financial impairment methodology to estimate the value at risk from SLR for each property. We base value and impairment estimates on the Gordon (1963) model, which is used by other researchers to estimate SLR timing (Bernstein et al., 2019). The Gordon model assumes that the value of property (V_i) is the sum of all future cash flows (CF_i) discounted by some discount rate (r) and that cash flows for unimpaired properties continue in perpetuity (forever). For our purposes, we make an additional simplifying assumption that cash flows to a property cease when it is exposed to SLR at time (T) and the value of the property immediately becomes worthless. For our impairment analysis, we use the following equations:

$$\begin{aligned} V_i &= \sum_{t=1}^{\infty} \frac{CF_{i,t}}{(1+r)^t} = \frac{CF_i}{r} \\ V_{impaired} &= \frac{V_i}{(1+r)^T} = \frac{\frac{CF_i}{r}}{(1+r)^T} \\ \%\ \text{Total Value Impaired} &= \frac{\frac{V_i}{(1+r)^T}}{V_i} = \frac{1}{(1+r)^T} \approx e^{-(r*T)} \end{aligned} \tag{1}$$

where:

V_i = present value; property value i

CF_i = cash flow for property i

T = year of impairment; year of SLR impact

r = discount rate

By summing up impairment values for individually impaired properties and the unimpaired values for all properties, we arrive at a total value impairment for an entire housing market (e.g., city, county, state, country) and the share of total value that may be at risk from SLR:

$$\text{Market Value Impaired} = \sum_{i=1}^{n} V_i(e^{-(r*T)})$$
$$\% \text{ Market Value Impaired} = \frac{\sum_{i=1}^{n} V_i(e^{-(r*T)})}{\sum_{i=1}^{n} V_i} \tag{2}$$

6.2.2 Impairment Values and Discount Rate Sensitivity

Our baseline impairment estimates use an easy to communicate and understand 0 percent discount rate, which means that those impairment estimates over time reflect the current estimated property values. However, using some other (positive) discount would result in lower overall impairment value estimates, as future property impairments are discounted compared to properties impaired in the near-term. The higher the discount rate, the lower the impairment value. Below, we provide aggregated impairment results across the 15 metros using three different discount rates (i.e., 0%, 2.6%, and 4%):

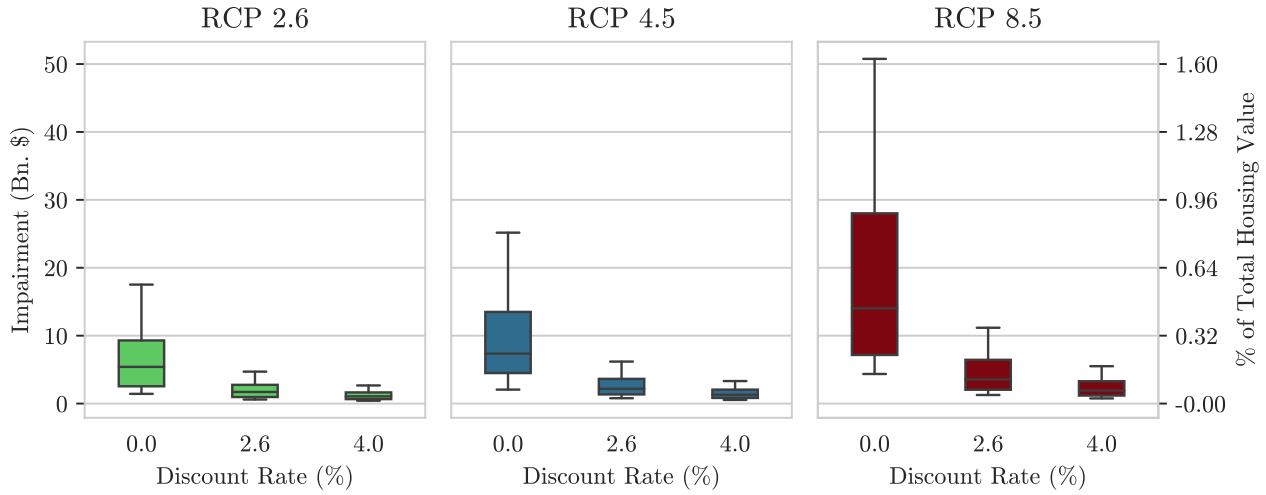

Figure 6: Interest Rate Sensitivity

The median results across all GHG concentration paths for Kopp et al. (2014, 2017), using three different discount rates, illustrate the sensitivity of impairment value estimates over time for a chosen interest rate. As an example, the median impairment value estimate with a 0 percent discount rate through 2100 is $7.0 billion for RCP 4.5. Using the 2.6% and 4% discount rates, this estimate drops to $1.9 billion, and $1.0 billion, respectively. As the discount rate

rises, the value impairment declines due to the time value of money, illustrating the importance of choosing a discount rate for this type of long-term analysis.

6.3 Deconto and Pollard (2016) Results: Antarctic Ice Sheet Physics

The main housing market impairment results in this paper use local SLR projections available in Kopp et al. (2014, 2017) (K14). These local SLR projections are commonly used by NOAA and other scientific agencies in their own local SLR projections (Sweet et al., 2017). The K14 results are a useful baseline for estimating local SLR and the economic consequences. However, K14 SLR projections do not account for factors that may cause accelerated ice sheet melt such as ice shelf hydrofracturing and ice cliff collapse. Deconto and Pollard (2016) (DP16) produce local sea-level projections that account for both the mechanisms of ice sheet hydrofracturing and ice-cliff collapse, which are reinforcing factors that accelerate global mean sea-level (GMSL) rise and exacerbate risk to local coastal communities. To provide some context, the median projected 21st century GMSL rise is expected to reach 0.59m for the medium GHG concentration scenarios (RCP 4.5) in K14, but under DP16, GMSL is expected to rise by 0.91m. Local, relative SLR differences can be even more pronounced. We provide a comparison of aggregated SLR impairment results across our 15 metros between K14 and DP16 (see figure 7) to demonstrate how accounting for additional influences, such as the rapid disintegration of ice sheets, can add to the economic costs of SLR.

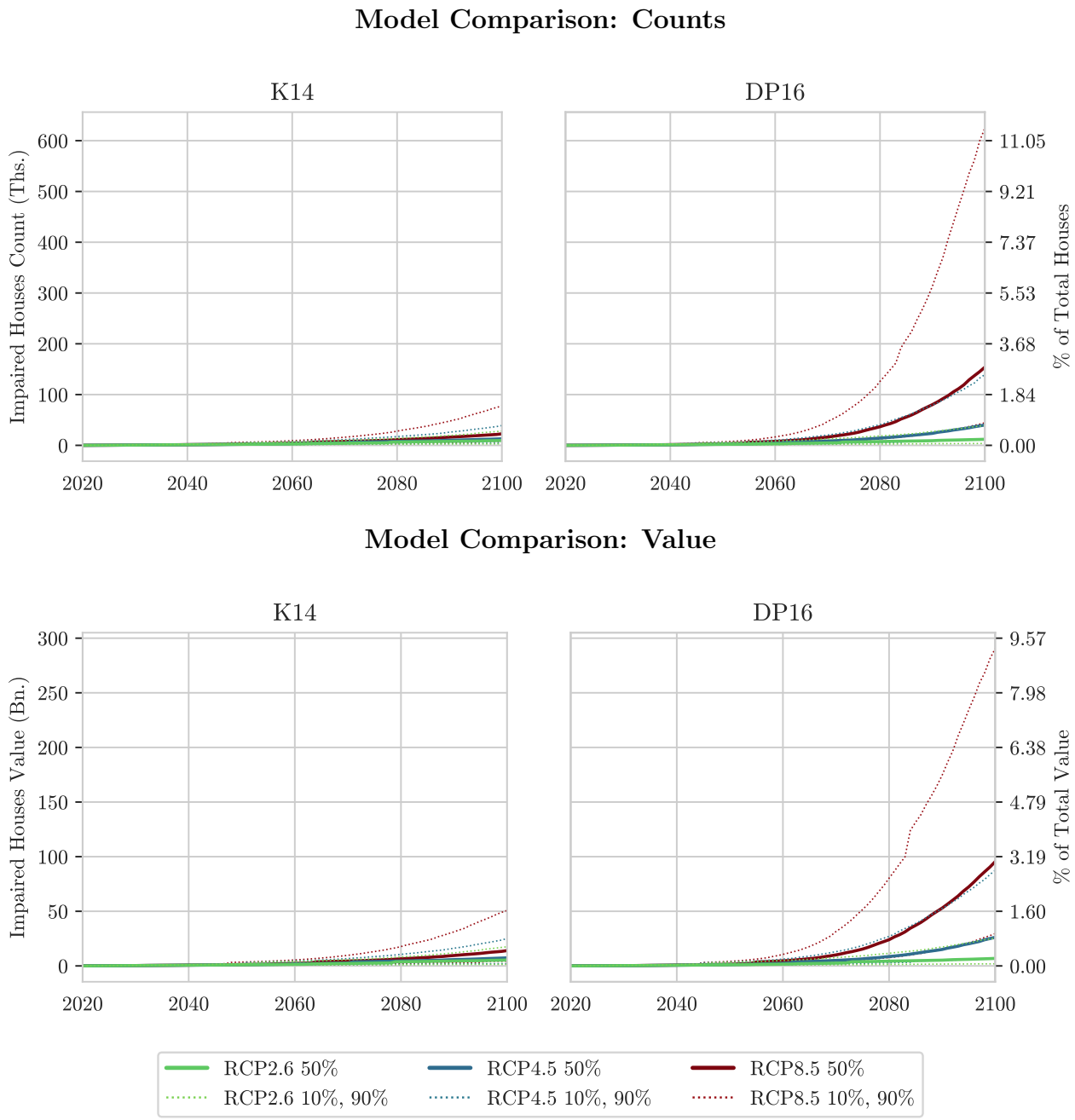

Figure 7: Combined 15 Metro Kopp et al. (2014) and Deconto and Pollard (2016) Comparison

The median impairment results across all GHG concentration paths for K14 compared to DP16 demonstrate how additional feedback loops in ice sheet melt can increase SLR impairment estimates. Using the medium GHG concentration path (RCP 4.5) as an example, the median impaired property counts though 2100 are estimated at 12,200 in K14, but are much larger at 39,300 in DP16. The median estimated impairment value is $7.0 billion in K14 for RCP 4.5 compared to $25.7 billion under DP16. Given the accelerated path of SLR in DP16 compared to K14, the number of properties and estimated impairment value is higher under all three of the GHG concentration scenarios. Accounting for potentially reinforcing feedback processes in ice sheet melt can be important when assessing the full spectrum of potential economic effects from more extreme SLR projections.

6.4 Metro-Level Results

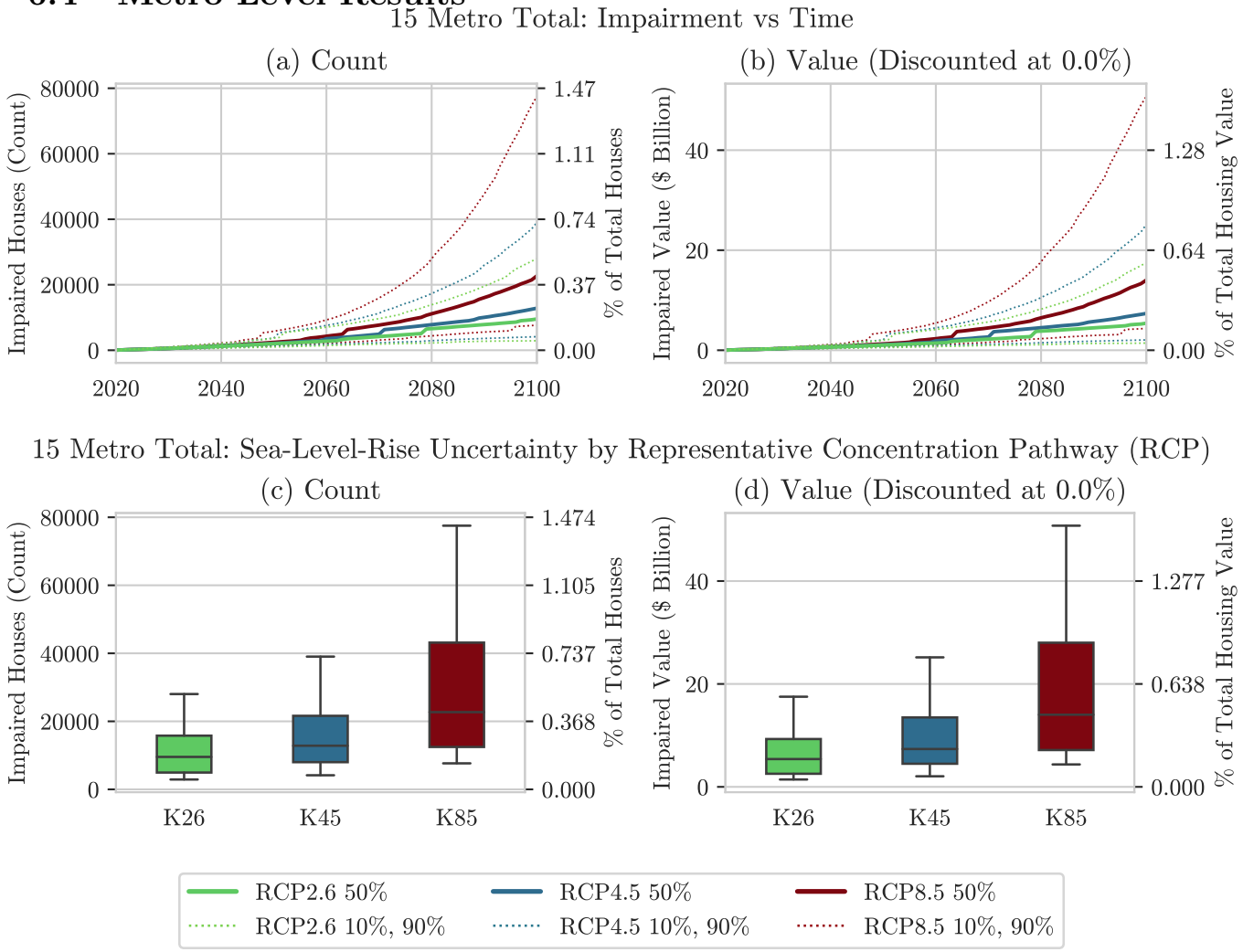

RCP	Ptile	Cnt. 2050	Cnt. 2100	% Cnt. 2100	Bn. $ 2050	Bn. $ 2100	% Value 2100	Avg. Year	Std. Year
RCP-26	**0.1**	253	2016	0.04	0.11	0.91	0.03	2070	15
	0.5	1367	8917	0.16	0.66	5.04	0.16	2072	18
	0.9	3360	27693	0.51	1.80	17.32	0.55	2075	19
RCP-45	**0.1**	351	3182	0.06	0.15	1.48	0.05	2073	16
	0.5	1466	12202	0.22	0.73	6.99	0.22	2074	18
	0.9	3399	38720	0.71	1.88	24.97	0.80	2077	18
RCP-85	**0.1**	515	6737	0.12	0.22	3.82	0.12	2077	16
	0.5	1785	22080	0.41	0.91	13.66	0.44	2077	17
	0.9	5510	77226	1.42	3.32	50.57	1.61	2081	16

*All values in charts and table are undiscounted.

a) Inundation path and uncertainty bands for impaired property counts (left vertical axis) and percent of housing market (right vertical axis) for RCP 2.6, 4.5, and 8.5; b) Inundation path and uncertainty bands for total value at an undiscounted rate (left vertical axis) and percent of housing market value (right vertical axis) for RCP 2.6, 4.5, and 8.5; c)Box and whisker plot for impaired property counts through 2100 (left vertical axis) and share of housing market (right vertical axis) for RCP 2.6, 4.5, and 8.5 - lower whisker 10th quantile, lower box 25th quantile, center line median, upper box 75th quantile, and upper whisker 90th quantile; d)Box and whisker plot for total value at risk through 2100 at an undiscounted rate (left vertical axis) and percent of housing market value (right vertical axis) for RCP 2.6, 4.5, and 8.5 – lower whisker 10th quantile, lower box 25th quantile, center line median, upper box 75th quantile, and upper whisker 90th quantile. K26, K45, and K85 refer to results associated with RCP2.6, RCP4.5, and RCP 8.5 from (Kopp et al., 2014, 2017)

Metro Summary Statistics and Results

	Properties	Housing Stock		K14 RCP26 by 2100 (50th ptile)			K14 RCP45 by 2100 (50th ptile)			K14 RCP85 by 2100 (50th ptile)		
	Count	Total Value	Median Price	Cnt. Share	Count	Value	Cnt. Share	Count	Value	Cnt. Share	Count	Value
Metro												
DC Metro	545,713	306.7 B	453.0 K	0.0 pct	1	1.8 M	0.0 pct	3	3.1 M	0.0 pct	11	7.0 M
Mobile, AL	110,265	12.5 B	84.7 K	0.1 pct	117	40.9 M	0.1 pct	157	46.5 M	0.2 pct	241	58.2 M
Houston, TX	746,861	192.1 B	152.6 K	0.0 pct	151	62.5 M	0.0 pct	182	74.9 M	0.0 pct	253	104.3 M
San Diego, CA	280,903	184.4 B	526.5 K	0.0 pct	73	72.7 M	0.0 pct	123	119.9 M	0.1 pct	330	311.3 M
Fort Lauderdale, FL	176,473	65.0 B	269.2 K	0.0 pct	40	49.7 M	0.1 pct	121	135.6 M	0.3 pct	535	550.9 M
Los Angeles, CA	616,092	489.1 B	495.8 K	0.0 pct	69	116.6 M	0.0 pct	152	206.2 M	0.1 pct	485	582.2 M
New York City, NY	658,622	536.5 B	671.7 K	0.0 pct	268	139.4 M	0.1 pct	511	232.9 M	0.2 pct	1,235	512.4 M
Wilmington, NC	67,559	20.6 B	205.0 K	0.2 pct	161	245.5 M	0.3 pct	221	291.9 M	0.5 pct	343	376.8 M
Seattle, WA	215,074	153.1 B	598.8 K	0.0 pct	16	509.3 M	0.0 pct	15	509.3 M	0.0 pct	21	516.9 M
Jacksonville, FL	302,428	62.3 B	154.4 K	0.2 pct	720	421.0 M	0.3 pct	1,055	561.5 M	0.6 pct	1,964	977.3 M
Miami, FL	330,512	131.4 B	263.4 K	0.1 pct	200	304.5 M	0.2 pct	589	731.2 M	0.8 pct	2,585	2,747.2 M
Norfolk, VA	202,585	55.5 B	221.0 K	0.4 pct	844	622.9 M	0.6 pct	1,159	740.2 M	1.0 pct	2,036	1,071.4 M
Galveston, TX	21,163	5.5 B	177.1 K	12.4 pct	2,622	999.6 M	15.6 pct	3,310	1,187.9 M	23.1 pct	4,886	1,645.9 M
Charleston, SC	113,444	45.1 B	275.2 K	0.8 pct	876	1,195.7 M	1.3 pct	1,495	1,647.5 M	2.5 pct	2,838	2,630.6 M
San Francisco, CA	1,041,061	873.7 B	618.8 K	0.3 pct	3,384	3,159.2 M	0.4 pct	3,740	3,401.2 M	0.5 pct	4,943	4,471.0 M
15 Metro Summary	5,428,755	3,133.5 B	396.2 K	0.2 pct	9,542	7,941.4 M	0.2 pct	12,833	9,889.8 M	0.4 pct	22,706	16,563.5 M

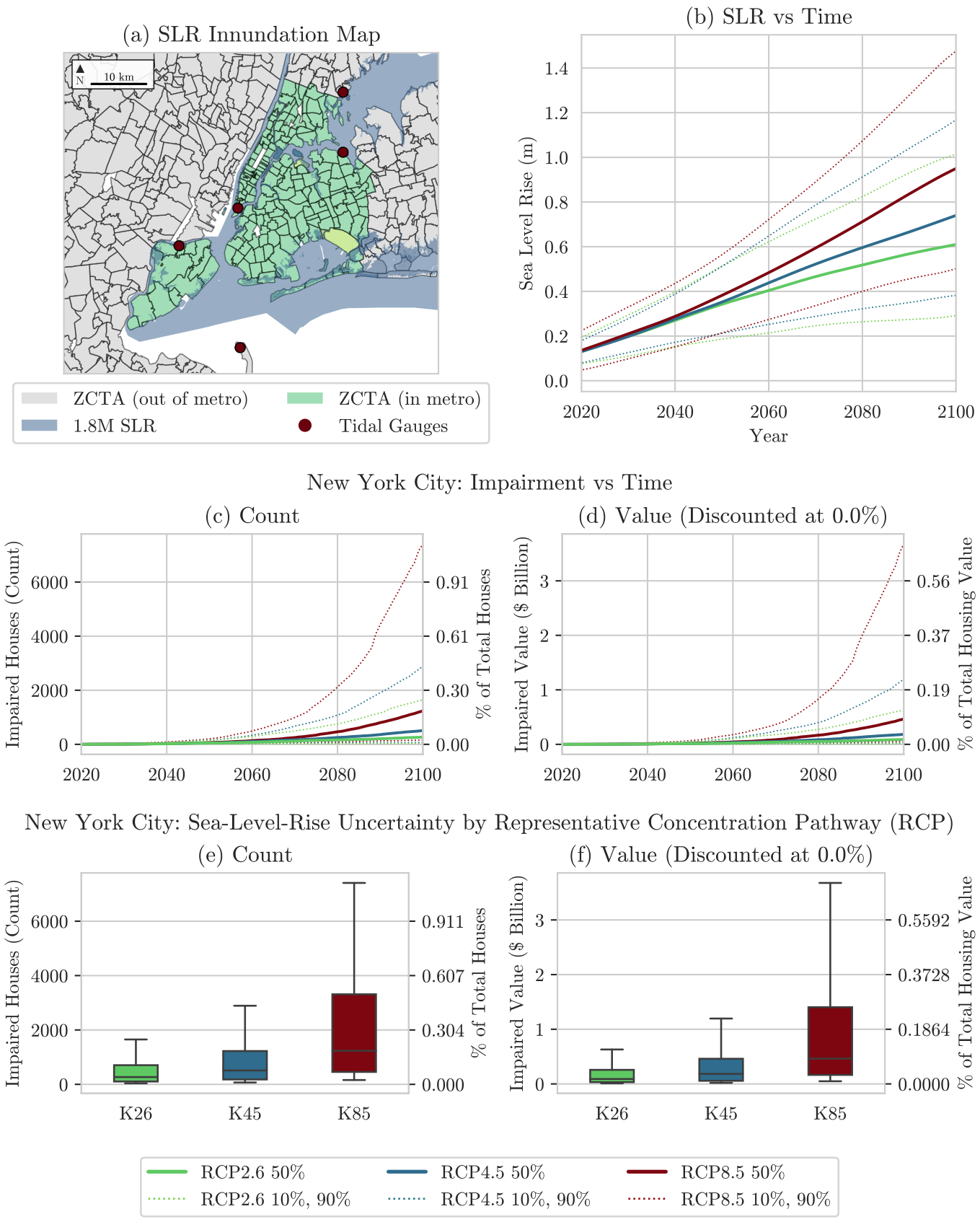
New York City: Sea-Level-Rise vs Time
(a) SLR Innundation Map
N
10 km
ZCTA (out of metro)
ZCTA (in metro)
1.8M SLR
Tidal Gauges
(b) SLR vs Time
Sea Level Rise (m)
Year
New York City: Impairment vs Time
(c) Count
Impaired Houses (Count)
% of Total Houses
(d) Value (Discounted at 0.0%)
Impaired Value ($ Billion)
% of Total Housing Value
New York City: Sea-Level-Rise Uncertainty by Representative Concentration Pathway (RCP)
(e) Count
(f) Value (Discounted at 0.0%)
K26
K45
K85
RCP2.6 50%
RCP2.6 10%, 90%
RCP4.5 50%
RCP4.5 10%, 90%
RCP8.5 50%
RCP8.5 10%, 90%

RCP	Ptile	Cnt. 2050	Cnt. 2100	% Cnt. 2100	Bn. $ 2050	Bn. $ 2100	% Value 2100	Avg. Year	Std. Year
RCP-26	**0.1**	0	16	0.00	0.00	0.01	0.00	2080	13
	0.5	36	256	0.04	0.01	0.09	0.02	2073	18
	0.9	150	1645	0.25	0.05	0.63	0.12	2077	17
RCP-45	**0.1**	0	47	0.01	0.00	0.01	0.00	2077	13
	0.5	37	496	0.08	0.01	0.18	0.03	2077	16
	0.9	150	2883	0.44	0.05	1.19	0.22	2081	15
RCP-85	**0.1**	0	132	0.02	0.00	0.04	0.01	2080	13
	0.5	53	1223	0.19	0.02	0.46	0.09	2082	14
	0.9	201	7405	1.12	0.07	3.68	0.69	2084	13

*All values in charts and table are undiscounted.

a) Map of ZIP Code Tabulation Areas (ZCTA) included in metro and 1.8m (6ft) inundation area; b) Sea level rise Path and 10-90th uncertainty band for greenhouse gas concentration pathways (representative concentration pathways) - RCP 2.6 (green), 4.5 (blue), and 8.5 (red) for; c) Inundation path and uncertainty bands for impaired property counts (left vertical axis) and percent of housing market (right vertical axis) for RCP 2.6, 4.5, and 8.5; d) Inundation path and uncertainty bands for total value at an undiscounted rate (left vertical axis) and percent of housing market value (right vertical axis) for RCP 2.6, 4.5, and 8.5; e)Box and whisker plot for impaired property counts through 2100 (left vertical axis) and share of housing market (right vertical axis) for RCP 2.6, 4.5, and 8.5 - lower whisker 10th quantile, lower box 25th quantile, center line median, upper box 75th quantile, and upper whisker 90th quantile; f)Box and whisker plot for total value at risk through 2100 at an undiscounted rate (left vertical axis) and percent of housing market value (right vertical axis) for RCP 2.6, 4.5, and 8.5 – lower whisker 10th quantile, lower box 25th quantile, center line median, upper box 75th quantile, and upper whisker 90th quantile. K26, K45, and K85 refer to results associated with RCP2.6, RCP4.5, and RCP 8.5 from (Kopp et al., 2014, 2017)

Miami: Sea-Level-Rise vs Time

(a) SLR Innundation Map

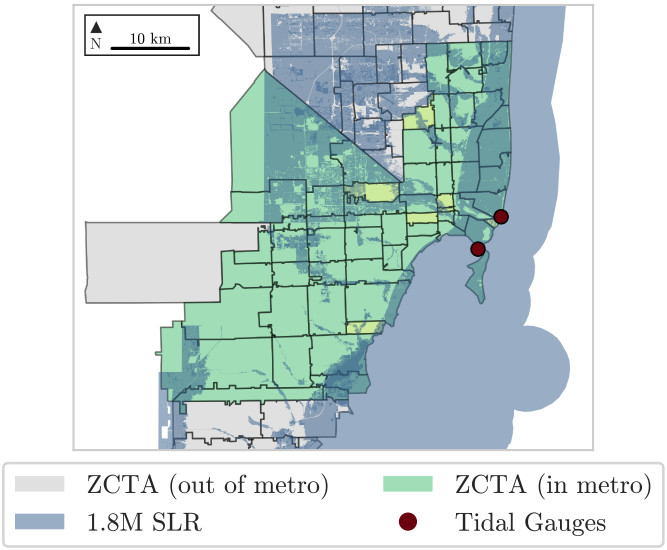

(b) SLR vs Time

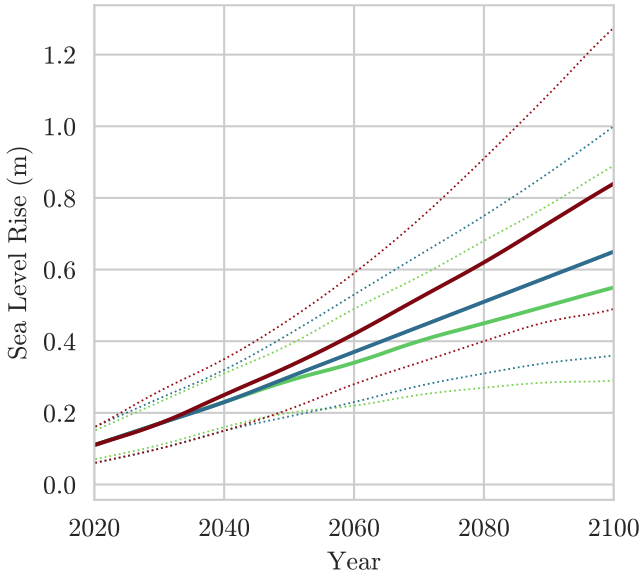

Miami: Impairment vs Time

(c) Count

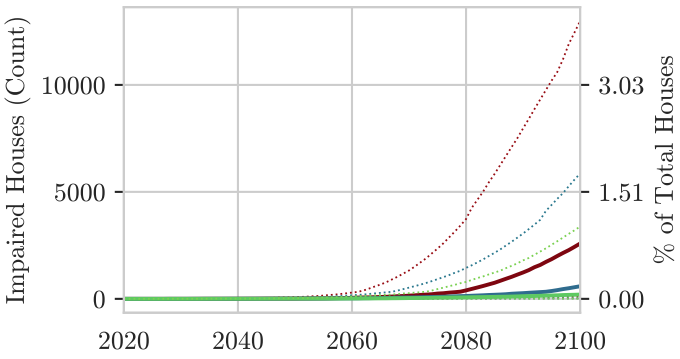

(d) Value (Discounted at 0.0%)

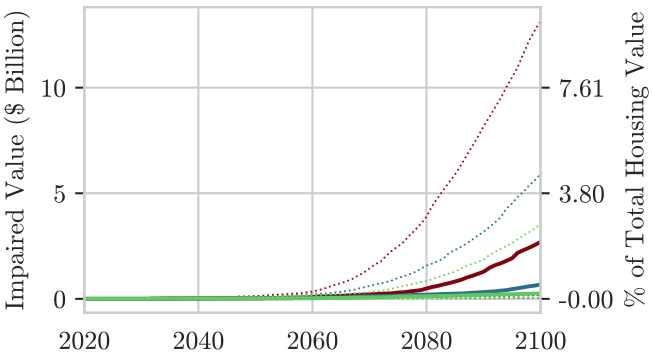

Miami: Sea-Level-Rise Uncertainty by Representative Concentration Pathway (RCP)

(e) Count

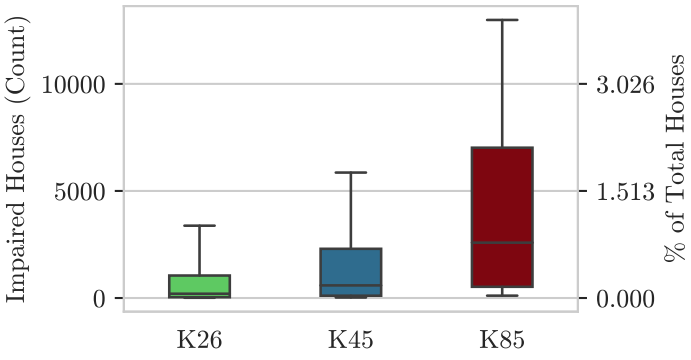

(f) Value (Discounted at 0.0%)

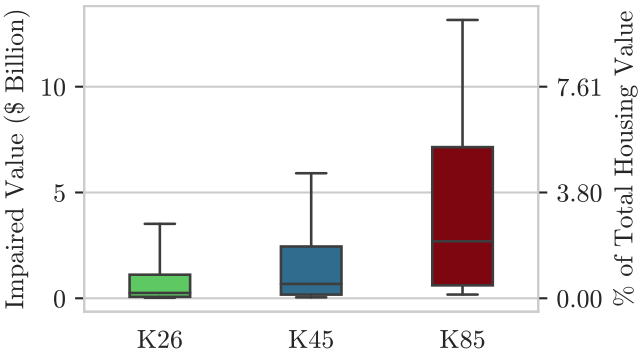

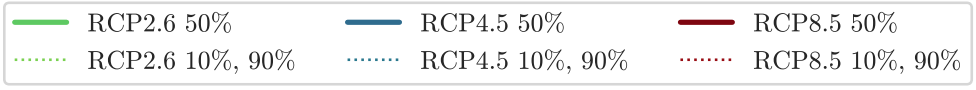

RCP	Ptile	Cnt. 2050	Cnt. 2100	% Cnt. 2100	Bn. $ 2050	Bn. $ 2100	% Value 2100	Avg. Year	Std. Year
RCP-26	**0.1**	3	11	0.00	0.01	0.02	0.02	2068	16
	0.5	11	199	0.06	0.02	0.25	0.19	2082	15
	0.9	30	3377	1.02	0.06	3.52	2.68	2086	11
RCP-45	**0.1**	1	20	0.01	0.01	0.04	0.03	2075	16
	0.5	11	588	0.18	0.02	0.68	0.52	2087	13
	0.9	45	5857	1.77	0.08	5.91	4.50	2086	11
RCP-85	**0.1**	3	107	0.03	0.01	0.17	0.13	2082	12
	0.5	12	2584	0.78	0.02	2.69	2.05	2088	10
	0.9	79	12984	3.93	0.13	13.15	10.01	2085	11

*All values in charts and table are undiscounted.

a) Map of ZIP Code Tabulation Areas (ZCTA) included in metro and 1.8m (6ft) inundation area; b) Sea level rise Path and 10-90th uncertainty band for greenhouse gas concentration pathways (representative concentration pathways) - RCP 2.6 (green), 4.5 (blue), and 8.5 (red) for; c) Inundation path and uncertainty bands for impaired property counts (left vertical axis) and percent of housing market (right vertical axis) for RCP 2.6, 4.5, and 8.5; d) Inundation path and uncertainty bands for total value at an undiscounted rate (left vertical axis) and percent of housing market value (right vertical axis) for RCP 2.6, 4.5, and 8.5; e)Box and whisker plot for impaired property counts through 2100 (left vertical axis) and share of housing market (right vertical axis) for RCP 2.6, 4.5, and 8.5 - lower whisker 10th quantile, lower box 25th quantile, center line median, upper box 75th quantile, and upper whisker 90th quantile; f)Box and whisker plot for total value at risk through 2100 at an undiscounted rate (left vertical axis) and percent of housing market value (right vertical axis) for RCP 2.6, 4.5, and 8.5 – lower whisker 10th quantile, lower box 25th quantile, center line median, upper box 75th quantile, and upper whisker 90th quantile. K26, K45, and K85 refer to results associated with RCP2.6, RCP4.5, and RCP 8.5 from (Kopp et al., 2014, 2017)

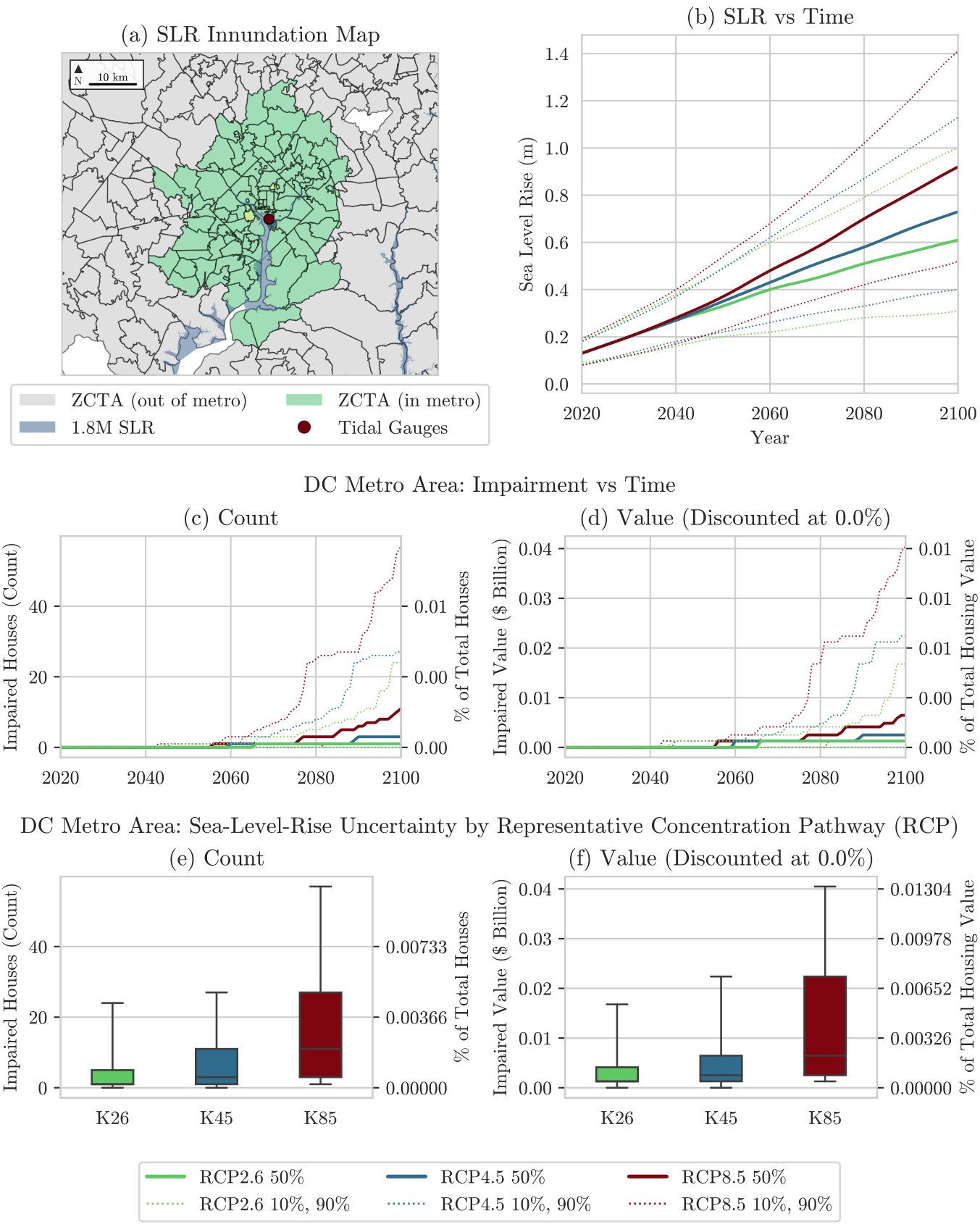
DC Metro Area: Sea-Level-Rise vs Time
(a) SLR Innundation Map
N
10 km
ZCTA (out of metro)
ZCTA (in metro)
1.8M SLR
Tidal Gauges
(b) SLR vs Time
Sea Level Rise (m)
Year
DC Metro Area: Impairment vs Time
(c) Count
Impaired Houses (Count)
% of Total Houses
(d) Value (Discounted at 0.0%)
Impaired Value ($ Billion)
% of Total Housing Value
DC Metro Area: Sea-Level-Rise Uncertainty by Representative Concentration Pathway (RCP)
(e) Count
(f) Value (Discounted at 0.0%)
K26
K45
K85
RCP2.6 50%
RCP2.6 10%, 90%
RCP4.5 50%
RCP4.5 10%, 90%
RCP8.5 50%
RCP8.5 10%, 90%

RCP	Ptile	Cnt. 2050	Cnt. 2100	% Cnt. 2100	Bn. $ 2050	Bn. $ 2100	% Value 2100	Avg. Year	Std. Year
RCP-26	**0.1**	NaN	0	0.00	NaN	0.00	0.00	nan	nan
	0.5	NaN	1	0.00	NaN	0.00	0.00	2066	nan
	0.9	NaN	24	0.00	NaN	0.02	0.01	2088	13
RCP-45	**0.1**	NaN	0	0.00	NaN	0.00	0.00	nan	nan
	0.5	NaN	3	0.00	NaN	0.00	0.00	2080	17
	0.9	NaN	27	0.00	NaN	0.02	0.01	2082	11
RCP-85	**0.1**	NaN	1	0.00	NaN	0.00	0.00	2082	nan
	0.5	NaN	11	0.00	NaN	0.01	0.00	2085	13
	0.9	NaN	57	0.01	NaN	0.04	0.01	2084	13

*All values in charts and table are undiscounted.

a) Map of ZIP Code Tabulation Areas (ZCTA) included in metro and 1.8m (6ft) inundation area; b) Sea level rise Path and 10-90th uncertainty band for greenhouse gas concentration pathways (representative concentration pathways) - RCP 2.6 (green), 4.5 (blue), and 8.5 (red) for; c) Inundation path and uncertainty bands for impaired property counts (left vertical axis) and percent of housing market (right vertical axis) for RCP 2.6, 4.5, and 8.5; d) Inundation path and uncertainty bands for total value at an undiscounted rate (left vertical axis) and percent of housing market value (right vertical axis) for RCP 2.6, 4.5, and 8.5; e)Box and whisker plot for impaired property counts through 2100 (left vertical axis) and share of housing market (right vertical axis) for RCP 2.6, 4.5, and 8.5 - lower whisker 10th quantile, lower box 25th quantile, center line median, upper box 75th quantile, and upper whisker 90th quantile; f)Box and whisker plot for total value at risk through 2100 at an undiscounted rate (left vertical axis) and percent of housing market value (right vertical axis) for RCP 2.6, 4.5, and 8.5 – lower whisker 10th quantile, lower box 25th quantile, center line median, upper box 75th quantile, and upper whisker 90th quantile. K26, K45, and K85 refer to results associated with RCP2.6, RCP4.5, and RCP 8.5 from (Kopp et al., 2014, 2017)

Norfolk: Sea-Level-Rise vs Time

(a) SLR Innundation Map

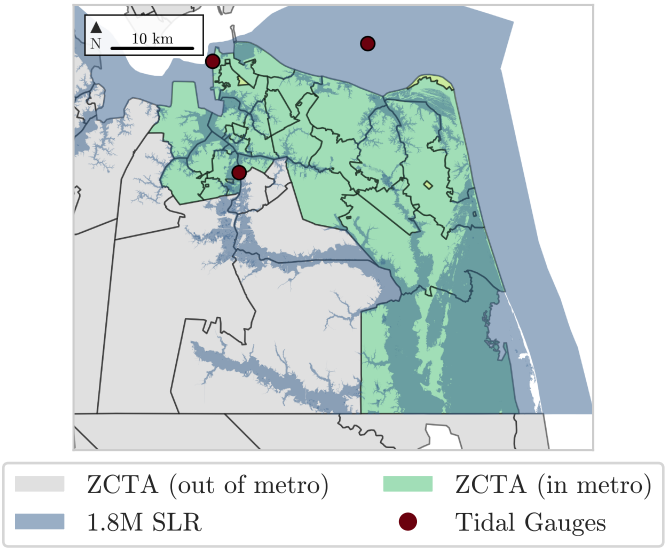

(b) SLR vs Time

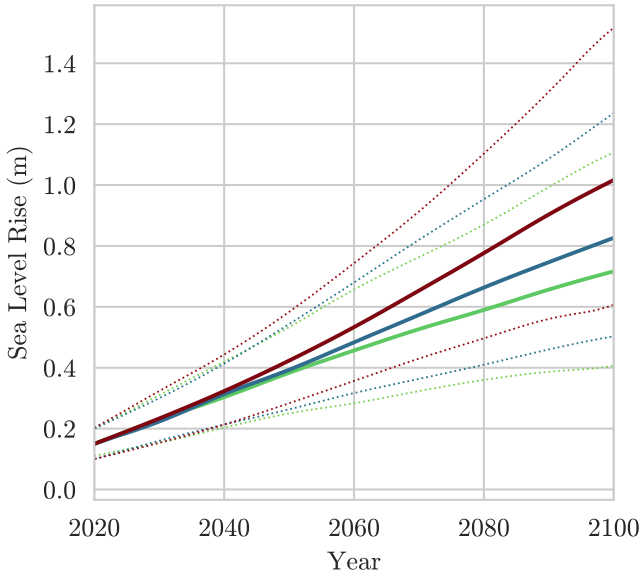

Norfolk: Impairment vs Time

(c) Count

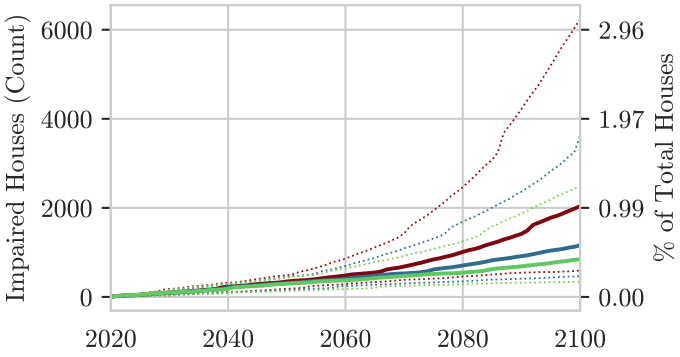

(d) Value (Discounted at 0.0%)

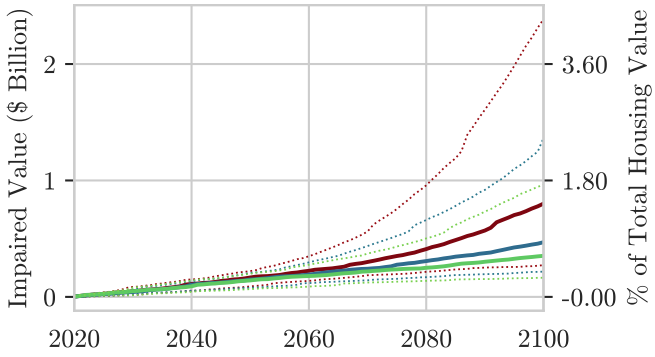

Norfolk: Sea-Level-Rise Uncertainty by Representative Concentration Pathway (RCP)

(e) Count

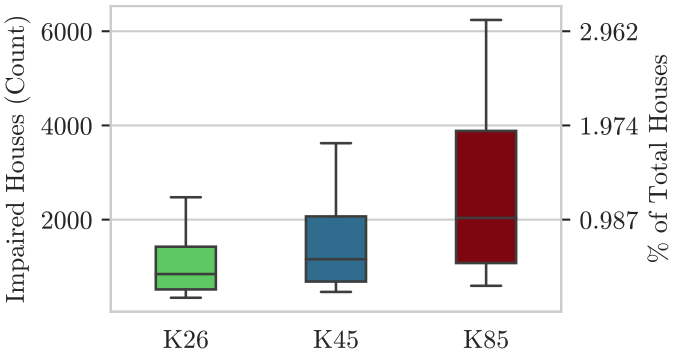

(f) Value (Discounted at 0.0%)

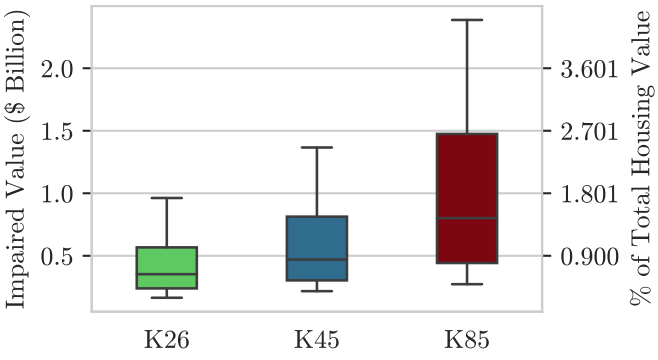

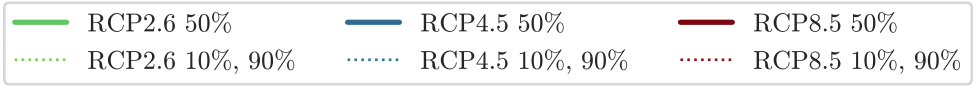

RCP	Ptile	Cnt. 2050	Cnt. 2100	% Cnt. 2100	Bn. $ 2050	Bn. $ 2100	% Value 2100	Avg. Year	Std. Year
RCP-26	**0.1**	33	241	0.12	0.02	0.11	0.20	2068	14
	0.5	219	766	0.38	0.10	0.31	0.56	2067	22
	0.9	404	2446	1.21	0.18	0.95	1.71	2073	21
RCP-45	**0.1**	51	359	0.18	0.03	0.16	0.30	2069	17
	0.5	234	1082	0.53	0.11	0.43	0.78	2071	20
	0.9	424	3595	1.77	0.19	1.35	2.44	2075	19
RCP-85	**0.1**	77	489	0.24	0.04	0.22	0.40	2068	16
	0.5	268	1958	0.97	0.13	0.76	1.37	2076	19
	0.9	460	6212	3.07	0.21	2.37	4.27	2079	17

*All values in charts and table are undiscounted.

a) Map of ZIP Code Tabulation Areas (ZCTA) included in metro and 1.8m (6ft) inundation area; b) Sea level rise Path and 10-90th uncertainty band for greenhouse gas concentration pathways (representative concentration pathways) - RCP 2.6 (green), 4.5 (blue), and 8.5 (red) for; c) Inundation path and uncertainty bands for impaired property counts (left vertical axis) and percent of housing market (right vertical axis) for RCP 2.6, 4.5, and 8.5; d) Inundation path and uncertainty bands for total value at an undiscounted rate (left vertical axis) and percent of housing market value (right vertical axis) for RCP 2.6, 4.5, and 8.5; e)Box and whisker plot for impaired property counts through 2100 (left vertical axis) and share of housing market (right vertical axis) for RCP 2.6, 4.5, and 8.5 - lower whisker 10th quantile, lower box 25th quantile, center line median, upper box 75th quantile, and upper whisker 90th quantile; f)Box and whisker plot for total value at risk through 2100 at an undiscounted rate (left vertical axis) and percent of housing market value (right vertical axis) for RCP 2.6, 4.5, and 8.5 – lower whisker 10th quantile, lower box 25th quantile, center line median, upper box 75th quantile, and upper whisker 90th quantile. K26, K45, and K85 refer to results associated with RCP2.6, RCP4.5, and RCP 8.5 from (Kopp et al., 2014, 2017)

Wilmington: Sea-Level-Rise vs Time

(a) SLR Innundation Map

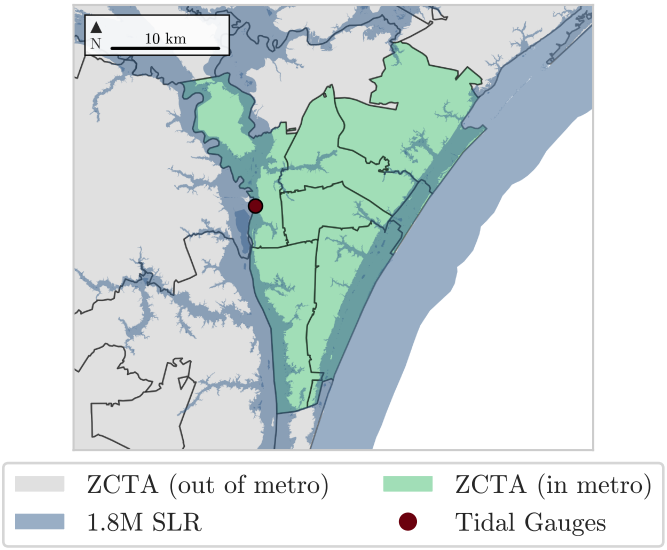

(b) SLR vs Time

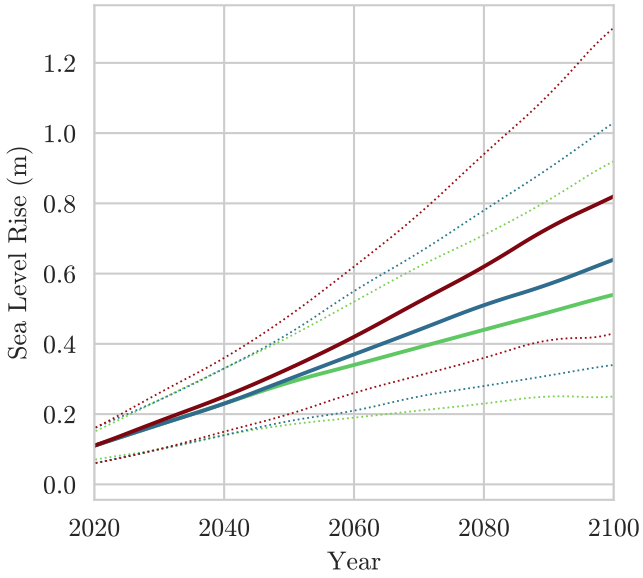

Wilmington: Impairment vs Time

(c) Count

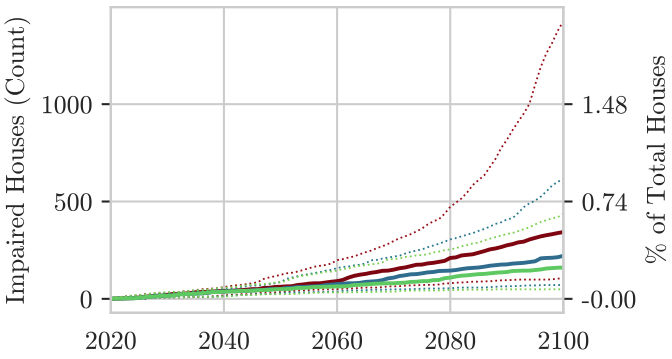

(d) Value (Discounted at 0.0%)

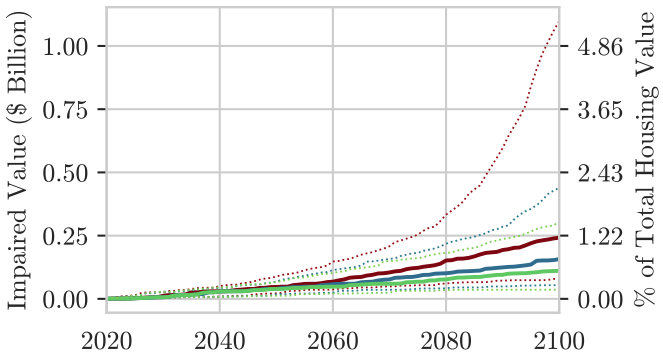

Wilmington: Sea-Level-Rise Uncertainty by Representative Concentration Pathway (RCP)

(e) Count

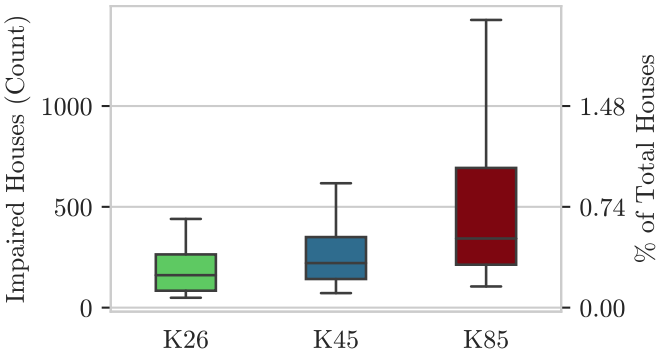

(f) Value (Discounted at 0.0%)

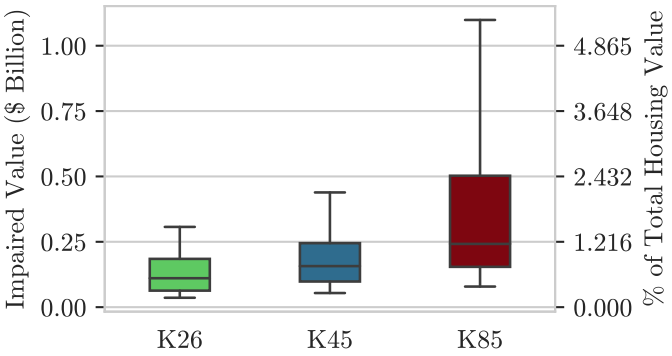

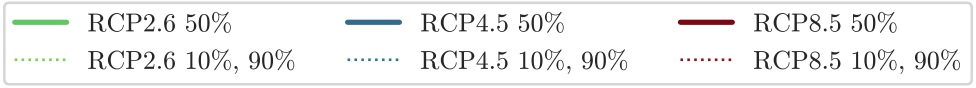

RCP	Ptile	Cnt. 2050	Cnt. 2100	% Cnt. 2100	Bn. $ 2050	Bn. $ 2100	% Value 2100	Avg. Year	Std. Year
RCP-26	**0.1**	0	25	0.04	0.00	0.02	0.12	2068	11
	0.5	34	145	0.21	0.03	0.10	0.51	2069	20
	0.9	75	429	0.64	0.06	0.30	1.47	2070	21
RCP-45	**0.1**	5	48	0.07	0.01	0.04	0.20	2071	16
	0.5	35	205	0.30	0.03	0.15	0.73	2070	19
	0.9	81	612	0.91	0.07	0.44	2.12	2075	21
RCP-85	**0.1**	11	81	0.12	0.01	0.07	0.32	2070	16
	0.5	46	327	0.48	0.04	0.24	1.15	2073	19
	0.9	118	1422	2.10	0.09	1.10	5.33	2082	18

*All values in charts and table are undiscounted.

a) Map of ZIP Code Tabulation Areas (ZCTA) included in metro and 1.8m (6ft) inundation area; b) Sea level rise Path and 10-90th uncertainty band for greenhouse gas concentration pathways (representative concentration pathways) - RCP 2.6 (green), 4.5 (blue), and 8.5 (red) for; c) Inundation path and uncertainty bands for impaired property counts (left vertical axis) and percent of housing market (right vertical axis) for RCP 2.6, 4.5, and 8.5; d) Inundation path and uncertainty bands for total value at an undiscounted rate (left vertical axis) and percent of housing market value (right vertical axis) for RCP 2.6, 4.5, and 8.5; e)Box and whisker plot for impaired property counts through 2100 (left vertical axis) and share of housing market (right vertical axis) for RCP 2.6, 4.5, and 8.5 - lower whisker 10th quantile, lower box 25th quantile, center line median, upper box 75th quantile, and upper whisker 90th quantile; f)Box and whisker plot for total value at risk through 2100 at an undiscounted rate (left vertical axis) and percent of housing market value (right vertical axis) for RCP 2.6, 4.5, and 8.5 – lower whisker 10th quantile, lower box 25th quantile, center line median, upper box 75th quantile, and upper whisker 90th quantile. K26, K45, and K85 refer to results associated with RCP2.6, RCP4.5, and RCP 8.5 from (Kopp et al., 2014, 2017)

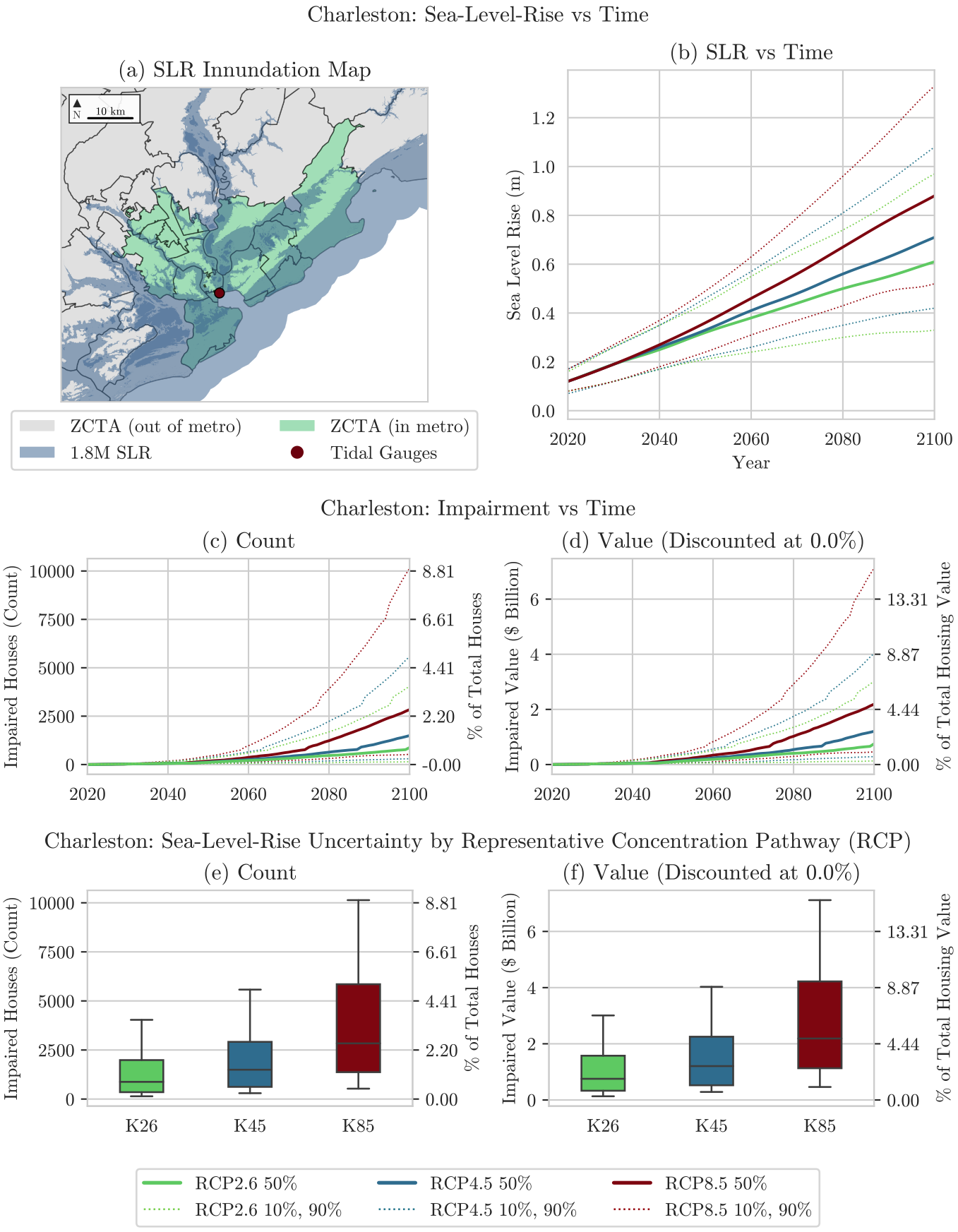
Charleston: Sea-Level-Rise vs Time
(a) SLR Innundation Map
N
10 km
ZCTA (out of metro)
ZCTA (in metro)
1.8M SLR
Tidal Gauges
(b) SLR vs Time
Sea Level Rise (m)
Year
Charleston: Impairment vs Time
(c) Count
Impaired Houses (Count)
% of Total Houses
(d) Value (Discounted at 0.0%)
Impaired Value ($ Billion)
% of Total Housing Value
Charleston: Sea-Level-Rise Uncertainty by Representative Concentration Pathway (RCP)
(e) Count
(f) Value (Discounted at 0.0%)
K26
K45
K85
RCP2.6 50%
RCP2.6 10%, 90%
RCP4.5 50%
RCP4.5 10%, 90%
RCP8.5 50%
RCP8.5 10%, 90%

RCP	Ptile	Cnt. 2050	Cnt. 2100	% Cnt. 2100	Bn. $ 2050	Bn. $ 2100	% Value 2100	Avg. Year	Std. Year
RCP-26	**0.1**	8	99	0.09	0.01	0.09	0.20	2075	16
	0.5	83	848	0.75	0.07	0.73	1.62	2074	17
	0.9	289	4021	3.54	0.27	2.99	6.64	2079	17
RCP-45	**0.1**	14	247	0.22	0.01	0.23	0.52	2078	14
	0.5	99	1467	1.29	0.09	1.18	2.62	2079	16
	0.9	343	5563	4.90	0.31	4.01	8.90	2080	16
RCP-85	**0.1**	24	486	0.43	0.02	0.42	0.93	2075	13
	0.5	148	2810	2.48	0.14	2.16	4.80	2080	15
	0.9	418	10121	8.92	0.37	7.10	15.75	2082	15

*All values in charts and table are undiscounted.

a) Map of ZIP Code Tabulation Areas (ZCTA) included in metro and 1.8m (6ft) inundation area; b) Sea level rise Path and 10-90th uncertainty band for greenhouse gas concentration pathways (representative concentration pathways) - RCP 2.6 (green), 4.5 (blue), and 8.5 (red) for; c) Inundation path and uncertainty bands for impaired property counts (left vertical axis) and percent of housing market (right vertical axis) for RCP 2.6, 4.5, and 8.5; d) Inundation path and uncertainty bands for total value at an undiscounted rate (left vertical axis) and percent of housing market value (right vertical axis) for RCP 2.6, 4.5, and 8.5; e)Box and whisker plot for impaired property counts through 2100 (left vertical axis) and share of housing market (right vertical axis) for RCP 2.6, 4.5, and 8.5 - lower whisker 10th quantile, lower box 25th quantile, center line median, upper box 75th quantile, and upper whisker 90th quantile; f)Box and whisker plot for total value at risk through 2100 at an undiscounted rate (left vertical axis) and percent of housing market value (right vertical axis) for RCP 2.6, 4.5, and 8.5 – lower whisker 10th quantile, lower box 25th quantile, center line median, upper box 75th quantile, and upper whisker 90th quantile. K26, K45, and K85 refer to results associated with RCP2.6, RCP4.5, and RCP 8.5 from (Kopp et al., 2014, 2017)

Jacksonville: Sea-Level-Rise vs Time

(a) SLR Innundation Map

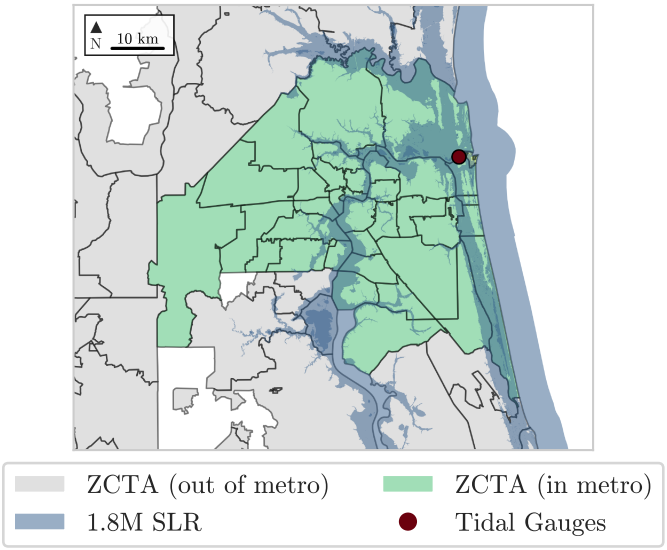

(b) SLR vs Time

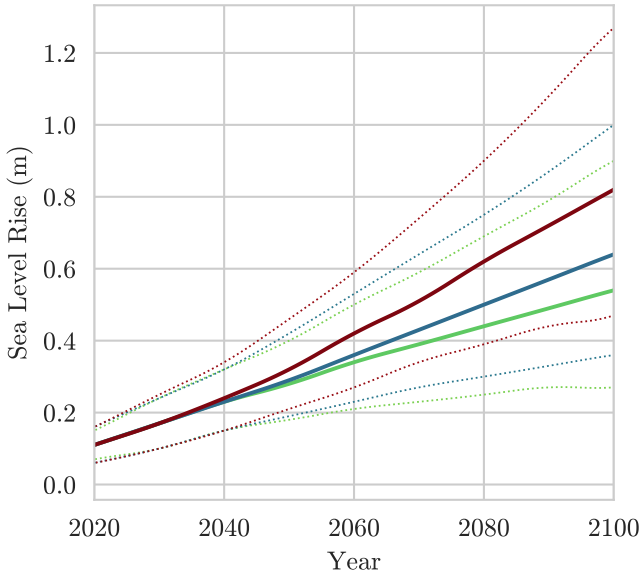

Jacksonville: Impairment vs Time

(c) Count

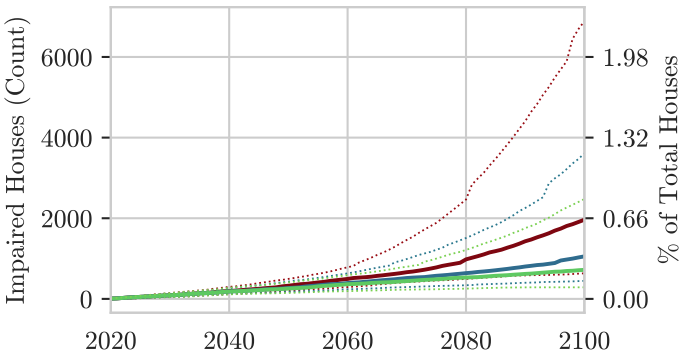

(d) Value (Discounted at 0.0%)

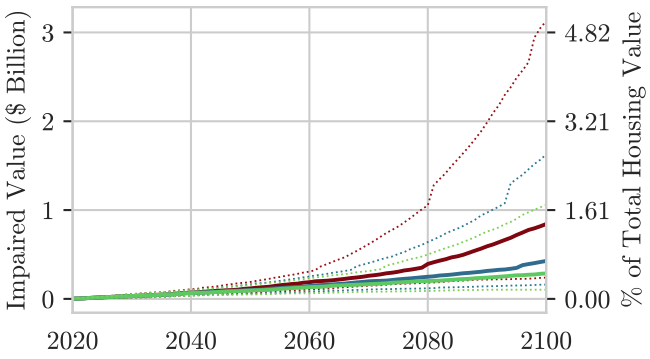

Jacksonville: Sea-Level-Rise Uncertainty by Representative Concentration Pathway (RCP)

(e) Count

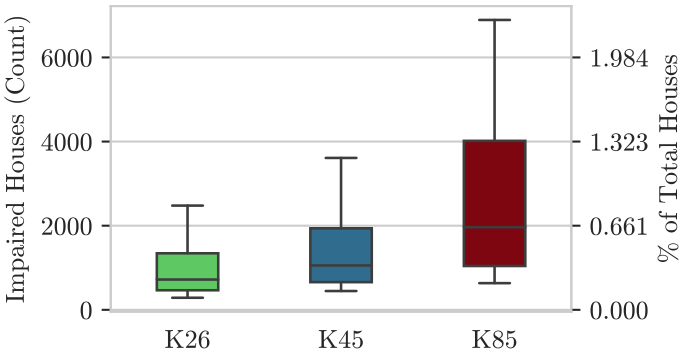

(f) Value (Discounted at 0.0%)

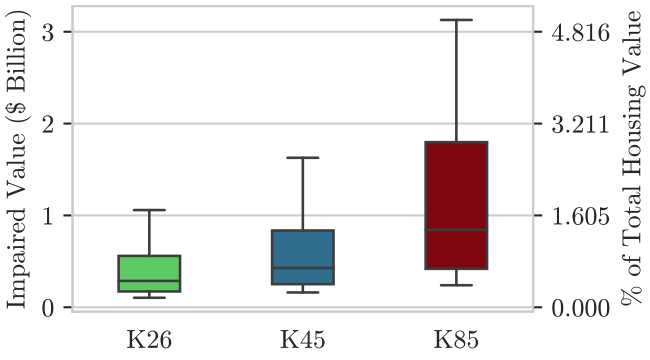

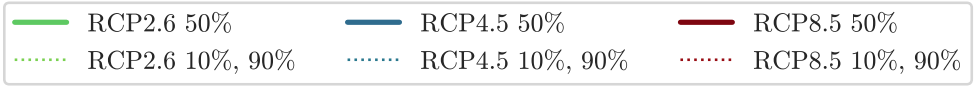

RCP	Ptile	Cnt. 2050	Cnt. 2100	% Cnt. 2100	Bn. $ 2050	Bn. $ 2100	% Value 2100	Avg. Year	Std. Year
RCP-26	**0.1**	13	152	0.05	0.00	0.06	0.09	2067	13
	0.5	167	631	0.21	0.06	0.25	0.41	2066	20
	0.9	373	2441	0.81	0.14	1.04	1.68	2075	21
RCP-45	**0.1**	30	304	0.10	0.01	0.11	0.18	2071	15
	0.5	181	966	0.32	0.07	0.39	0.63	2072	20
	0.9	406	3588	1.19	0.16	1.62	2.60	2078	19
RCP-85	**0.1**	57	492	0.16	0.02	0.19	0.31	2069	15
	0.5	238	1875	0.62	0.09	0.81	1.30	2076	18
	0.9	473	6868	2.27	0.18	3.12	5.01	2081	17

*All values in charts and table are undiscounted.

a) Map of ZIP Code Tabulation Areas (ZCTA) included in metro and 1.8m (6ft) inundation area; b) Sea level rise Path and 10-90th uncertainty band for greenhouse gas concentration pathways (representative concentration pathways) - RCP 2.6 (green), 4.5 (blue), and 8.5 (red) for; c) Inundation path and uncertainty bands for impaired property counts (left vertical axis) and percent of housing market (right vertical axis) for RCP 2.6, 4.5, and 8.5; d) Inundation path and uncertainty bands for total value at an undiscounted rate (left vertical axis) and percent of housing market value (right vertical axis) for RCP 2.6, 4.5, and 8.5; e)Box and whisker plot for impaired property counts through 2100 (left vertical axis) and share of housing market (right vertical axis) for RCP 2.6, 4.5, and 8.5 - lower whisker 10th quantile, lower box 25th quantile, center line median, upper box 75th quantile, and upper whisker 90th quantile; f)Box and whisker plot for total value at risk through 2100 at an undiscounted rate (left vertical axis) and percent of housing market value (right vertical axis) for RCP 2.6, 4.5, and 8.5 – lower whisker 10th quantile, lower box 25th quantile, center line median, upper box 75th quantile, and upper whisker 90th quantile. K26, K45, and K85 refer to results associated with RCP2.6, RCP4.5, and RCP 8.5 from (Kopp et al., 2014, 2017)

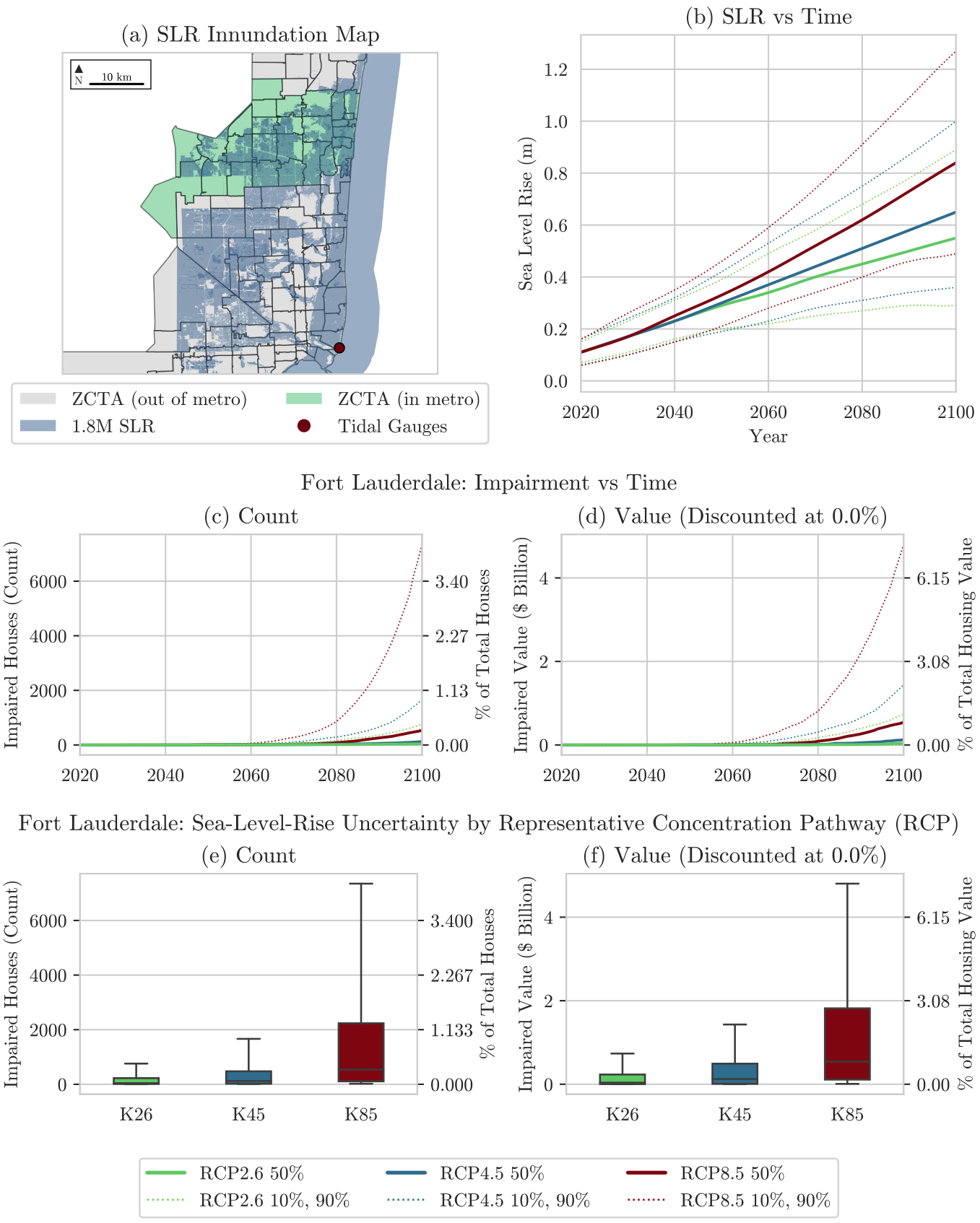
Fort Lauderdale: Sea-Level-Rise vs Time
(a) SLR Innundation Map
N
10 km
ZCTA (out of metro)
ZCTA (in metro)
1.8M SLR
Tidal Gauges
(b) SLR vs Time
Sea Level Rise (m)
Year
Fort Lauderdale: Impairment vs Time
(c) Count
Impaired Houses (Count)
% of Total Houses
(d) Value (Discounted at 0.0%)
Impaired Value ($ Billion)
% of Total Housing Value
Fort Lauderdale: Sea-Level-Rise Uncertainty by Representative Concentration Pathway (RCP)
(e) Count
(f) Value (Discounted at 0.0%)
K26
K45
K85
RCP2.6 50%
RCP2.6 10%, 90%
RCP4.5 50%
RCP4.5 10%, 90%
RCP8.5 50%
RCP8.5 10%, 90%

RCP	Ptile	Cnt. 2050	Cnt. 2100	% Cnt. 2100	Bn. $ 2050	Bn. $ 2100	% Value 2100	Avg. Year	Std. Year
RCP-26	**0.1**	0	2	0.00	0.00	0.00	0.00	2074	21
	0.5	2	39	0.02	0.00	0.04	0.06	2081	18
	0.9	10	757	0.43	0.00	0.74	1.13	2087	11
RCP-45	**0.1**	0	9	0.01	0.00	0.00	0.00	2077	9
	0.5	5	120	0.07	0.00	0.12	0.19	2086	14
	0.9	11	1663	0.94	0.00	1.43	2.20	2089	11
RCP-85	**0.1**	0	20	0.01	0.00	0.01	0.01	2077	14
	0.5	8	534	0.30	0.00	0.54	0.83	2088	10
	0.9	14	7347	4.16	0.01	4.80	7.39	2090	9

*All values in charts and table are undiscounted.

a) Map of ZIP Code Tabulation Areas (ZCTA) included in metro and 1.8m (6ft) inundation area; b) Sea level rise Path and 10-90th uncertainty band for greenhouse gas concentration pathways (representative concentration pathways) - RCP 2.6 (green), 4.5 (blue), and 8.5 (red) for; c) Inundation path and uncertainty bands for impaired property counts (left vertical axis) and percent of housing market (right vertical axis) for RCP 2.6, 4.5, and 8.5; d) Inundation path and uncertainty bands for total value at an undiscounted rate (left vertical axis) and percent of housing market value (right vertical axis) for RCP 2.6, 4.5, and 8.5; e)Box and whisker plot for impaired property counts through 2100 (left vertical axis) and share of housing market (right vertical axis) for RCP 2.6, 4.5, and 8.5 - lower whisker 10th quantile, lower box 25th quantile, center line median, upper box 75th quantile, and upper whisker 90th quantile; f)Box and whisker plot for total value at risk through 2100 at an undiscounted rate (left vertical axis) and percent of housing market value (right vertical axis) for RCP 2.6, 4.5, and 8.5 – lower whisker 10th quantile, lower box 25th quantile, center line median, upper box 75th quantile, and upper whisker 90th quantile. K26, K45, and K85 refer to results associated with RCP2.6, RCP4.5, and RCP 8.5 from (Kopp et al., 2014, 2017)

Mobile: Sea-Level-Rise vs Time

(a) SLR Innundation Map

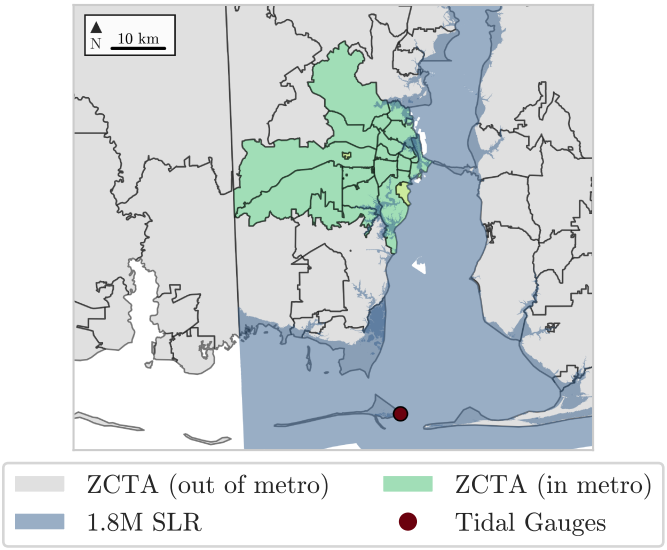

(b) SLR vs Time

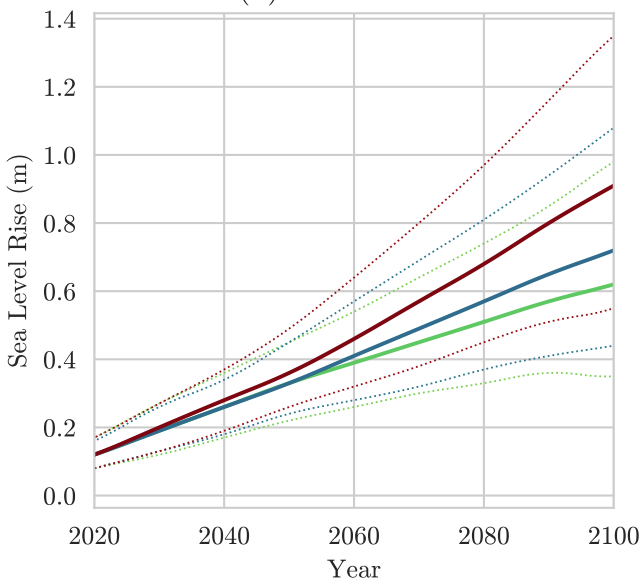

Mobile: Impairment vs Time

(c) Count

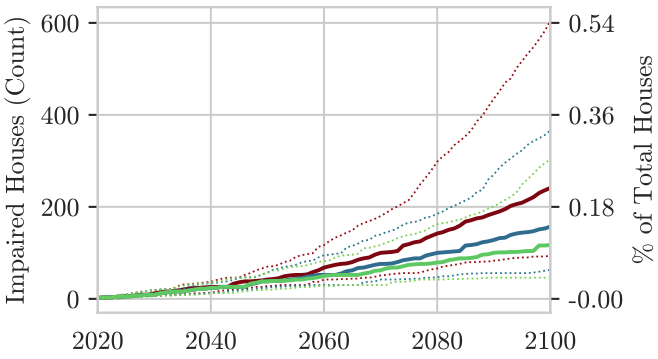

(d) Value (Discounted at 0.0%)

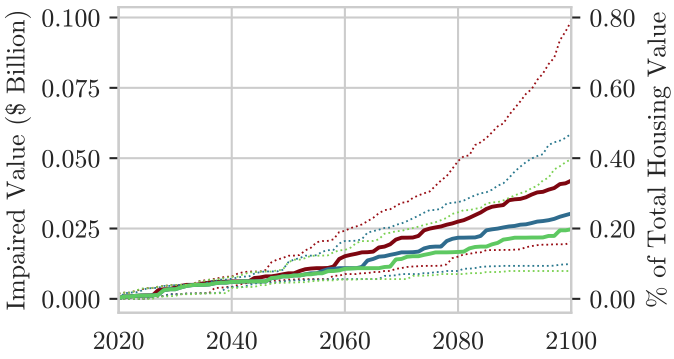

Mobile: Sea-Level-Rise Uncertainty by Representative Concentration Pathway (RCP)

(e) Count

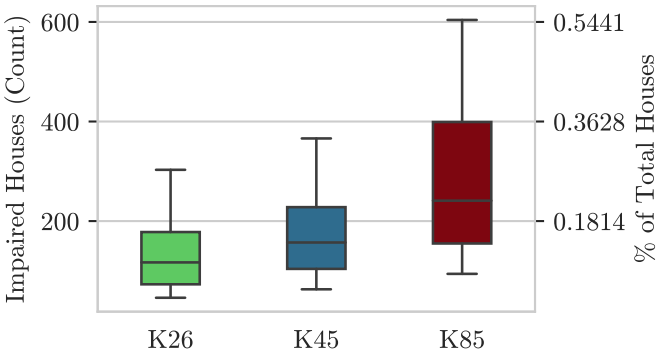

(f) Value (Discounted at 0.0%)

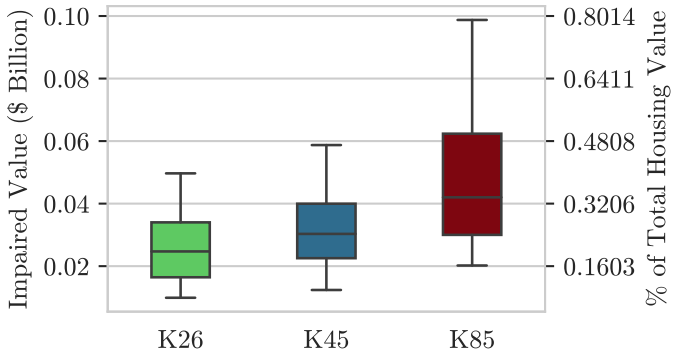

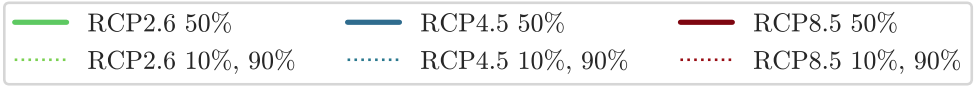

RCP	Ptile	Cnt. 2050	Cnt. 2100	% Cnt. 2100	Bn. $ 2050	Bn. $ 2100	% Value 2100	Avg. Year	Std. Year
RCP-26	**0.1**	7	33	0.03	0.00	0.01	0.05	2064	14
	0.5	29	108	0.10	0.00	0.02	0.17	2068	21
	0.9	53	300	0.27	0.01	0.05	0.38	2073	22
RCP-45	**0.1**	11	50	0.05	0.00	0.01	0.07	2068	17
	0.5	29	148	0.13	0.00	0.03	0.22	2071	19
	0.9	53	362	0.33	0.01	0.06	0.45	2074	20
RCP-85	**0.1**	15	81	0.07	0.00	0.02	0.13	2070	16
	0.5	33	232	0.21	0.01	0.04	0.31	2073	19
	0.9	67	601	0.55	0.01	0.10	0.77	2076	18

*All values in charts and table are undiscounted.

a) Map of ZIP Code Tabulation Areas (ZCTA) included in metro and 1.8m (6ft) inundation area; b) Sea level rise Path and 10-90th uncertainty band for greenhouse gas concentration pathways (representative concentration pathways) - RCP 2.6 (green), 4.5 (blue), and 8.5 (red) for; c) Inundation path and uncertainty bands for impaired property counts (left vertical axis) and percent of housing market (right vertical axis) for RCP 2.6, 4.5, and 8.5; d) Inundation path and uncertainty bands for total value at an undiscounted rate (left vertical axis) and percent of housing market value (right vertical axis) for RCP 2.6, 4.5, and 8.5; e)Box and whisker plot for impaired property counts through 2100 (left vertical axis) and share of housing market (right vertical axis) for RCP 2.6, 4.5, and 8.5 - lower whisker 10th quantile, lower box 25th quantile, center line median, upper box 75th quantile, and upper whisker 90th quantile; f)Box and whisker plot for total value at risk through 2100 at an undiscounted rate (left vertical axis) and percent of housing market value (right vertical axis) for RCP 2.6, 4.5, and 8.5 – lower whisker 10th quantile, lower box 25th quantile, center line median, upper box 75th quantile, and upper whisker 90th quantile. K26, K45, and K85 refer to results associated with RCP2.6, RCP4.5, and RCP 8.5 from (Kopp et al., 2014, 2017)

Galveston: Sea-Level-Rise vs Time

(a) SLR Innundation Map

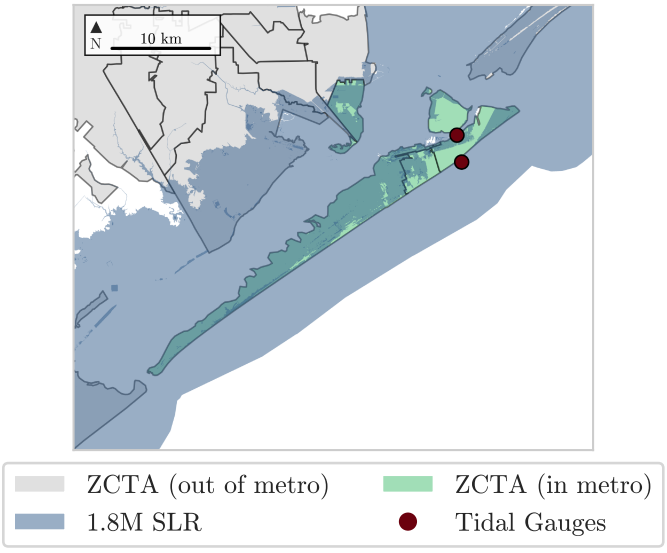

(b) SLR vs Time

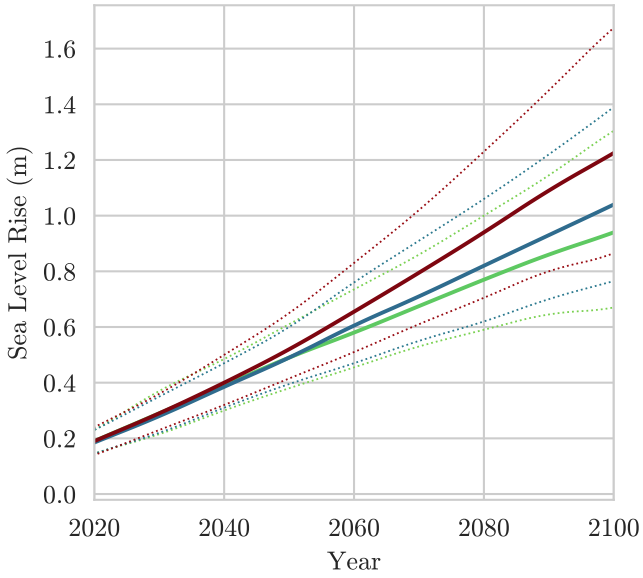

Galveston: Impairment vs Time

(c) Count

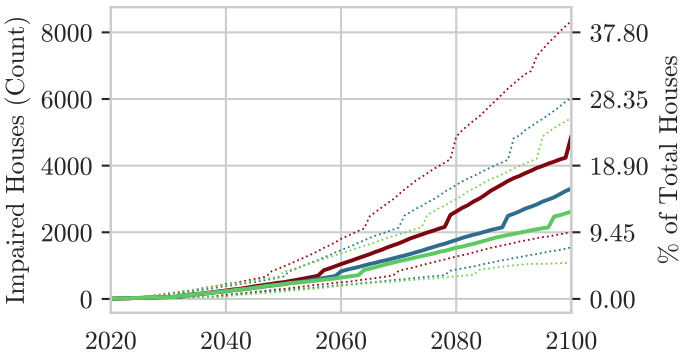

(d) Value (Discounted at 0.0%)

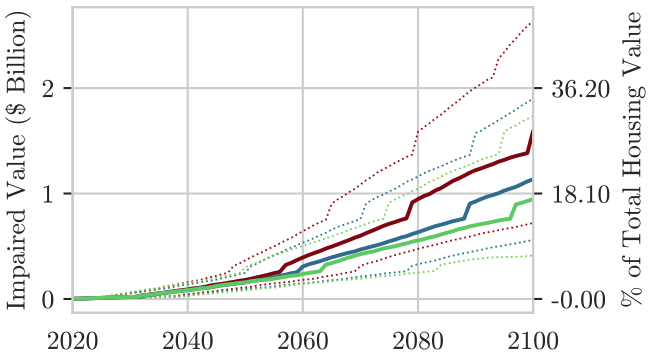

Galveston: Sea-Level-Rise Uncertainty by Representative Concentration Pathway (RCP)

(e) Count

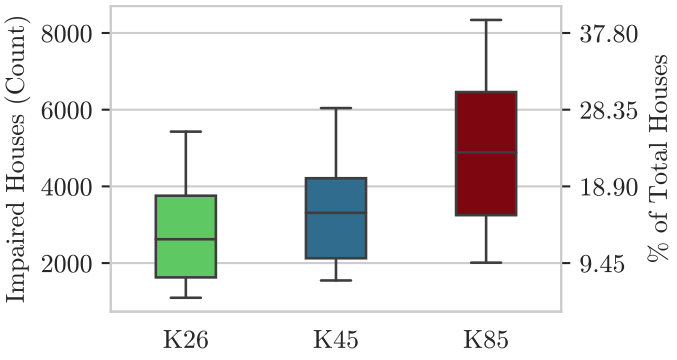

(f) Value (Discounted at 0.0%)

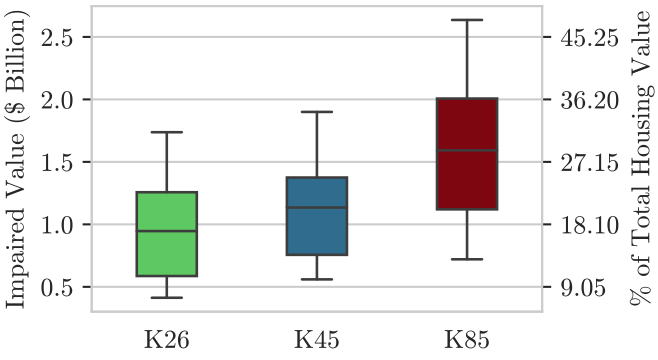

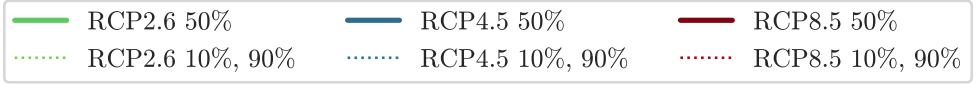

RCP	Ptile	Cnt. 2050	Cnt. 2100	% Cnt. 2100	Bn. $ 2050	Bn. $ 2100	% Value 2100	Avg. Year	Std. Year
RCP-26	**0.1**	179	1051	4.97	0.07	0.40	7.18	2070	17
	0.5	408	2587	12.22	0.15	0.93	16.91	2073	19
	0.9	792	5413	25.58	0.30	1.73	31.34	2074	20
RCP-45	**0.1**	215	1502	7.10	0.08	0.54	9.84	2074	18
	0.5	408	3275	15.48	0.15	1.12	20.32	2074	18
	0.9	655	6027	28.48	0.24	1.89	34.28	2074	18
RCP-85	**0.1**	253	1964	9.28	0.09	0.70	12.71	2073	16
	0.5	466	4851	22.92	0.17	1.58	28.61	2073	17
	0.9	962	8330	39.36	0.36	2.63	47.64	2074	18

*All values in charts and table are undiscounted.

a) Map of ZIP Code Tabulation Areas (ZCTA) included in metro and 1.8m (6ft) inundation area; b) Sea level rise Path and 10-90th uncertainty band for greenhouse gas concentration pathways (representative concentration pathways) - RCP 2.6 (green), 4.5 (blue), and 8.5 (red) for; c) Inundation path and uncertainty bands for impaired property counts (left vertical axis) and percent of housing market (right vertical axis) for RCP 2.6, 4.5, and 8.5; d) Inundation path and uncertainty bands for total value at an undiscounted rate (left vertical axis) and percent of housing market value (right vertical axis) for RCP 2.6, 4.5, and 8.5; e)Box and whisker plot for impaired property counts through 2100 (left vertical axis) and share of housing market (right vertical axis) for RCP 2.6, 4.5, and 8.5 - lower whisker 10th quantile, lower box 25th quantile, center line median, upper box 75th quantile, and upper whisker 90th quantile; f)Box and whisker plot for total value at risk through 2100 at an undiscounted rate (left vertical axis) and percent of housing market value (right vertical axis) for RCP 2.6, 4.5, and 8.5 – lower whisker 10th quantile, lower box 25th quantile, center line median, upper box 75th quantile, and upper whisker 90th quantile. K26, K45, and K85 refer to results associated with RCP2.6, RCP4.5, and RCP 8.5 from (Kopp et al., 2014, 2017)

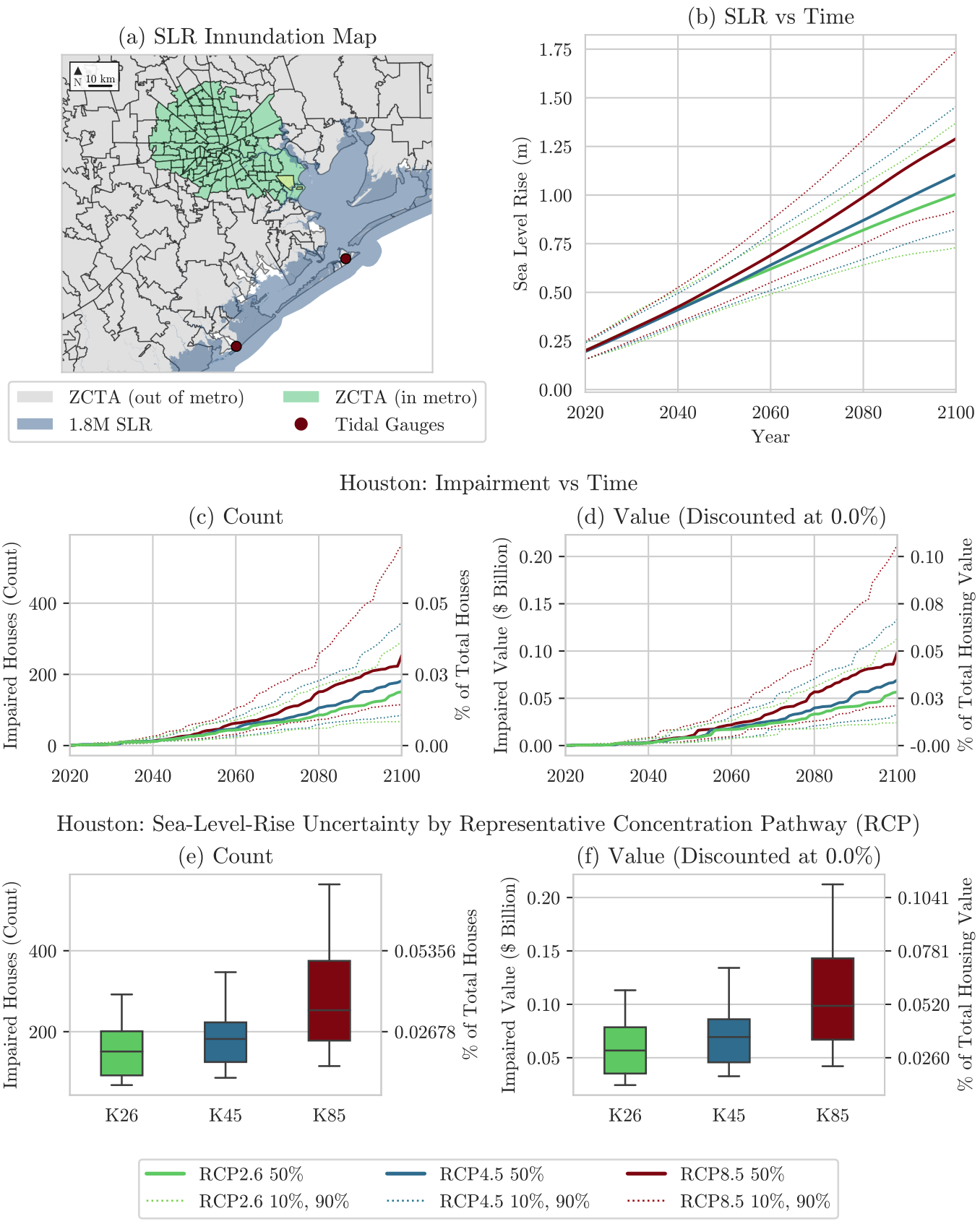
Houston: Sea-Level-Rise vs Time
(a) SLR Innundation Map
N 10 km
(b) SLR vs Time
Sea Level Rise (m)
1.75
1.50
1.25
1.00
0.75
0.50
0.25
0.00
2020
2040
2060
2080
2100
Year
ZCTA (out of metro)
ZCTA (in metro)
1.8M SLR
Tidal Gauges
Houston: Impairment vs Time
(c) Count
Impaired Houses (Count)
400
200
0
0.05
0.03
0.00
% of Total Houses
(d) Value (Discounted at 0.0%)
Impaired Value ($ Billion)
0.20
0.15
0.10
0.05
0.00
0.10
0.08
0.05
0.03
-0.00
% of Total Housing Value
Houston: Sea-Level-Rise Uncertainty by Representative Concentration Pathway (RCP)
(e) Count
Impaired Houses (Count)
400
200
0.05356
0.02678
% of Total Houses
K26
K45
K85
(f) Value (Discounted at 0.0%)
Impaired Value ($ Billion)
0.20
0.15
0.10
0.05
0.1041
0.0781
0.0520
0.0260
% of Total Housing Value
K26
K45
K85
RCP2.6 50%
RCP2.6 10%, 90%
RCP4.5 50%
RCP4.5 10%, 90%
RCP8.5 50%
RCP8.5 10%, 90%

RCP	Ptile	Cnt. 2050	Cnt. 2100	% Cnt. 2100	Bn. $ 2050	Bn. $ 2100	% Value 2100	Avg. Year	Std. Year
RCP-26	**0.1**	10	63	0.01	0.00	0.02	0.01	2068	16
	0.5	24	149	0.02	0.01	0.06	0.03	2073	20
	0.9	51	292	0.04	0.02	0.11	0.06	2073	20
RCP-45	**0.1**	10	81	0.01	0.00	0.03	0.02	2071	17
	0.5	24	179	0.02	0.01	0.07	0.04	2073	18
	0.9	44	347	0.05	0.02	0.13	0.07	2074	19
RCP-85	**0.1**	13	110	0.01	0.00	0.04	0.02	2072	17
	0.5	30	251	0.03	0.01	0.10	0.05	2072	17
	0.9	61	564	0.08	0.02	0.21	0.11	2077	18

*All values in charts and table are undiscounted.

a) Map of ZIP Code Tabulation Areas (ZCTA) included in metro and 1.8m (6ft) inundation area; b) Sea level rise Path and 10-90th uncertainty band for greenhouse gas concentration pathways (representative concentration pathways) - RCP 2.6 (green), 4.5 (blue), and 8.5 (red) for; c) Inundation path and uncertainty bands for impaired property counts (left vertical axis) and percent of housing market (right vertical axis) for RCP 2.6, 4.5, and 8.5; d) Inundation path and uncertainty bands for total value at an undiscounted rate (left vertical axis) and percent of housing market value (right vertical axis) for RCP 2.6, 4.5, and 8.5; e)Box and whisker plot for impaired property counts through 2100 (left vertical axis) and share of housing market (right vertical axis) for RCP 2.6, 4.5, and 8.5 - lower whisker 10th quantile, lower box 25th quantile, center line median, upper box 75th quantile, and upper whisker 90th quantile; f)Box and whisker plot for total value at risk through 2100 at an undiscounted rate (left vertical axis) and percent of housing market value (right vertical axis) for RCP 2.6, 4.5, and 8.5 – lower whisker 10th quantile, lower box 25th quantile, center line median, upper box 75th quantile, and upper whisker 90th quantile. K26, K45, and K85 refer to results associated with RCP2.6, RCP4.5, and RCP 8.5 from (Kopp et al., 2014, 2017)

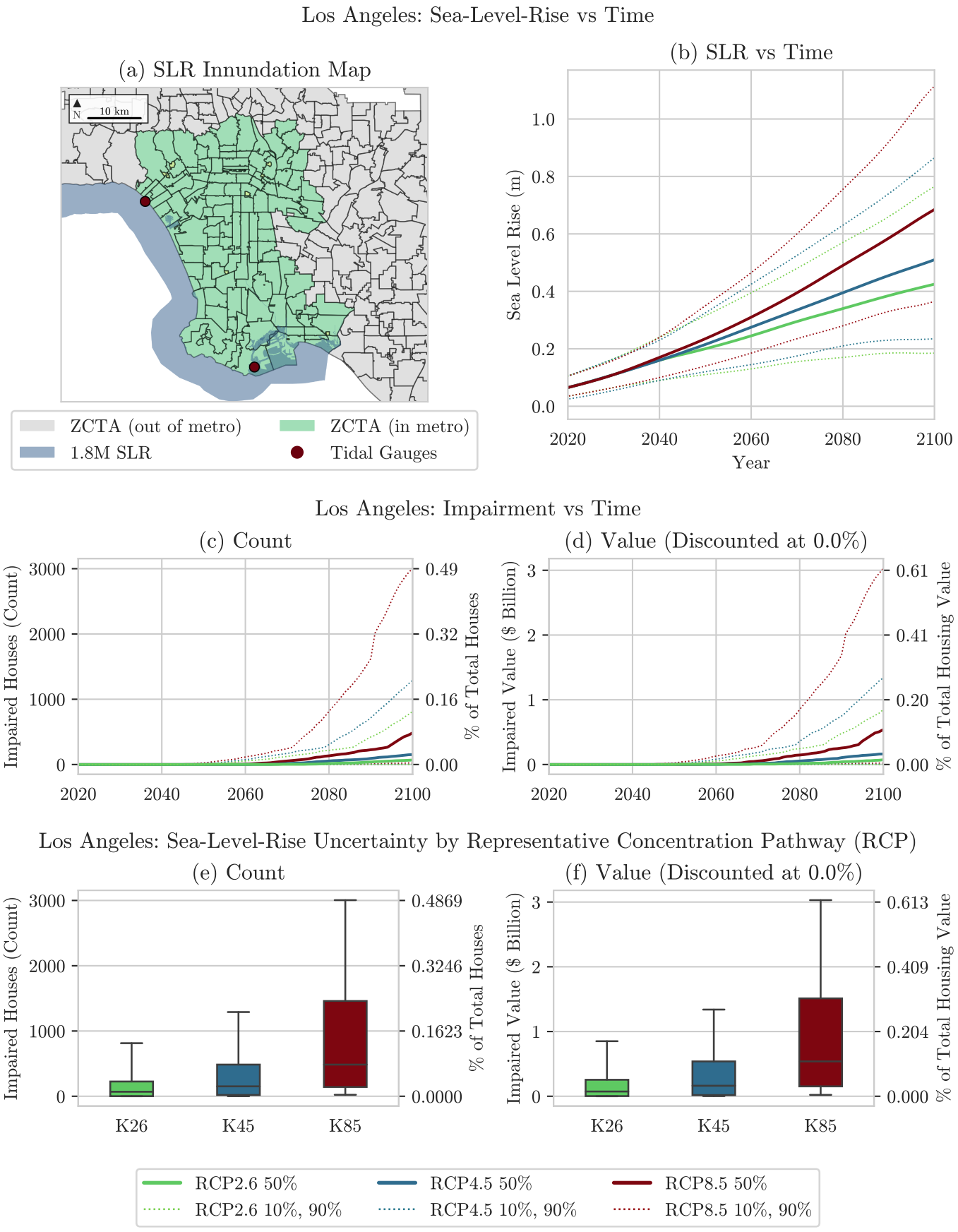
Los Angeles: Sea-Level-Rise vs Time
(a) SLR Innundation Map
N
10 km
ZCTA (out of metro)
ZCTA (in metro)
1.8M SLR
Tidal Gauges
(b) SLR vs Time
Sea Level Rise (m)
Year
Los Angeles: Impairment vs Time
(c) Count
Impaired Houses (Count)
% of Total Houses
(d) Value (Discounted at 0.0%)
Impaired Value ($ Billion)
% of Total Housing Value
Los Angeles: Sea-Level-Rise Uncertainty by Representative Concentration Pathway (RCP)
(e) Count
(f) Value (Discounted at 0.0%)
K26
K45
K85
RCP2.6 50%
RCP2.6 10%, 90%
RCP4.5 50%
RCP4.5 10%, 90%
RCP8.5 50%
RCP8.5 10%, 90%

RCP	Ptile	Cnt. 2050	Cnt. 2100	% Cnt. 2100	Bn. $ 2050	Bn. $ 2100	% Value 2100	Avg. Year	Std. Year
RCP-26	**0.1**	0	0	0.00	0.00	0.00	0.00	nan	nan
	0.5	0	69	0.01	0.00	0.07	0.01	2087	9
	0.9	5	813	0.13	0.01	0.85	0.17	2085	13
RCP-45	**0.1**	0	1	0.00	0.00	0.00	0.00	2082	nan
	0.5	1	152	0.02	0.00	0.16	0.03	2085	10
	0.9	7	1290	0.21	0.01	1.34	0.27	2085	12
RCP-85	**0.1**	0	23	0.00	0.00	0.02	0.00	2091	7
	0.5	1	485	0.08	0.00	0.54	0.11	2087	11
	0.9	23	3005	0.49	0.02	3.03	0.62	2085	11

*All values in charts and table are undiscounted.

a) Map of ZIP Code Tabulation Areas (ZCTA) included in metro and 1.8m (6ft) inundation area; b) Sea level rise Path and 10-90th uncertainty band for greenhouse gas concentration pathways (representative concentration pathways) - RCP 2.6 (green), 4.5 (blue), and 8.5 (red) for; c) Inundation path and uncertainty bands for impaired property counts (left vertical axis) and percent of housing market (right vertical axis) for RCP 2.6, 4.5, and 8.5; d) Inundation path and uncertainty bands for total value at an undiscounted rate (left vertical axis) and percent of housing market value (right vertical axis) for RCP 2.6, 4.5, and 8.5; e)Box and whisker plot for impaired property counts through 2100 (left vertical axis) and share of housing market (right vertical axis) for RCP 2.6, 4.5, and 8.5 - lower whisker 10th quantile, lower box 25th quantile, center line median, upper box 75th quantile, and upper whisker 90th quantile; f)Box and whisker plot for total value at risk through 2100 at an undiscounted rate (left vertical axis) and percent of housing market value (right vertical axis) for RCP 2.6, 4.5, and 8.5 – lower whisker 10th quantile, lower box 25th quantile, center line median, upper box 75th quantile, and upper whisker 90th quantile. K26, K45, and K85 refer to results associated with RCP2.6, RCP4.5, and RCP 8.5 from (Kopp et al., 2014, 2017)

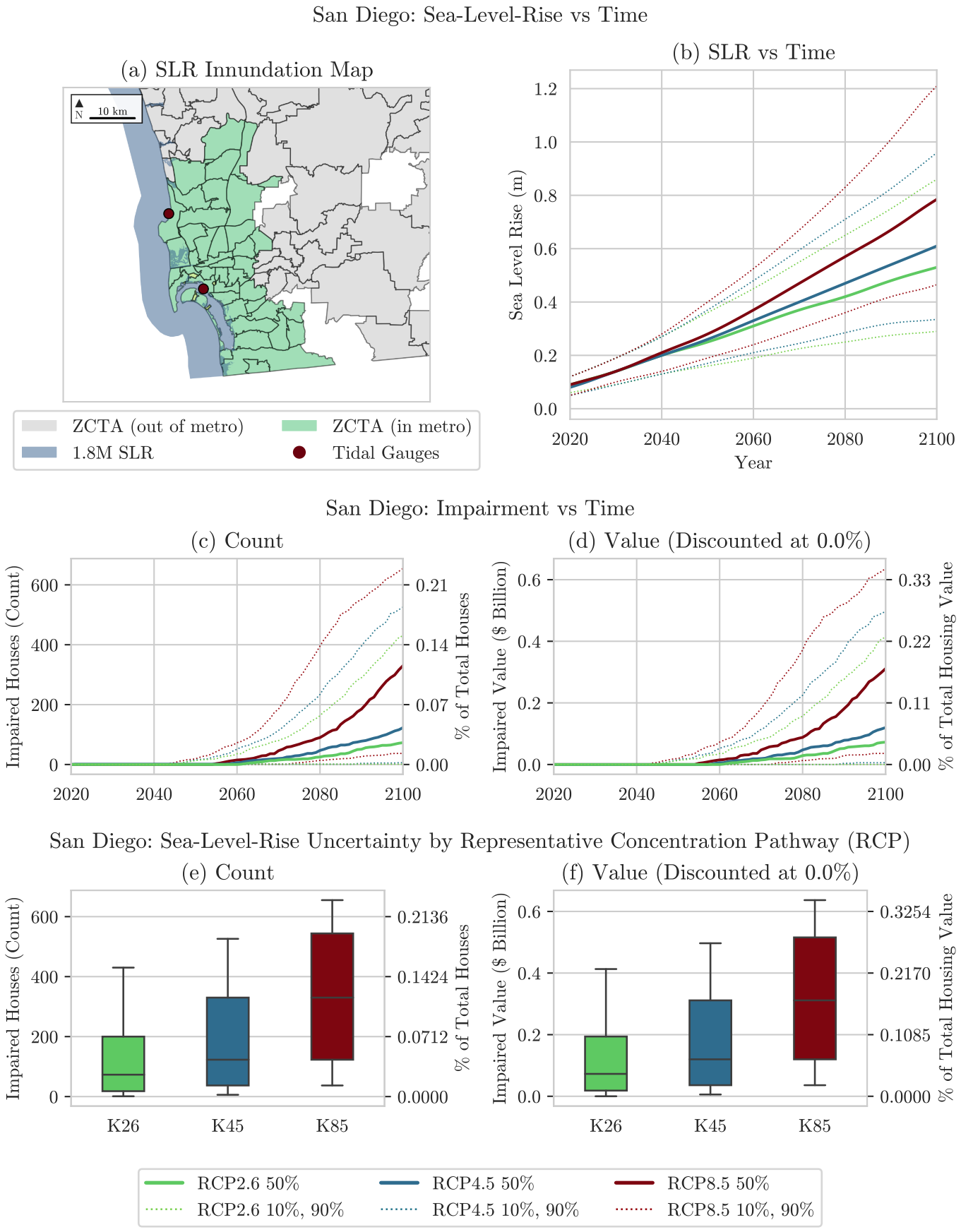
San Diego: Sea-Level-Rise vs Time
(a) SLR Innundation Map
N
10 km
(b) SLR vs Time
Sea Level Rise (m)
Year
ZCTA (out of metro)
ZCTA (in metro)
1.8M SLR
Tidal Gauges
San Diego: Impairment vs Time
(c) Count
(d) Value (Discounted at 0.0%)
Impaired Houses (Count)
% of Total Houses
Impaired Value ($ Billion)
% of Total Housing Value
San Diego: Sea-Level-Rise Uncertainty by Representative Concentration Pathway (RCP)
(e) Count
(f) Value (Discounted at 0.0%)
K26
K45
K85
RCP2.6 50%
RCP2.6 10%, 90%
RCP4.5 50%
RCP4.5 10%, 90%
RCP8.5 50%
RCP8.5 10%, 90%

RCP	Ptile	Cnt. 2050	Cnt. 2100	% Cnt. 2100	Bn. $ 2050	Bn. $ 2100	% Value 2100	Avg. Year	Std. Year
RCP-26	**0.1**	0	0	0.00	0.00	0.00	0.00	nan	nan
	0.5	0	73	0.03	0.00	0.07	0.04	2083	11
	0.9	13	430	0.15	0.01	0.41	0.22	2082	13
RCP-45	**0.1**	0	5	0.00	0.00	0.01	0.00	2092	4
	0.5	0	122	0.04	0.00	0.12	0.07	2083	12
	0.9	15	526	0.19	0.01	0.50	0.27	2080	13
RCP-85	**0.1**	0	36	0.01	0.00	0.04	0.02	2085	8
	0.5	0	330	0.12	0.00	0.31	0.17	2085	11
	0.9	19	655	0.23	0.02	0.64	0.35	2076	12

*All values in charts and table are undiscounted.

a) Map of ZIP Code Tabulation Areas (ZCTA) included in metro and 1.8m (6ft) inundation area; b) Sea level rise Path and 10-90th uncertainty band for greenhouse gas concentration pathways (representative concentration pathways) - RCP 2.6 (green), 4.5 (blue), and 8.5 (red) for; c) Inundation path and uncertainty bands for impaired property counts (left vertical axis) and percent of housing market (right vertical axis) for RCP 2.6, 4.5, and 8.5; d) Inundation path and uncertainty bands for total value at an undiscounted rate (left vertical axis) and percent of housing market value (right vertical axis) for RCP 2.6, 4.5, and 8.5; e)Box and whisker plot for impaired property counts through 2100 (left vertical axis) and share of housing market (right vertical axis) for RCP 2.6, 4.5, and 8.5 - lower whisker 10th quantile, lower box 25th quantile, center line median, upper box 75th quantile, and upper whisker 90th quantile; f)Box and whisker plot for total value at risk through 2100 at an undiscounted rate (left vertical axis) and percent of housing market value (right vertical axis) for RCP 2.6, 4.5, and 8.5 – lower whisker 10th quantile, lower box 25th quantile, center line median, upper box 75th quantile, and upper whisker 90th quantile. K26, K45, and K85 refer to results associated with RCP2.6, RCP4.5, and RCP 8.5 from (Kopp et al., 2014, 2017)

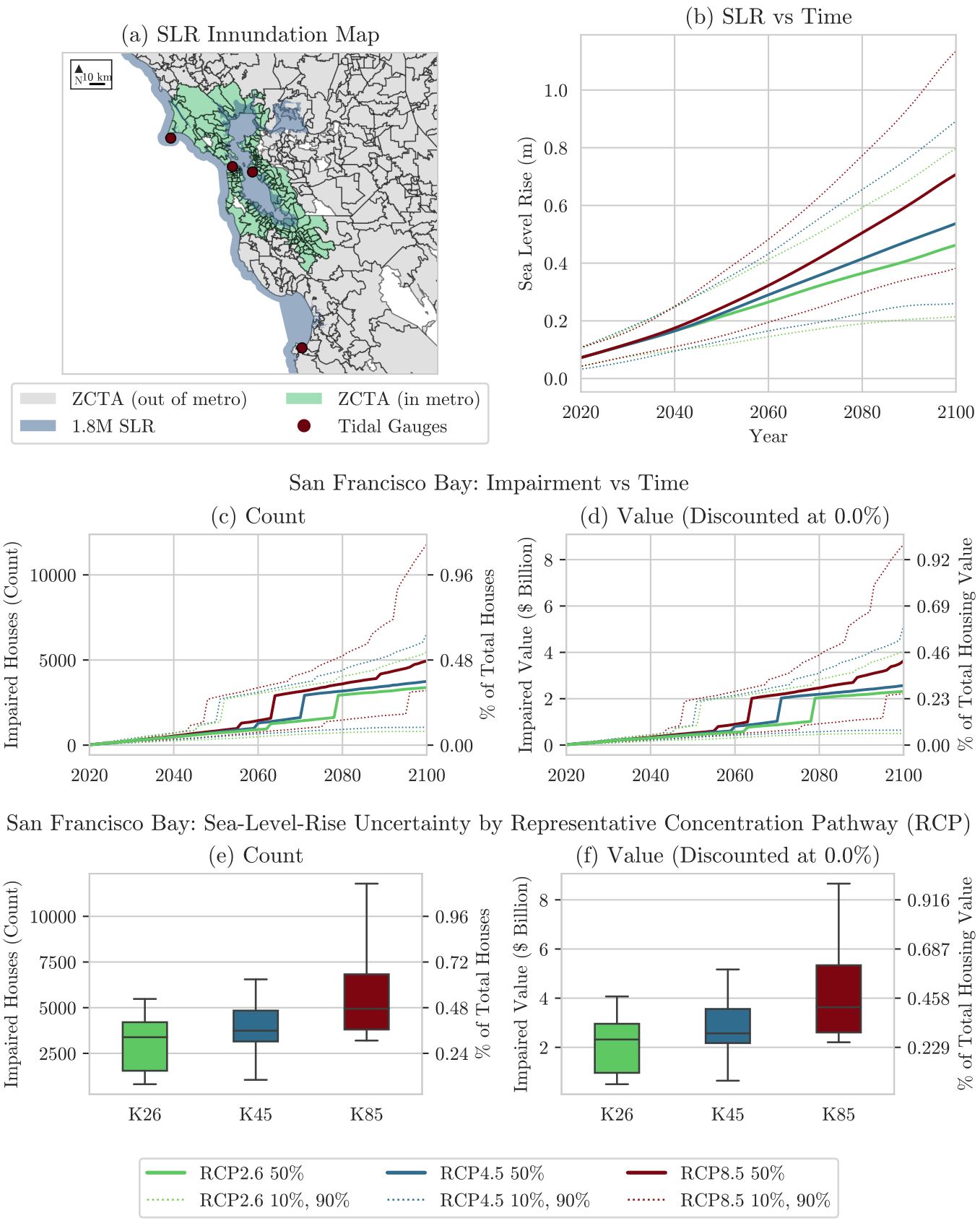
San Francisco Bay: Sea-Level-Rise vs Time
(a) SLR Innudation Map
N 10 km
ZCTA (out of metro)
ZCTA (in metro)
1.8M SLR
Tidal Gauges
(b) SLR vs Time
Sea Level Rise (m)
Year
San Francisco Bay: Impairment vs Time
(c) Count
Impaired Houses (Count)
% of Total Houses
(d) Value (Discounted at 0.0%)
Impaired Value ($ Billion)
% of Total Housing Value
San Francisco Bay: Sea-Level-Rise Uncertainty by Representative Concentration Pathway (RCP)
(e) Count
(f) Value (Discounted at 0.0%)
K26
K45
K85
RCP2.6 50%
RCP2.6 10%, 90%
RCP4.5 50%
RCP4.5 10%, 90%
RCP8.5 50%
RCP8.5 10%, 90%

RCP	Ptile	Cnt. 2050	Cnt. 2100	% Cnt. 2100	Bn. $ 2050	Bn. $ 2100	% Value 2100	Avg. Year	Std. Year
RCP-26	**0.1**	0	322	0.03	0.00	0.17	0.02	2072	11
	0.5	353	3034	0.29	0.20	2.08	0.24	2072	14
	0.9	1110	5268	0.51	0.67	3.93	0.45	2064	20
RCP-45	**0.1**	14	506	0.05	0.01	0.28	0.03	2070	12
	0.5	401	3387	0.33	0.23	2.33	0.27	2068	14
	0.9	1160	6339	0.61	0.71	5.02	0.57	2065	20
RCP-85	**0.1**	62	2707	0.26	0.03	1.87	0.21	2085	14
	0.5	481	4591	0.44	0.28	3.40	0.39	2070	16
	0.9	2608	11581	1.11	1.82	8.51	0.97	2076	21

*All values in charts and table are undiscounted.

a) Map of ZIP Code Tabulation Areas (ZCTA) included in metro and 1.8m (6ft) inundation area; b) Sea level rise Path and 10-90th uncertainty band for greenhouse gas concentration pathways (representative concentration pathways) - RCP 2.6 (green), 4.5 (blue), and 8.5 (red) for; c) Inundation path and uncertainty bands for impaired property counts (left vertical axis) and percent of housing market (right vertical axis) for RCP 2.6, 4.5, and 8.5; d) Inundation path and uncertainty bands for total value at an undiscounted rate (left vertical axis) and percent of housing market value (right vertical axis) for RCP 2.6, 4.5, and 8.5; e)Box and whisker plot for impaired property counts through 2100 (left vertical axis) and share of housing market (right vertical axis) for RCP 2.6, 4.5, and 8.5 - lower whisker 10th quantile, lower box 25th quantile, center line median, upper box 75th quantile, and upper whisker 90th quantile; f)Box and whisker plot for total value at risk through 2100 at an undiscounted rate (left vertical axis) and percent of housing market value (right vertical axis) for RCP 2.6, 4.5, and 8.5 – lower whisker 10th quantile, lower box 25th quantile, center line median, upper box 75th quantile, and upper whisker 90th quantile. K26, K45, and K85 refer to results associated with RCP2.6, RCP4.5, and RCP 8.5 from (Kopp et al., 2014, 2017)

Seattle: Sea-Level-Rise vs Time

(a) SLR Innundation Map

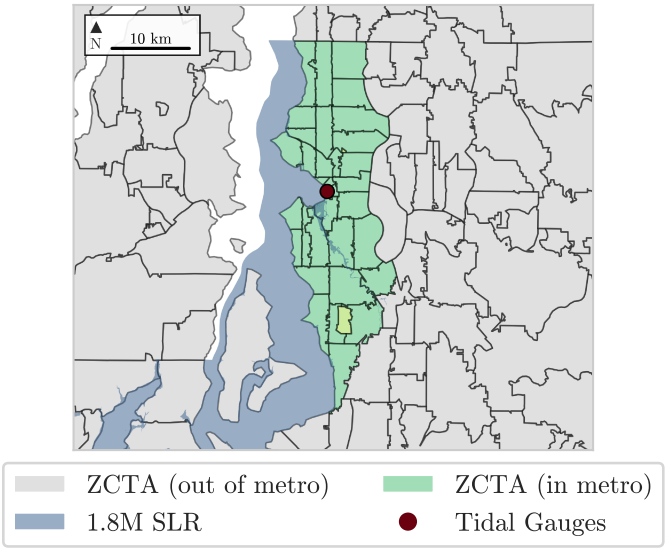

(b) SLR vs Time

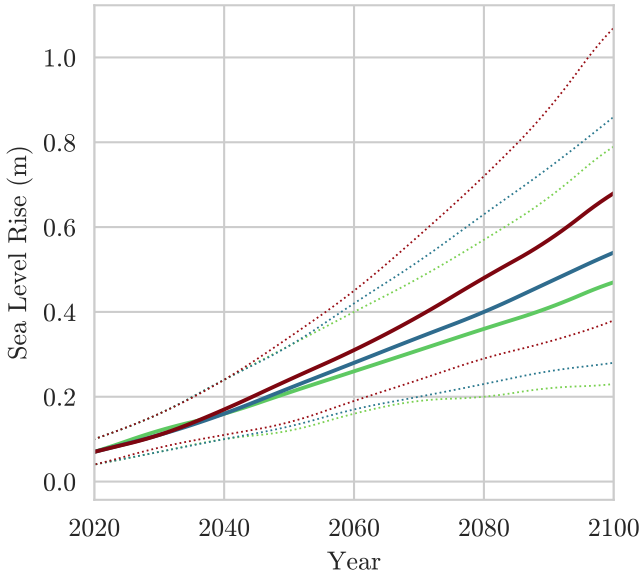

Seattle: Impairment vs Time

(c) Count

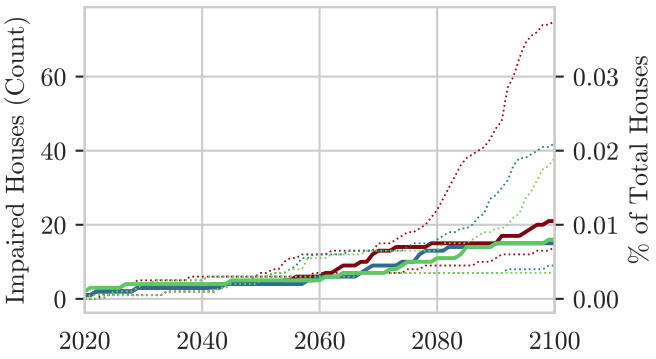

(d) Value (Discounted at 0.0%)

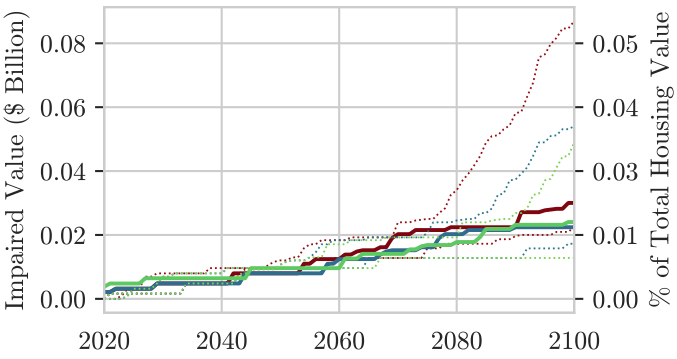

Seattle: Sea-Level-Rise Uncertainty by Representative Concentration Pathway (RCP)

(e) Count

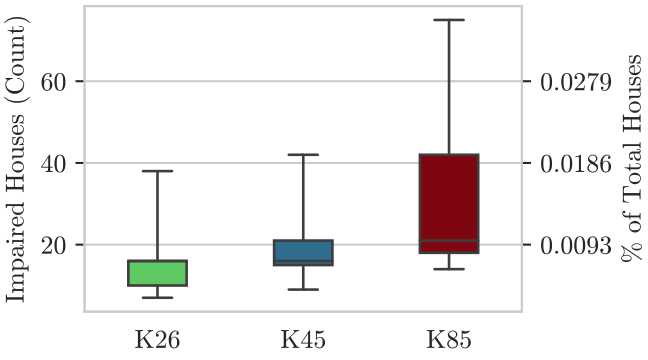

(f) Value (Discounted at 0.0%)

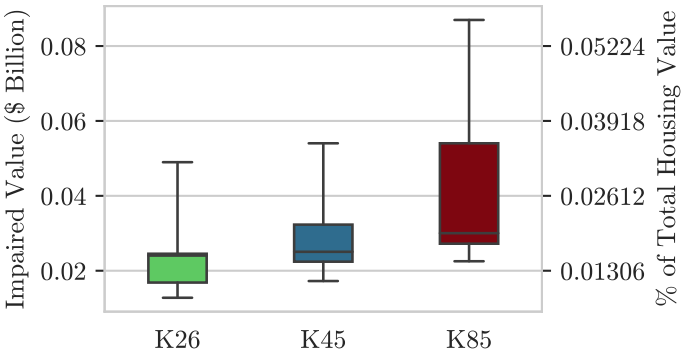

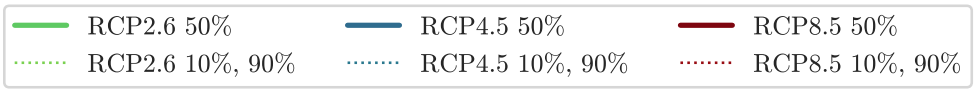

RCP	Ptile	Cnt. 2050	Cnt. 2100	% Cnt. 2100	Bn. $ 2050	Bn. $ 2100	% Value 2100	Avg. Year	Std. Year
RCP-26	**0.1**	0	1	0.00	0.00	0.00	0.00	2067	nan
	0.5	1	12	0.01	0.00	0.02	0.01	2076	15
	0.9	4	37	0.02	0.01	0.05	0.03	2079	21
RCP-45	**0.1**	0	3	0.00	0.00	0.01	0.00	2085	18
	0.5	1	12	0.01	0.00	0.02	0.01	2070	12
	0.9	4	41	0.02	0.01	0.05	0.03	2078	18
RCP-85	**0.1**	0	8	0.00	0.00	0.01	0.01	2082	13
	0.5	1	18	0.01	0.00	0.03	0.02	2074	17
	0.9	6	74	0.03	0.01	0.09	0.06	2081	16

*All values in charts and table are undiscounted.

a) Map of ZIP Code Tabulation Areas (ZCTA) included in metro and 1.8m (6ft) inundation area; b) Sea level rise Path and 10-90th uncertainty band for greenhouse gas concentration pathways (representative concentration pathways) - RCP 2.6 (green), 4.5 (blue), and 8.5 (red) for; c) Inundation path and uncertainty bands for impaired property counts (left vertical axis) and percent of housing market (right vertical axis) for RCP 2.6, 4.5, and 8.5; d) Inundation path and uncertainty bands for total value at an undiscounted rate (left vertical axis) and percent of housing market value (right vertical axis) for RCP 2.6, 4.5, and 8.5; e)Box and whisker plot for impaired property counts through 2100 (left vertical axis) and share of housing market (right vertical axis) for RCP 2.6, 4.5, and 8.5 - lower whisker 10th quantile, lower box 25th quantile, center line median, upper box 75th quantile, and upper whisker 90th quantile; f)Box and whisker plot for total value at risk through 2100 at an undiscounted rate (left vertical axis) and percent of housing market value (right vertical axis) for RCP 2.6, 4.5, and 8.5 – lower whisker 10th quantile, lower box 25th quantile, center line median, upper box 75th quantile, and upper whisker 90th quantile. K26, K45, and K85 refer to results associated with RCP2.6, RCP4.5, and RCP 8.5 from (Kopp et al., 2014, 2017)